Identification of Process Models Using Relay Feedback Response

Venkata Ramana Kasi

Identification of Process Models Using Relay Feedback Response

A

Thesis Submitted

in Partial Fulfilment of the Requirements

for the Degree of

DOCTOR OF PHILOSOPHY

By

VENKATA RAMANA KASI

Department of Electronics and Electrical Engineering

Indian Institute of Technology Guwahati

Guwahati - 781 039, INDIA.

November, 2018

Certificate

This is to certify that the thesis entitled "**IDENTIFICATION OF PROCESS MODELS USING RELAY FEEDBACK RESPONSE**", submitted by **Venkata Ramana Kasi** (126102002), a research scholar in the *Department of Electronics & Electrical Engineering, Indian Institute of Technology Guwahati*, for the award of the degree of **Doctor of Philosophy**, has been carried out by him under my supervision and guidance. The thesis has fulfilled all requirements as per the regulations of the institute and in my opinion has reached the standard needed for submission. The results embodied in this thesis have not been submitted to any other University or Institute for the award of any degree or diploma.

Dated:
Guwahati.

Prof. Somanath Majhi
Dept. of Electronics and Electrical Engg.
Indian Institute of Technology Guwahati
Guwahati - 781039, Assam, India.

Dated:
Guwahati.

Prof. Anup Kumar Gogoi
Dept. of Electronics and Electrical Engg.
Indian Institute of Technology Guwahati
Guwahati - 781039, Assam, India.

To my family ...

Acknowledgements

At the outset, I express gratitude heartily to my supervisors, Prof. Somanath Majhi and Prof. Anup Kumar Gogoi, for their excellent guidance and constant motivation during the thesis work. They gave me strength to overcome the difficulties faced during the course. I am grateful to them for their constant monitoring of my thesis work. Without that, the thesis might not have reached its current form.

I also thank my doctoral committee members Prof. C. Mahanta, Dr. Sisir Kumar Nayak and Dr. H. S. Shekhawat for their continuous scrutiny of my thesis work and suggestions to improvise the thesis. The support provided by the previous and the current Head of the Department, and other faculty members during the course is commendable. I thank specially to Mr. Samim, Mr. Sanjib, Mr. Dimpul, Mr. Bharali, Mr. Sonowal and all the members of the Power and control lab for providing necessary lab facilities required for the research work.

I am grateful to my parents and sister, for their love, care and support that made me the person today I am.

I had immense pleasure spending great time with friends during my stay at IIT Guwahati, including Krishna, Radak, Gargi, Dibyajyoti, Kannan, Brijesh, Ramesh, Dwivedi, Upendra, Rituraj, Kashyap, Prosenjit, Mridul, Kitaba, Umesh, Jagath, Trusna, and Arvin. They stood by me during my difficult times. Their support and encouragement gave me immense strength.

I am thankful to Ministry of Human Resource Development (MHRD) for providing assistantship during the course. The nice weather of the city of Guwahati made my stay pleasant. The stay at this place also gave me an opportunity to know the rich diversity of the north-eastern states.

Finally, I thank those invisible hands of the Almighty, which always shower blessings on me.

(Venkata Ramana Kasi)

Abstract

Relay based identification is widely used for the identification of process dynamics. The dynamic behavior of the process can be obtained from the limit cycle output. The process models are affected during abnormal conditions such as load disturbance and parameter variations. In this thesis, the dynamic model of first order plus dead-time (FOPDT) and second order plus dead-time (SOPDT) are identified during load and no-load disturbances and a controller is designed to reject the load disturbances. Due to the ease of implementation, relay identification is used in many practical applications. Here, the identification methods are implemented on DC-DC buck converter.

An ideal relay is used during the identification. The relay is approximated as Dual-input-describing-function (DIDF) which is used for the identification during load and no-load disturbances. During the load disturbance, the relay settings are not modified to restore the symmetric limit cycle. Instead, the asymmetric limit cycle information is used to observe the variation in process parameters during the load disturbance. The DIDF approximation is applied to identify the process parameters of a DC-DC buck converter. A systematic procedure is developed to induce limit cycle oscillations. Utilizing the limit cycle measurements, the control to output transfer function of the converter is extracted. To show the effectiveness of the identified model, it is evaluated with the closed-loop response.

As DIDF is an approximated method, state-space approach is used to obtain better accuracy in the identification. Required analytical expressions are derived to estimate the unknown process parameters. Half-limit cycle data is sufficient for identification. The performance of the buck converter model obtained from the proposed state-space method is analyzed. Further, a model-based controller (PID) is designed for the control of FOPDT and SOPDT processes. The controller parameters are tuned using direct-synthesis method with a single tuning parameter. The best value of the tuning parameter is obtained using particle

swarm optimization (PSO) with optimal performance measure. The objective of the controller design is to achieve better performance during load disturbance. A set-point filter is used for satisfactory set-point tracking. The method is tested on standard benchmark examples available in the literature.

CONTENTS

भारतीय प्रौद्योगिकी संस्थान गुवाहाटी
Indian Institute of Technology Guwahati

LIST OF FIGURES

LIST OF TABLES

NOMENCLATURE

DF	Describing function
DIDF	Dual Input Describing function
FOPDT	First order plus dead-time
DPWT	Discrete parameter wavelet transform
TBPRD	Time-base Period Register
PID	Proportional-integral-derivative controller
ESR	Equivalent series resistance
RHP	Right half of the s-plane
ePWM	enhanced Pulse Width Modulation
SOPDT	Second order plus dead-time
SNR	Signal to noise ratio
ISE	Integral square error
IAE	Integral square error

भारतीय प्रौद्योगिकी संस्थान गुवाहाटी
Indian Institute of Technology Guwahati

MATHEMATICAL NOTATIONS

A_p	Peak amplitude of limit cycle output
δ_0	Bias term
h	Amplitude of a relay
K	Steady state gain of a process model
θ	Time delay of a process model
τ_1, τ_2	Time constants of a process model
T_c	Tuning parameter
τ_s	Time constant of SOPDT process
K_P	Proportional gain
T_I	Integral time constant
T_D	Derivative time constant
h	Amplitude of a relay
n	Order of the system
D	Duty cycle
L	Inductance
R_{el}	Inductor ESR
C	Capacitance
R_{ec}	Capacitor ESR
R_o	Load resistance
i_L	Current through inductor
f_s	Switching frequency
f_{p_clk}	processor clock frequency

v_c	Voltage across capacitor
β	set-point coefficient
$C1, C2$	Acceleration constants
T_p	Half period of the limit cycle output
t_p	Time at which peak amplitude of limit cycle occurs
$y(t)$	Output signal
$y_n(t)$	Noisy signal
$u(t)$	Process input
$r(t)$	Set-point / reference input
$e(t)$	Error signal
t	Time
$G(s)$	Transfer function of a process
$G_m(s)$	Transfer function of a process model
$G_c(s)$	Transfer function of a controller
$G_f(s)$	Set-point filter
N	Describing function of the relay with hystereis
E_I	Identification error
ω_c	Critical frequency of the process
M_s	Maximum sensitivity

भारतीय प्रौद्योगिकी संस्थान गुवाहाटी
Indian Institute of Technology Guwahati

भारतीय प्रौद्योगिकी संस्थान गुवाहाटी
Indian Institute of Technology Guwahati

CHAPTER 1

INTRODUCTION

1.1 Research Background

There are several identification methods (step and frequency response) available to estimate the model parameters, out of which the relay identification method has gained more importance due to its advantages as mentioned below [1–3].

1. It identifies the process at ultimate frequency (the frequency where the phase angle corresponds to $-\pi$).
2. As it is a closed-loop test, the process will not drift away from the operating point.
3. It is less sensitive to the parameter variations and the disturbance.
4. It requires less measurements for the identification.

A. Identification of FOPDT and SOPDT processes using dual-input describing function (DIDF) technique

Identification refers to the estimation of the transfer function model of a plant. Once the mathematical model of the plant is available, analysis regarding its operation and controller design can be done. Before commissioning in real-time application, the performance of the plant can be analyzed for different conditions. With the available plant input-output data, the overall transfer function can be obtained. The relay feedback identification has become popular for identifying the process dynamics. This method was initially tested by Åström and Hägglund [4] to induce limit cycle oscillation for autotuning purpose. It is referred as autotune variation method (ATV). For the controller tuning, the ultimate gain and the period of the limit cycle at critical frequency is utilized. Later, using Åström's autotune method, Luyben [5] obtained the transfer function of a nonlinear distillation column. During the identification, the relay is approximated by describing function (DF). The gain and phase criteria are used to estimate the unknown process parameters. The critical frequency information of the limit cycle can help in the modeling of any complex plant in terms of the first-order-plus-dead-time (FOPDT) and the second-order-plus-dead-time (SOPDT) systems. Several researchers have successfully extended the DF approximation for the identification of various processes [6–10]. Some modifications were made to the conventional relay test by Li et al. [11] and Leva [12] to get additional information during the identification. In their methods, two relay feedback tests were conducted to get two points on the Nyquist curve. But this increases the time for identifying the plant transfer function. The DF method can estimate a maximum of two parameters. Using the method reported in [11], Scali et al. [13] identified five parameters with three relay tests and with additional delay. More time is required to perform the overall test. Using a biased-relay, Shen et al. [14] obtained two points on the Nyquist curve with a single test in their analysis dual-input describing function (DIDF) during the identification. In many processes, frequent load changes occur. This may affect the limit cycle output. Considering this, shen et al. [15] modified the relay

settings to compensate the effect of disturbance. Panda [16] identified the SOPDT process parameters during disturbance as suggested by [15]. Sung and Lee [17] proposed a relay feedback method to reject the load disturbance using PI controller. In [18], Atherton gave an overview of relay autotuning in which the author has reported in detail about how the relay feedback method has succeeded Z-N identification. Padhy and Majhi [19] identified the stable and the unstable FOPDT processes using DF method. A relay with hysteresis is used by Bajarangabali and Majhi to overcome the issue of measurement noise [20]. During the practical implementation, the model obtained from the relay test may not be accurate as obtained from simulation due to non-ideal conditions. But the identified model should give a satisfactory performance. The practical feasibility of the relay autotuner in the industry is reported in by Berner et al. [21]. The advancements in digital processors have reduced the complexity of the real-time implementation. Therefore, utilizing these the identification algorithms can be implemented in an effective way.

B. State-Space approach for the Identification of FOPDT and SOPDT Processes

In the DF method, the relay gain is approximated considering the fundamental component of the relay output. This approximation leads to an error in the parameter estimation. To overcome this, alternative methods were developed by researchers to obtain accurate modeling. Chang et al. [6] used Z-transform to improve the identification accuracy, but this method requires information obtained from the DF method. The time domain approach for the process identification was first presented by Wang et al. [22]. The processes are estimated as FOPDT. Majhi and Atherton [23], Majhi [24]- [25] proposed state-space approach for the identification of various processes. Utilizing the derivatives of the half limit cycle data, one extra parameter is obtained with a single relay feedback test [25]. Kaya and Atherton [26]-[27] estimated the process parameters using A-locus method with the relay response data. Marchetti et al. [7] extended ATV method to identify the unstable processes using two relay tests. Depending on the shape of the relay feedback response for different dead-time

to time constant ratios, the types of the models are categorized (FOPDT, critically damped SOPDT and higher order) by Thyagarajan and Yu [28]. Using the shape factor, Panda and Yu [29]- [30] derived analytical expressions to identify different types of processes (overdamped, critically damped and underdamped). Srinivasan and Chidambaram [31] estimated FOPDT model parameters using the Laplace transform method. In the closed-loop test, an asymmetrical relay with displacement factor is utilized to obtain a fitted model for the stable and the unstable processes. Panda et al. [32] identified process parameters of different types of integrating processes using the relay test. Lee at al. [33] proposed a method to get more accurate models by taking the integrals of the fundamental frequency term. Liu and Gao [34]- [35] proposed an on-line identification method using the biased/unbiased relay. In the same, authors proposed a low-pass Butterworth filter to recover a noisy signal. A multiloop relay feedback structure is given by Bajrangabali et al. [36] to obtain FOPDT and SOPDT process models using the relay with hysteresis. But due to the presence of derivative term in the forward path, the sampling time should be selected carefully to yield a bounded output during noise. Apart from the relay test, different methods are also used for identification. Park et al. [37] identified a SOPDT model using the least-squares method in the frequency domain. Ananth and Chidambaram identified the unstable FOPDT process from step response with the PID controller in the loop [38]. This method has stability issues, which is later solved by Padma Sree and Chidambaram in [39]. A detailed review of the step and the relay feedback identification methods are reported by Liu et al. [40]. Due to the advantages in relay test, it is most widely used for estimating the unknown processes. Using the exact methods, the identification error can be reduced and the methods can be modified to be hardware-effective for real-time application.

C. Identification and Control of FOPDT and SOPDT Processes

In many process industries, model-based controller design is opted for the effective operation of the plant. An accurate dynamic model will enhance the controller performance. Using the modified ATV method, Marchetti et al. [7] identified the unstable process and the con-

troller is tuned with the obtained parameters. Many autotuning techniques for the control of various process are presented in the literature. An autotune procedure for the design of a model-based control is given by Huang et al. [8]. Based on the identified model, Vivek and Chidambaram [41] designed a PID controller for unstable systems. Padhy and Majhi [19] proposed an identification and control scheme with a PI-PD structure for FOPDT processes. After estimating the dynamic model, a model based controller can be designed using the identified plant dynamics. Åström and Eykhoff [42] presented a detailed survey on process identification and also mentioned about the importance of identification for designing a control strategy. Numerous advancements have taken place in the control design, such as optimal, adaptive, Fuzzy etc.. but still PID controllers are employed in process industries. Many techniques are available in the literature for PID tuning [43–48]. In some of the methods, the tuning rules cannot be applied for the stable processes. Internal model control (IMC) is one of the popular methods for tuning PI/PID controllers. On the same line of the IMC method, Chen and Seborg [45] proposed the direct synthesis method. Here, more emphasis is given to the load disturbance rejection. Set-point weighted PID controller is designed by Prashanti and Chidambaram [49] to track set-point response with less peak overshoot for an unstable process. Most of the methods reported in the literature give a good set-point response but the disturbance rejection is sluggish. In general, the designer should compromise on achieving either good set-point response or disturbance rejection. To bring a good trade-off between set-point tracking and disturbance rejection, a two-degree-of-freedom (2-DoF) controller is used by many researchers [50–52]. This require tuning of extra parameters. In 2DoF control, the two responses can be individually controlled. Different closed-loop control structures are proposed by authors in [19, 53, 54] to control both set-point and load disturbance responses. During the controller design, the system robustness measure is important. Gain and phase margins are used as a performance measure in the literature [46, 55, 56]. The controller parameters are tuned by setting the desired gain and phase margins. Maximum sensitivity is also considered as a performance measure for controller tuning [52,54,57]. Over the last few years, optimization techniques are used in controller tuning considering integral square error

(ISE) or integral absolute error (IAE) as performance index [58]. Numerical optimization is used in [59] to design PI/PID controller for FOPDT and SOPDT processes. This method requires complex mathematical formulation to derive the analytical expressions for controller parameters. During the controller tuning for any process, the performance measure is chosen according to the design requirement. The tuning rules should guarantee system robustness even in presence of parameter variations.

1.2 Motivation

Relay feedback test has emerged as one of the best identification methods for identifying various process models in many process industries. In literature, it is observed that many researchers used the relay test for the identification of the stable and the unstable processes. Different types of relays, such as ideal relay, asymmetric and relay with hysteresis are used. According to the requirement, the type of the relay is selected. Mostly, an ideal relay is used as it involves less complexity. When the relay test is conducted with the ideal relay, the limit cycle becomes asymmetric either if the process is subjected to disturbance during its operation or due to the drift caused by the sensors used in the real-time environment. Many authors in the literature suggested to compensate the bias present in an asymmetric limit cycle by modifying the relay settings to restore the symmetric limit cycle output. However, the process parameters will change in presence of disturbance or due to the drift. This motivates us to extend the relay based identification method to identify the process parameters during normal and abnormal conditions. As a part of this, at first dual input describing function is used for the identification under different situations. DIDF method is an approximate method so to get better identification accuracy state space method is utilized for the identification. Once the process model is obtained, a controller can be designed. A model-based controller is designed which works well for nominal and during disturbance condition.

1.3 Contributions of this Thesis

Identification of process models using the relay feedback test has been extensively used to obtain the dynamic models. There is still much scope left in the relay identification. The objective of this thesis is to extend the relay method to identify the process models and to conduct a real-time implementation of the same. The following are the contributions of this thesis:

I. Identification of FOPDT and SOPDT processes using dual-input describing function (DIDF) technique

Identification of different processes is done from the closed-loop test using the dual input describing function. An ideal relay is connected in the loop during the test. Explicit expressions of the process parameters of the dynamic models are derived for both the off-line and the on-line methods and then the models are identified during the nominal and the load disturbance conditions. For both the conditions, DIDF approximation is utilized to obtain the process parameters. The proposed identification method is demonstrated through a real-time application on the DC-DC buck converter. The converter transfer function is obtained under different parameter variations. The issue of measurement noise is taken care of using the wavelet transform.

II. State-Space approach for the Identification of FOPDT and SOPDT Processes

The DIDF technique is an approximate method, so the error between the identified models and actual model is more. Therefore, the state space method is used to determine different classes of process model. The necessary mathematical expressions are derived to get the process models using the limit cycle conditions. To show the effectiveness of the proposed method, the identified models are compared with the existing models in the literature. The identification is done in presence of the load disturbance and the no-load disturbances. The state-space method is used to identify the dynamic model of the DC-DC buck converter. The

performance of the identified model is observed using the step response.

III. Identification and Control of FOPDT and SOPDT Processes

At first, the identification of process models are carried out using the state-space method. Then the analytical expressions for the process parameters are derived using the limit cycle information. The derived mathematical expressions are a function of the time domain data of the limit cycle. The required measurements of the limit cycle are made to obtain the process parameters. After obtaining the process models, a model based controller is designed to control the process. The controller is designed to get good load disturbance attenuation and satisfactory set-point response. During the design, more emphasis is given to reject the disturbances that occur in the plant operation. The closed-loop responses are compared with the methods reported in the literature.

1.4 Thesis Organization

In this section, a brief description of each section of the thesis is presented. The thesis consists of five chapters

- **Chapter 2:** In this chapter, the process models of FOPDT and SOPDT plants are identified using the DIDF technique. The approximated relay gain in the form of DIDF is used to obtain process parameters under different conditions. The symmetric and asymmetric limit cycle measurements are measured to get the process parameters during load and no-load disturbance. The identification error is determined for both the conditions. The DIDF approximation is applied to identify the dynamic model of a DC-DC buck converter. The transfer function of the converter is obtained for nominal and during parameter variations. The performance of the identified model is verified with the closed loop response. A prototype of the converter model is developed for the real-time implementation of the proposed identification method.

- **Chapter 3:** In this chapter, the state space approach is used to model the FOPDT and

the SOPDT processes. Analytical equations are derived to get a better identification accuracy of the process models. The peak amplitude condition in the output equation is utilized to derive the expressions. Different low load disturbances are considered to illustrate the identification method. Then we apply the identification method to DC-DC converter model. The performance of the identified converter model is compared with the model obtained using the DIDF method.

- **Chapter 4:** In this chapter, the identification and control of the FOPDT and the SOPDT stable/unstable process is performed. The process models are obtained using the time domain equations obtained from the state-space method. Using the identified model, a model based controller is designed employing the direct synthesis method. The required tuning parameter, to tune the controller parameters, is obtained with help of the particle swarm optimization technique. The optimization algorithm with error minimization as the objective function is chosen to get the best tuning parameter. The obtained closed-loop responses are compared with the methods existing in the literature.

- **Chapter 5:** In Chapter 5, the conclusions drawn from the research work and scope for future work are presented.

भारतीय प्रौद्योगिकी संस्थान गुवाहाटी
Indian Institute of Technology Guwahati

CHAPTER 2

IDENTIFICATION OF FOPDT AND SOPDT PROCESSES USING DUAL-INPUT DESCRIBING FUNCTION (DIDF)

2.1 Introduction

In control theory, obtaining process parameter is very important to control the process. Relay-based identification has received more attention in process industries for the identification of various process models. Åström and Hägglund [4] proposed a relay feedback method to generate sustained oscillatory output. Luyben [5] represented the relay in terms of a gain known as describing function (DF). Later, many researchers explored relay identification to identify different processes. Atherton [18] proposed relay auto-tuning using limit cycle information by using the DF method. Using the critical information, such as critical frequency and critical gain from the oscillatory output, many authors identified different types of processes which includes first-order plus dead time (FOPDT), second-order plus dead time (SOPDT) and integrating processes [10, 25, 32, 34]. During nominal condition, the limit cycle output will be symmetric. Whereas during the load disturbance the limit cycle becomes asymmetric with some bias, it becomes difficult to get the required limit cycle measurements from the asymmetric limit cycle. Shen et al. [15] compensated the bias caused due to load disturbance by adjusting the relay setting. Panda [16] estimated the parameters of an

underdamped process during disturbance by changing the relay settings as suggested in [15]. The exact dynamic model during disturbance or with bias in the output cannot be seen with the modified relay heights. In general, there will be a small amount of drift (bias) in the output of any process due to the sensors used in practical applications. So it is necessary to identify the process parameters under these small drifts as well along with the nominal condition.

In this chapter, FOPDT and SOPDT processes are identified. The process parameters are identified for nominal and during load disturbance condition. During the identification, the relay gain is approximated by DIDF. Required analytical expressions are derived to determine the unknown process parameters. The following processes are identified: Stable and unstable FOPDT processes, stable and unstable SOPDT processes, underdamped and critically damped processes. The limit cycle corrupted with noise is recovered using the wavelet transform. The DIDF approximation is applied to identify the dynamics of a DC-DC buck converter. The transfer function of the converter is obtained for nominal and during parameter variations. The performance of the identified model is verified with the closed loop response. A prototype of the converter model is developed for the real-time implementation of the identification method.

2.2 Relay Identification using DIDF method

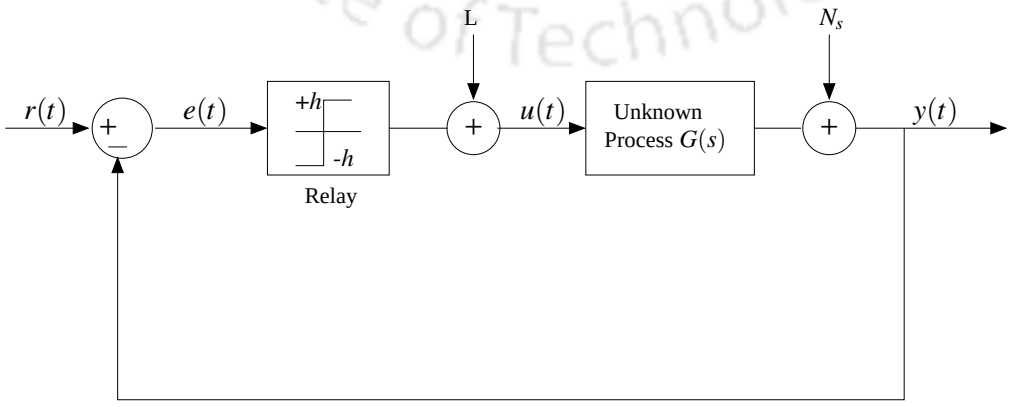

Figure 2.1: Off-line relay feedback scheme.

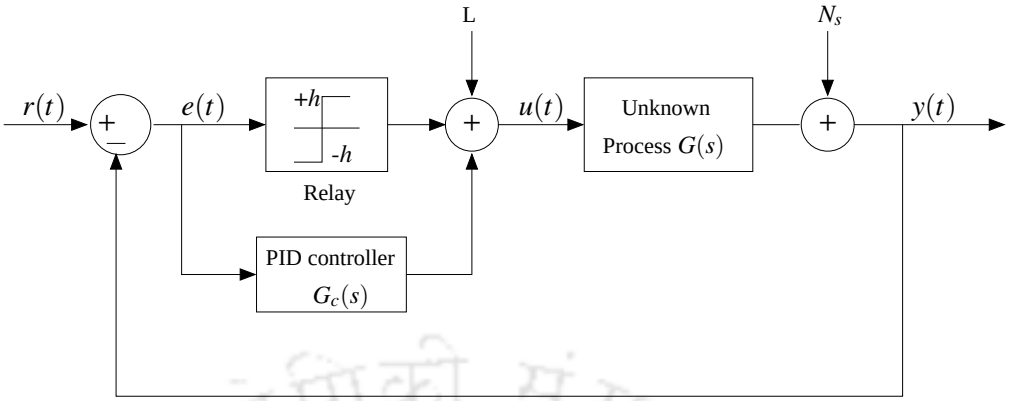

Figure 2.2: On-line relay feedback scheme.

In this section, identification of FOPDT and SOPDT processes using on-line and off-line method is presented. The off-line and on-line identification schemes are shown in Fig. 2.1 and Fig. 2.2, respectively. In the off-line scheme, only relay is connected with the feedback loop. Whereas in on-line identification both relay and controller are connected to the process. In both the identification schemes, $r(t)$ is reference input, $e(t)$ is input to relay, $u(t)$ is the input to process, $y(t)$ is the output of the process, L is load disturbance and N_s is noise at the process output. The controller present in the loop will induce a stabilized limit cycle during identification. An ideal symmetrical relay shown in Fig. 2.3 is used for the identification. The relay output switches to h or $-h$ at the zero crossing of the error. The limit cycle output

Figure 2.3: Ideal relay.

under ideal conditions with $r(t) = 0$ is shown in Fig. 2.4. The limit cycle is symmetric with respect to the reference value.

During disturbance condition, the limit cycle output becomes asymmetric. The shift in the limit cycle due to disturbance is shown in Fig. 2.5. The process parameters are identified

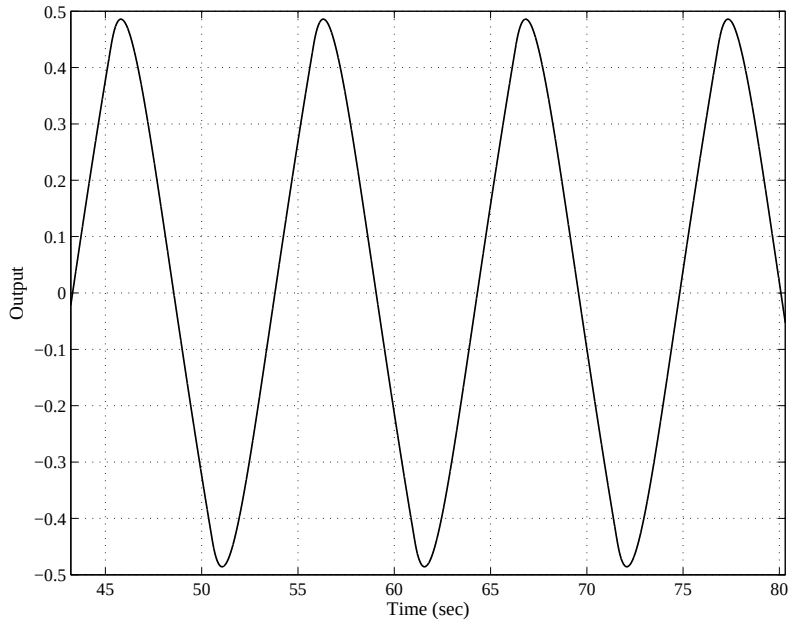

Figure 2.4: Limit cycle output under nominal conditions

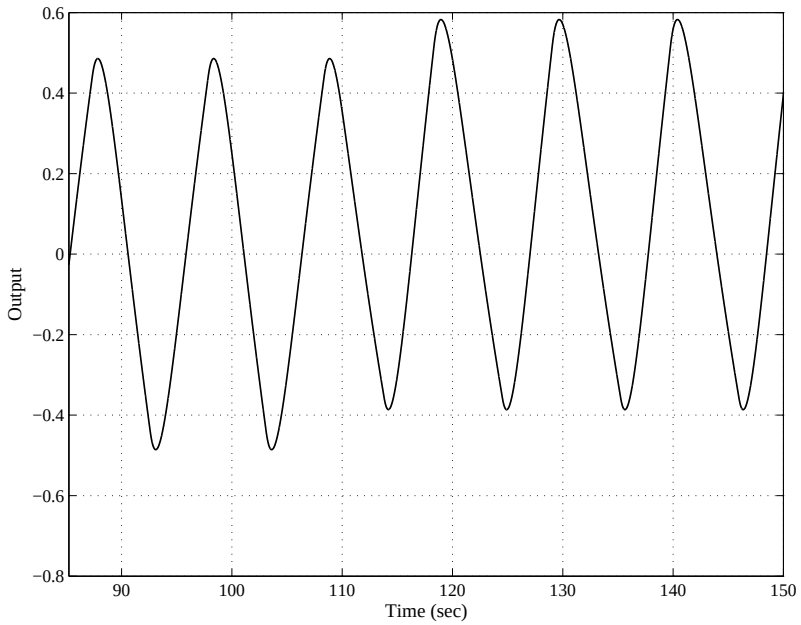

Figure 2.5: Limit cycle output during disturbance

under nominal and during load disturbance condition. The general limit cycle output with offset is considered to have a sinusoidal component and a bias component which is shown in Fig. 2.6. The expression for error signal is given in Eq. (2.1)

$$e(t) = \delta_0 + A_p \sin(\omega t) \tag{2.1}$$

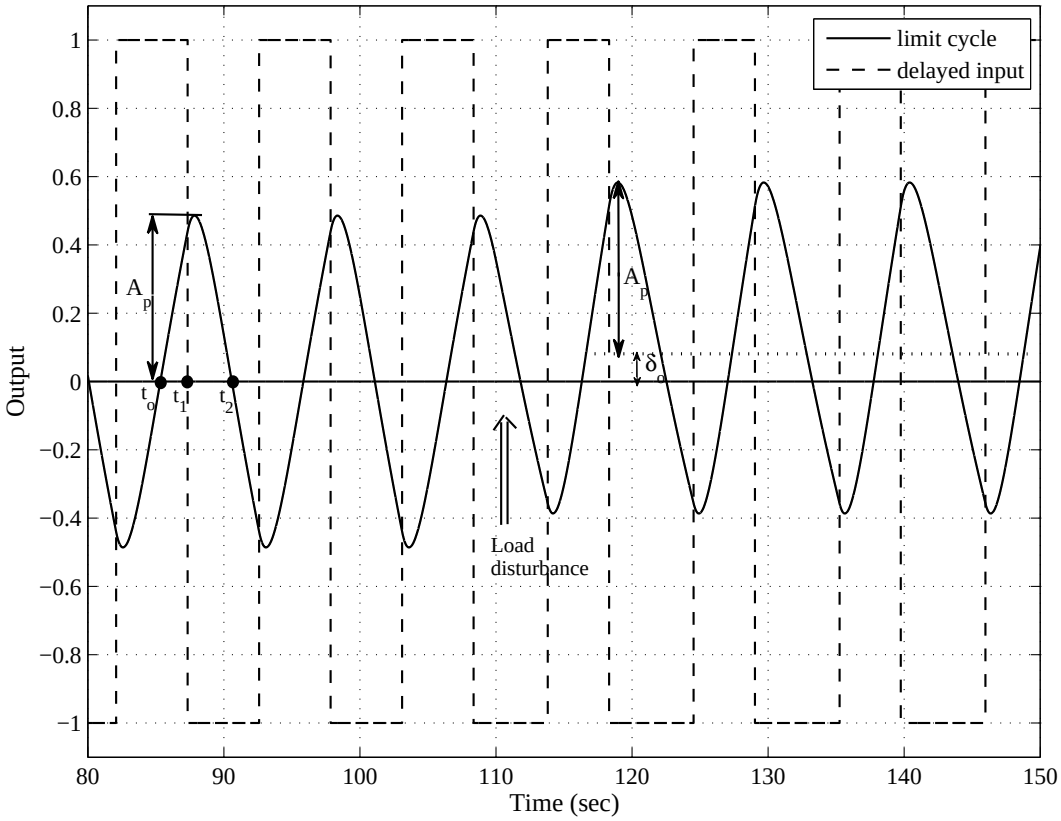

Figure 2.6: Limit cycle output measurements

where δ_0 is the bias in the limit cycle output. Under nominal conditions $\delta_0 = 0$.

The relay gain ($N(.)$) is approximated as dual input describing function [60].

$$N(.) = \frac{4h}{\pi A_p}\sqrt{1-\left(\frac{\delta_0}{A_p}\right)^2} \tag{2.2}$$

The sustained oscillatory output condition for on-line identification is given as

$$G_p(j\omega)[N(.)+G_c(j\omega)] = -1 \tag{2.3}$$

where $G_p(j\omega)$ and $G_c(j\omega)$ are the process and controller at the oscillatory frequency.

The form of the controller is chosen as

$$G_c(s) = K_P\left(1+\frac{1}{T_I s}+T_D s\right) \tag{2.4}$$

where K_P, T_I and T_D are the proportional gain, integral time constant and derivative time constant, respectively. The controller form can be expressed in the frequency domain by replacing s with $j\omega$. Therefore, (2.3) is written as

$$G_p(j\omega)\left[\frac{4h}{\pi A_p}\sqrt{1-\left(\frac{\delta_0}{A_p}\right)^2}+K_P\left(1+\frac{1}{j\omega T_I}+j\omega T_D\right)\right]=-1 \tag{2.5}$$

Rearranging the above equation results in

$$G_p(j\omega)\left[\frac{4h}{\pi A_p}\sqrt{1-\left(\frac{\delta_0}{A_p}\right)^2}+K_P+jK_P\left(T_D\omega-\frac{1}{\omega T_I}\right)\right]=-1 \tag{2.6}$$

The above expression is simplified as

$$G_p(j\omega)\,[u+jv]=-1 \tag{2.7}$$

where $u=\frac{4h}{\pi A_p}\sqrt{1-\left(\frac{\delta_0}{A_p}\right)^2}+K_P$ and $v=K_P\left(T_D\omega-\frac{1}{\omega T_I}\right)$. During the on-line relay feedback test the controller parameters are selected as K_P=0.01, $T_D=0.1$ and $T_I=\infty$.

In the off-line test, the controller ($G_c(s)$) is not present in the loop. Therefore, substituting K_P=0, $T_D=0$ and $T_I=\infty$ in (2.7) gives $u=\frac{4h}{\pi A_p}\sqrt{1-\left(\frac{\delta_0}{A_p}\right)^2}$ and $v=0$. The general expression for off-line can be obtained as

$$G_p(j\omega)\frac{4h}{\pi A_p}\sqrt{1-\left(\frac{\delta_0}{A_p}\right)^2}=-1 \tag{2.8}$$

Eqs. (2.7) and (2.8) are utilized for on-line and off-line identification of the process models. The required measurements for the limit cycle shown in Fig. 2.6 are A_p, δ_0, $T_p=t_2-t_o$ (half-period) and $\omega=\frac{T_p}{\pi}$. δ_0 is the average of the limit cycle for one period. Here, t_o and t_2 are zero-crossings of limit cycle output and t_1 is the zero crossing of delayed input.

2.3 Limit cycle corrupted with noise

Generally, in industries the process output is measured using sensors. These measuring devices cause noise during the measurement. Also sometimes noise is generated within the process. It becomes difficult to get the required data from the limit cycle corrupted by noise. Sensors devices will cause some drift in the process output. The wavelet transform is widely used in many applications to get good frequency resolution information of any noisy signal. This is mostly applied in electro-encephalogram (EEG) and image processing. During the identification process, wavelet transform can be applied to extract a de-noised signal. Discrete wavelet transform (DWT) is used for the analysis of noisy limit cycle. For computational efficiency, scaling and shifting are selected with the powers of 2.

The discrete parameter wavelet transform (DPWT) can be written as

$$DPWT(j,n) = \frac{1}{\sqrt{2^j}} \int y_n(t)\psi(2^{-j}t - n)dt \tag{2.9}$$

where $y_n(t)$ is the noisy signal.

To implement DPWT, Mallat [61] proposed a method to decompose the signal using low-pass and high-pass filters. The noisy signal $y_n(t)$ with sampling frequency f is decomposed into different frequency levels using low-pass (g(n)) and high-pass filters (h(n)). After decomposition of the signal $y(t)$ the frequencies are divided into various levels. An eight level decomposition is shown in Fig. 2.7. At each level the frequencies are divided into high frequency and low frequency components which are referred as detail (D_n) and approximation (A_n) coefficients, respectively. Initially, the corrupted signal is downsampled by 2 then the same procedure is opted in the successive levels. In the first level ($j = 1$), the frequency ranges of A_1 and D_1 are 0-$f/4$ and $f/4$-$f/2$, respectively. Similarly, at each level, the signal is downsampled by 2. The decomposition is performed until a noise-free signal is obtained. The required extracted signal lies in the approximation coefficients at the final level.

The advantage of wavelet decomposition is that it recovers the noisy signal precisely by per-

forming scaling and shifting. Selecting the required decomposition level, the high frequency components present in the noisy signal are eliminated. The important information of the limit cycle, such as peak amplitude and period of the signal is recovered with better accuracy.

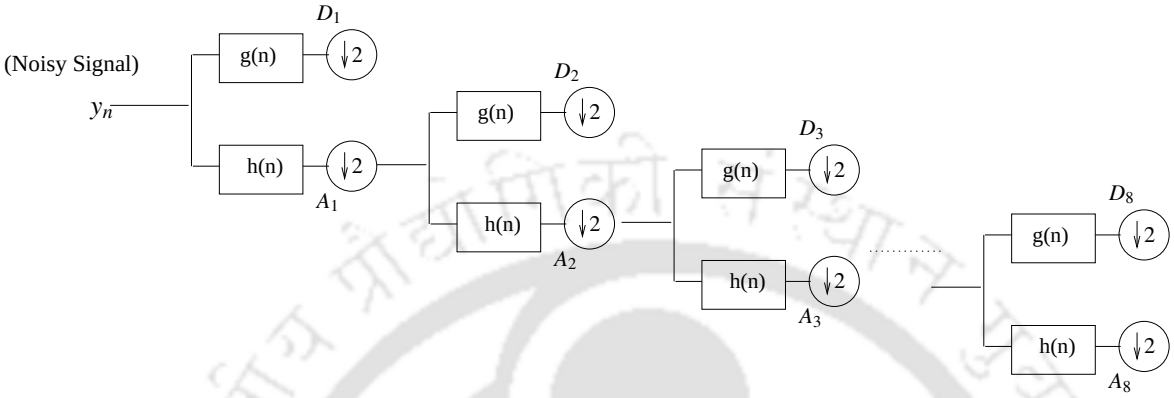

Figure 2.7: Wavelet Decomposition tree.

2.4 Identification of process models

2.4.1 FOPDT processes

The stable or unstable FOPDT process is considered as

$$G_p(s) = \frac{Ke^{-\theta s}}{\tau_1 s \pm 1} \tag{2.10}$$

The process transfer function in frequency domain is

$$G_p(j\omega) = \frac{Ke^{-j\omega\theta}}{j\omega\tau_1 \pm 1} \tag{2.11}$$

where the process parameters K, θ and τ_1 are the steady-state gain, time delay and process time constant, respectively. Using the limit cycle measurements in Fig. 2.6, the parameters θ and τ_1 are estimated. The expressions for the process parameters for on-line identification are obtained from (2.7) as

$$\frac{Ke^{-j\omega\theta}(u+jv)}{(j\omega\tau_1 \pm 1)} = -1 \tag{2.12}$$

Applying the magnitude condition to (2.12) results in

$$\frac{K\sqrt{u^2+v^2}}{\sqrt{((\omega\tau_1)^2+1)}} = 1 \tag{2.13}$$

By rearranging the above equation the expression for τ_1 for stable or unstable process is obtained as

$$\tau_1 = \frac{1}{\omega}\sqrt{K^2\sqrt{u^2+v^2}-1} \tag{2.14}$$

The phase angles for stable process can be written from Eq. (2.12) as

$$-\omega\theta + \tan^{-1}\left(\frac{v}{u}\right) - \tan^{-1}(\omega\tau_1) = -\pi \tag{2.15}$$

solving the above equation gives

$$\theta = \frac{1}{\omega}\left[\pi + \tan^{-1}\left(\frac{v-u\tau_1\omega}{u+v\tau_1\omega}\right)\right] \tag{2.16}$$

For unstable process

$$\theta = \frac{1}{\omega}\left[\tan^{-1}\left(\frac{v+u\tau_1\omega}{u-v\tau_1\omega}\right)\right] \tag{2.17}$$

The expressions for off-line identification can be obtained by replacing $u = \frac{4h}{\pi A_p}\sqrt{1-\left(\frac{\delta_0}{A_p}\right)^2}$ and $v = 0$ in (2.14), (2.16) and (2.17).

Two unknown process parameters can be estimated from the above equations. The other process parameter, K is assumed to be known a priori.

Example 1

Let us consider the following stable FOPDT process [11]

$$G(s) = \frac{e^{-2s}}{10s+1}$$

Initially, off-line test is performed by setting $h = 1$ to get the limit cycle output. The measurements of the limit cycle are $A_p = 0.1820$, $T_p = 3.680$ and $\delta_0 = 0$. The steady-state gain $K = 1$. The other parameters are obtained from the above expressions derived for off-line

identification as $\tau_1 = 8.1106$ and $\theta = 2.008$. The parameters are also identified for small step load disturbance of magnitude 0.1. The limit cycle measurements are $A_p = 0.1816$, $\delta_0 = 0.01816$ and the corresponding process parameters are $\tau_1 = 8.806$ and $\theta = 2.187$.

The on-line relay test is carried out with the initial controller settings. The limit cycle has $A_p = 0.1812$, $T_p = 3.670$, and $\delta_0 = 0$. Utilizing these measurements in (2.14) and (2.16) with $K = 1$ results in $\tau_1 = 8.137$, $\theta = 2.001$. The parameters for the load disturbance of 0.1 are $\tau_1 = 8.8195$ and $\theta = 2.177$. The identification results are also obtained in presence of measurement noise with SNR of 20dB for both on-line and off-line methods. Approximation coefficients during the extraction of the limit cycle with noise is shown in Fig. 2.8. The de-noised limit cycle output is obtained at 11^{th} level (a_{11}). The results of the identification tests are presented in Table 2.1. The limit cycle measurements and process parameters obtained for different SNR levels are shown in Table 2.2.

The accuracy of the identified model is obtained by calculating identification error (E_I) between the identified model ($G_p(s)$) and the actual model ($G(s)$) at the oscillatory frequency as

$$E_I = \int_0^{\omega_c} \left| \frac{G_p(j\omega) - G(j\omega)}{G_p(j\omega)} \right| d\omega \tag{2.18}$$

Table. 2.1: Identified process models for Example 1

Method	Process model	Error (E_I)
Off-line	$\frac{1.0e^{-2.008s}}{8.1106s+1}$	0.1429
Off-line with $L = 0.1$	$\frac{1.0e^{-2.187s}}{8.8063s+1}$	0.0891
On-line	$\frac{1.0e^{-2.001s}}{8.1372s+1}$	0.1417
On-line with $L = 0.1$	$\frac{1.0e^{-2.177s}}{8.8195s+1}$	0.0878
On-line with noise	$\frac{1.0e^{-2.006s}}{8.2202s+1}$	0.1347

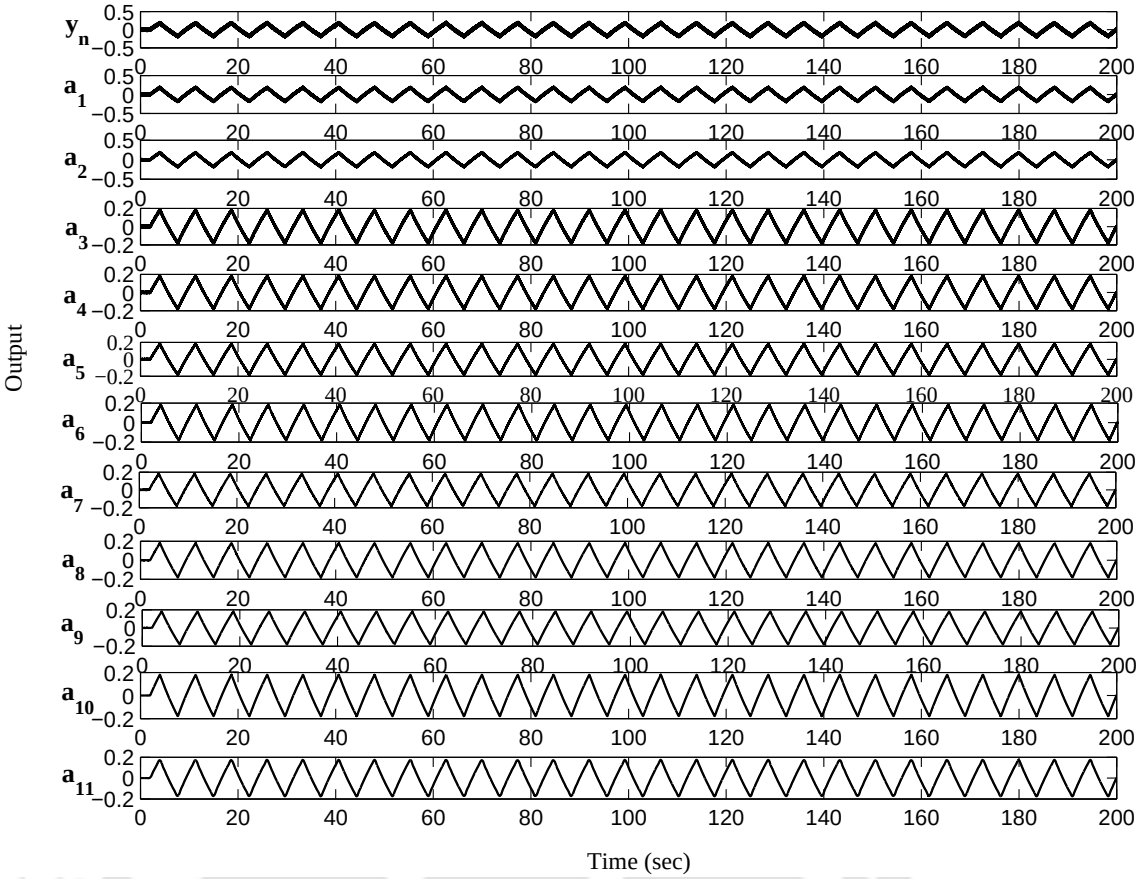

Figure 2.8: Approximation coefficients for Example 1

Table. 2.2: Limit cycle measurements of the extracted signal at different SNR levels for Example 1

Method	SNR (dB)	A_p	T_p	K	τ_1	θ
Off-line	10	0.179	3.65	1	8.1823	1.988
	15	0.178	3.68	1	8.2977	2.004
	20	0.178	3.68	1	8.2977	2.004
On-line	10	0.180	3.67	1	8.3072	2.039
	15	0.178	3.67	1	8.2863	1.998
	20	0.179	3.68	1	8.2202	2.006

2.4.2 SOPDT process model

The stable or unstable SOPDT process model is given as

$$G_p(s) = \frac{Ke^{-\theta s}}{(\tau_1 s \pm 1)(\tau_2 s + 1)} \tag{2.19}$$

where τ_1 and τ_2 are time constants, representing in frequency domain the model becomes

$$G_p(j\omega) = \frac{Ke^{-j\omega\theta}}{(j\omega\tau_1 \pm 1)(j\omega\tau_2 + 1)} \tag{2.20}$$

Utilizing the condition (2.7), the expression for on-line method is obtained by substituting (2.20) in (2.7) as

$$\frac{Ke^{-j\omega\theta}(u+jv)}{(j\omega\tau_1 \pm 1)(j\omega\tau_2 + 1)} = -1 \tag{2.21}$$

The magnitude condition for the above equation will be

$$\frac{K\sqrt{u^2+v^2}}{\sqrt{((\omega\tau_1)^2+1)((\omega\tau_2)^2+1)}} = 1 \tag{2.22}$$

Solving the equation further gives

$$\frac{K^2(u^2+v^2)-1}{\omega^2} = \tau_1^2 + \tau_2^2 + \tau_1^2\tau_2^2\omega^2 \tag{2.23}$$

$$\frac{K^2(u^2+v^2)-1}{\omega^2} = \tau_2^2(1+\tau_1^2\omega^2) + \tau_1^2 \tag{2.24}$$

Assuming $\tau_1^2\omega^2 >> 1$, the above equation becomes

$$\frac{K^2(u^2+v^2)-1}{\omega^2} = \tau_1^2(\tau_2^2\omega^2 + 1) \tag{2.25}$$

To simplify it further, it is assumed that $\tau_2^2\omega^2 << 1$ which gives τ_1 as

$$\tau_1 = \frac{\sqrt{K^2(u^2+v^2)-1}}{\omega} \tag{2.26}$$

According to Eq. (2.20) the phase angles for stable process will be

$$\tan^{-1}(\omega\tau_1) + \tan^{-1}(\omega\tau_2) = \pi - \omega\theta + \tan^{-1}\left(\frac{v}{u}\right) \tag{2.27}$$

for unstable process the phase angle equation is

$$\tan^{-1}(\omega\tau_1) - \tan^{-1}(\omega\tau_2) = \omega\theta - \tan^{-1}\left(\frac{v}{u}\right) \tag{2.28}$$

Therefore, using (2.27) and (2.28) the expression for τ_2 for the stable and unstable process is obtained as

$$\tau_2 = \frac{\tau_1 \omega \pm \tan(\Delta)}{\omega(\mp 1 + \omega \tan(\Delta))} \tag{2.29}$$

where $\Delta = \theta\omega - \tan^{-1}\left(\frac{v}{u}\right)$

Hence, the explicit expressions for τ_1 and τ_2 of the SOPDT model are obtained. θ is estimated from the limit cycle output shown in Fig. 2.6 as $\theta = t_2 - t_1$ and K is assumed to be known a priori.

Expressions for τ_1 and τ_2 for off-line identification can be obtained according to the conditions given in subsection 2.2.

Table. 2.3: Process models for Example 2

Method	Process model	Error (E_I)
Off-line	$\frac{e^{-1.998s}}{(10.827s+1)(0.983s+1)}$	0.040
Off-line with $L = 0.1$	$\frac{e^{-1.995s}}{(11.693s+1)(1.313s+1)}$	0.115
On-line	$\frac{e^{-2.003s}}{(10.833s+1)(0.976s+1)}$	0.039
On-line with noise	$\frac{e^{-2.008s}}{(10.898s+1)(0.975s+1)}$	0.043
Vivek & Chidambaram [62]	$\frac{1.03e^{-2.84s}}{(11.98s+1)}$	0.044

Example 2

The following stable SOPDT model is considered for the identification [11]

$$G(s) = \frac{e^{-2s}}{(10s+1)(s+1)}.$$

Relay feedback test is carried out with $h = 1$ to induce the limit cycle output. The off-line identification has the measurements $A_p = 0.1946$, $\delta_0 = 0$ and $T_p = 5.2598$. The steady-state gain is assumed to be $K = 1$ and $\theta = 1.998$. Substituting these in the analytical gives τ_1 and τ_2 as 10.827 and 0.983, respectively. During the on-line test with K_p =0.01, T_D = 0.1

and $T_I = \infty$ the limit cycle parameters are A_p=0.1948, $\delta = 0$, $T_p = 5.26$ and $\theta = 2.0$. Using the Eqs. (2.26) and (2.29) gives $\tau_1 = 10.833$ and $\tau_2 = 0.976$. The estimated process models are given in Table 2.3. The identified models are compared with the model obtained by

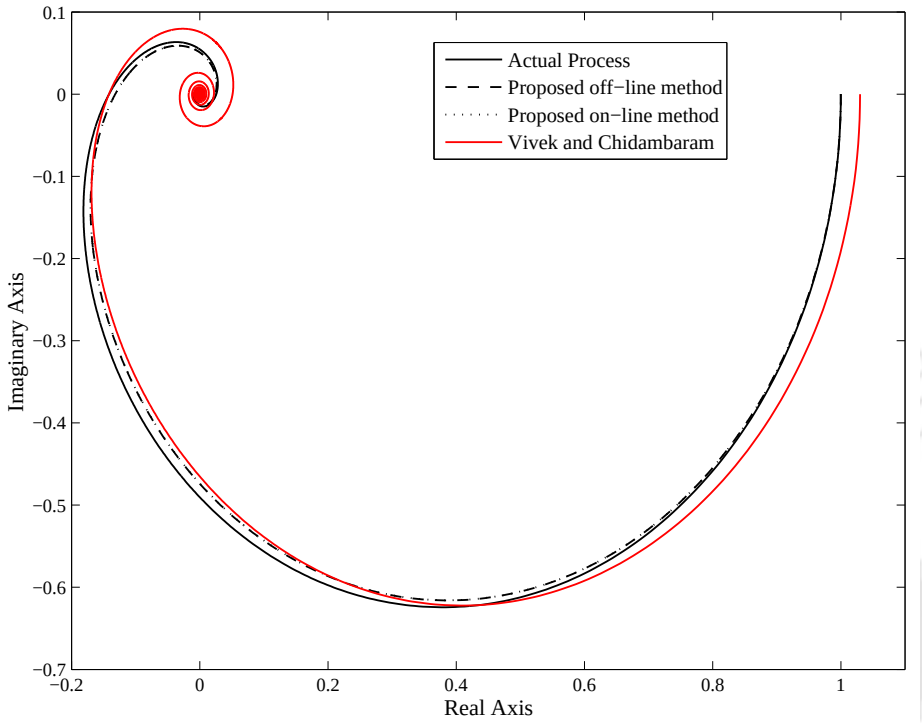

Figure 2.9: Nyquist plot Example 2

Table. 2.4: Limit cycle measurements of the extracted signal at different SNR levels for Example 2

Method	SNR (dB)	A_p	T_p	K	τ_1	τ_2	θ
Off-line	10	0.194	5.26	1	10.821	0.975	2.004
	15	0.194	5.26	1	10.861	0.987	1.994
	20	0.194	5.26	1	10.861	0.974	2.004
On-line	10	0.195	5.26	1	10.880	0.996	1.988
	15	0.195	5.24	1	10.836	0.981	1.988
	20	0.194	5.27	1	10.898	0.975	2.008

Vivek and Chidambaram [62] and the Nyquist plot in Fig. 2.9 shows that the identified model is near to the actual process. Process parameters for different noise levels are shown in Table 2.4. The measurements of the extracted limit cycle are close to the actual limit cycle measurements.

Example 3

An unstable SOPDT model is considered as [41]

$$G(s) = \frac{e^{-0.5s}}{(2s-1)(0.5s+1)}.$$

The off-line identification test with $h = 1$ gives $A_p = 0.4462$, $T_p = 2.77$, $\delta_0 = 0$, $\theta = 0.502$. The process parameters with steady state gain $K = 1$ are $\tau_1 = 2.356$ and $\tau_2 = 0.661$. During the on-line test the limit cycle output has $A_p = 0.4473$, $T_p = 2.75$, $\delta_0 = 0$ and $\theta = 0.496$. From the above equations derived for unstable process the process parameters are obtained as $K = 1$, $\tau_1 = 2.342$ and $\tau_2 = 0.661$. The parameters are obtained when the limit cycle is corrupted with a noise (SNR of 20dB). The recovered limit cycle output is shown in Fig. 2.10. Vivek and Chidambaram [41] identified the unstable model in FOPDT form and the identified models are given in Table 2.5. The variation in limit cycle measurements for different SNR levels are shown in Table 2.6.

Table. 2.5: Process models for Example 3

Method	Process model	Error (E_I)
Off-line	$\frac{e^{-0.502s}}{(2.356s-1)(0.661s+1)}$	0.1506
On-line	$\frac{e^{-0.496s}}{(2.342s-1)(0.661s+1)}$	0.148
Vivek & Chidambaram [41]	$\frac{0.753e^{-1.041s}}{(2.164s-1)}$	0.359

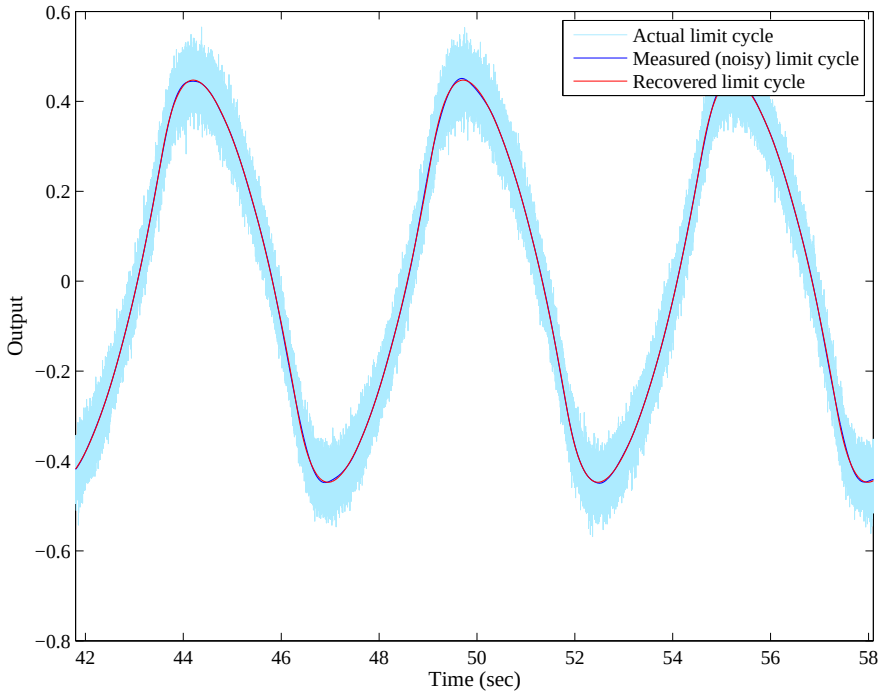

Figure 2.10: Nyquist plot Example 3

Table. 2.6: Limit cycle measurements of the extracted signal at different SNR levels for Example 3

Method	SNR (dB)	A_p	T_p	K	τ_1	τ_2	θ
Off-line	10	0.441	2.78	1	2.375	0.652	0.512
	15	0.444	2.77	1	2.368	0.663	0.502
	20	0.444	2.77	1	2.368	0.663	0.502
On-line	10	0.455	2.76	1	2.304	0.657	0.496
	15	0.451	2.76	1	2.325	0.661	0.496
	20	0.450	2.76	1	2.330	0.662	0.496

2.4.3 Critically damped process

An n^{th} order critically damped process is considered as

$$G_p(s) = \frac{Ke^{-\theta s}}{(\tau_1 s + 1)^n} \tag{2.30}$$

Expressing the above equation in the frequency domain as

$$G_p(j\omega) = \frac{Ke^{-\theta s}}{(j\omega\tau_1 + 1)^n} \tag{2.31}$$

Substituting (2.31) in (2.7) gives

$$\frac{Ke^{-\theta s}}{(j\omega\tau_1 + 1)^n}[u + jv] = -1 \tag{2.32}$$

The expressions for τ_1 and θ are obtained from the magnitude and the phase condition as

$$\tau_1 = \frac{1}{\omega}\sqrt{[K\sqrt{u^2+v^2}]^{\frac{2}{n}} - 1} \tag{2.33}$$

$$\theta = \frac{1}{\omega}\left[\pi - n\,\tan^{-1}(\tau_1\omega) + \tan^{-1}\left(\frac{v}{u}\right)\right] \tag{2.34}$$

The expressions for off-line identification can be obtained by substituting $K_p = 0$, $T_D = 0$ and $T_I = \infty$ in u and v expressions.

Table. 2.7: Process models for Example 4

Method	Process model	Error (E_I)
Off-line	$\frac{e^{-0.570s}}{(20.410s+1)^2}$	0.0177
On-line	$\frac{e^{-0.570s}}{(20.411s+1)^2}$	0.0178
On-line with $L = 0.1$	$\frac{e^{-0.632s}}{(22.511s+1)^2}$	0.0896
Vivek & Chidambaram [10]	$\frac{1.058e^{-0.548s}}{(20.818s+1)^2}$	0.0156

Example 4

An SOPDT critically damped system [10] is considered as

$$G(s) = \frac{e^{-0.5s}}{(20s+1)^2}.$$

The off-line relay test for the SOPDT system with $h = 1$ has the limit cycle parameters $A_p = 0.0176$ and $T_p = 7.6$. For the steady-state gain $K = 1$ the identified parameters are $\tau_1 = 20.410$ and $\theta = 0.570$. Using the initial PID controller settings, the on-line relay test

gives $A_p = 0.0176$ and $T_p = 7.6$. The process parameters are obtained as $K = 1$, $\tau_1 = 20.411$ and $\theta = 0.570$. For the same process, Vivek and Chidambaram [10] identified an SOPDT critically damped model. The identified models are tabulated in Table 2.7. The extracted limit cycle parameters during noise are given in Table 2.8.

Table. 2.8: Limit cycle measurements of the extracted signal at different SNR levels for Example 4

Method	SNR (dB)	A_p	T_p	K	τ_1	θ
Off-line	10	0.0177	7.6	1	20.346	0.572
	15	0.0176	7.6	1	20.387	0.571
	20	0.0176	7.6	1	20.387	0.571
On-line	10	0.0176	7.6	1	20.429	0.570
	15	0.0176	7.6	1	20.417	0.570
	20	0.0176	7.6	1	20.411	0.570

Example 5

The following higher order process is considered for identification [8]

$$G(s) = \frac{e^{-1.5s}}{(s+1)^5}.$$

Both off-line and on-line relay tests are performed to identify the higher order process. The models are identified with the same order as that of the actual process. This will give better identification accuracy. Huang et al. [8] identified an SOPDT model for the same higher order critically damped process. The obtained models are given in Table 2.9. Nyquist plot of the models given in Fig. 2.11 reveals that the identified models are near to the actual process. Using the proposed method the model is also estimated during noise for an SNR of 10dB, 15dB and 20dB and during small load disturbance and the results are given in Table 2.10.

Table. 2.9: Process models for Example 5

Method	Process model	Error (E_I)
Off-line	$\frac{e^{-1.513s}}{(0.969s+1)^5}$	0.0176
Off-line with $L = 0.1$	$\frac{e^{-1.598s}}{(1.015s+1)^5}$	0.0213
On-line	$\frac{e^{-1.512s}}{(0.970s+1)^5}$	0.0173
On-line with $L = 0.1$	$\frac{e^{-1.608s}}{(1.013s+1)^5}$	0.0212
Huang et al. [8]	$\frac{1.01e^{-2.91s}}{(4.162s^2+3.418s+1)}$	0.0173

Table. 2.10: Process models at different SNR levels for Example 5

Method	SNR(dB)	L	Process model	Error (E_I)
Off-line	10	0	$\frac{e^{-1.515s}}{(0.969s+1)^5}$	0.0175
	15	0	$\frac{e^{-1.507s}}{(0.971s+1)^5}$	0.0172
	20	0	$\frac{e^{-1.518s}}{(0.968s+1)^5}$	0.0176
	10	0.1	$\frac{e^{-1.628s}}{(1.030s+1)^5}$	0.0327
On-line	10	0	$\frac{e^{-1.505s}}{(0.972s+1)^5}$	0.0171
	15	0	$\frac{e^{-1.508s}}{(0.971s+1)^5}$	0.0172
	20	0	$\frac{e^{-1.514s}}{(0.969s+1)^5}$	0.0174
	10	0.1	$\frac{e^{-1.596s}}{(1.016s+1)^5}$	0.0214

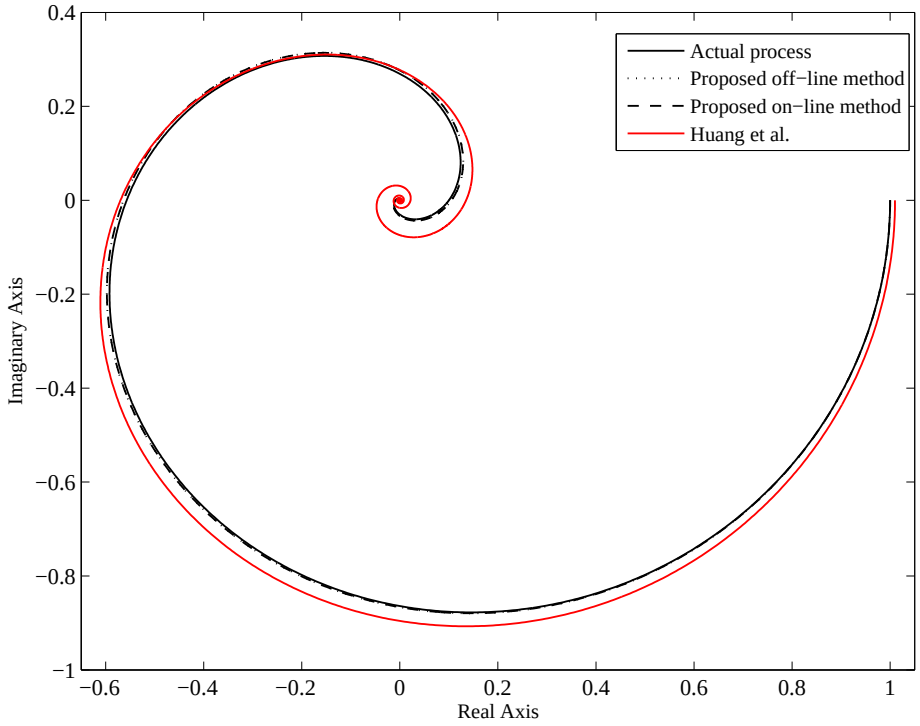

Figure 2.11: Nyquist plot Example 5

2.4.4 Underdamped SOPDT process

An underdamped SOPDT process is considered as

$$G_p(s) = \frac{Ke^{-\theta s}}{a_1 s^2 + a_2 s + 1} \tag{2.35}$$

In the frequency domain, the above equation is represented as

$$G_p(j\omega) = \frac{Ke^{-j\omega\theta}}{-\omega^2 a_1 + j\omega a_2 + 1} \tag{2.36}$$

Substituting (2.36) in (2.7) the characteristic equation becomes

$$\frac{Ke^{-j\omega\theta}\,[u + jv]}{-a_1\omega^2 + ja_2\omega + 1} = -1 \tag{2.37}$$

Applying magnitude condition we get

$$\frac{K\sqrt{u^2+v^2}}{\sqrt{(1-a_1\omega^2)^2 + (a_2\omega)^2}} = 1 \tag{2.38}$$

$$K^2(u^2+v^2) = (1-a_1\omega^2)^2 + (a_2\omega)^2 = 1 \tag{2.39}$$

The phase angle equation for (2.37) is

$$-\theta\omega+\tan^{-1}\left(\frac{v}{u}\right)-\tan^{-1}\left(\frac{a_2\omega}{1-a_1\omega^2}\right)=-\pi \tag{2.40}$$

The above equation is rearranged as

$$-\tan^{-1}\left(\frac{v}{u}\right)-\tan^{-1}\left(\frac{a_2\omega}{a_1\omega^2-1}\right)=\pi-\theta\omega \tag{2.41}$$

$$a_1\omega^2-1=a_2\omega\left[\frac{u\cos(\theta\omega)+v\sin(\theta\omega)}{u\sin(\theta\omega)-v\cos(\theta\omega)}\right] \tag{2.42}$$

Substituting (2.39) in (2.42) we obtain a_2 as

$$a_2=\frac{1}{\omega}K(u\sin(\theta\omega)-v\cos(\theta\omega)) \tag{2.43}$$

Substituting (2.43) in (2.42)

$$a_1=\frac{1}{\omega^2}K\left(1+u\cos(\theta\omega)+v\sin(\theta\omega)\right) \tag{2.44}$$

For off-line identification the analytical expressions for a_2 and a_1 are obtained by substituting $u=\frac{4h}{\pi A_p}\sqrt{1-\left(\frac{\delta_0}{A_p}\right)^2}$ and $v=0$ as

$$a_2=\frac{\sin(\theta\omega)}{\omega}\left(\frac{4hK}{\pi A_p}\sqrt{1-\left(\frac{\delta_0}{A_p}\right)^2}\right) \tag{2.45}$$

$$a_1=\frac{1}{\omega^2}K\left[1+\frac{4h}{\pi A_p}\sqrt{1-\left(\frac{\delta_0}{A_p}\right)^2}\cos(\theta\omega)\right] \tag{2.46}$$

The unknown process parameters a_1 and a_2 are estimated from (2.43) and (2.44), respectively. Time delay θ is estimated from Fig. 2.6. The steady state value K is obtained from step test by setting the reference value $r(t)$ greater than h ($r(t)>h$) and the ratio of steady state output to reference input gives K.

Example 6

The following underdamped process is considered to identify using the proposed identification method.

$$G(s)=\frac{e^{-s}}{(9s^2+2.4s+1)}.$$

The limit cycle parameters for the off-line relay test are $A_p = 0.525$, $T_p = 5.44$ and $\theta = 0.99$. The value of K is 1. Substituting the measured values in (2.43) and (2.44) gives a_1 and a_2 as 9.143 and 2.270, respectively. The identified process parameters during on-line test are $K = 1$, $\theta = 0.99$, $a_1 = 9.152$ and $a_2 = 2.271$. The obtained models are given in Table 2.11. The limit cycle measurements and identified parameters for different SNR levels are given in Table 2.12.

Table. 2.11: Process models for Example 6

Method	Process model	Error (E_I)
Off-line	$\frac{e^{-0.99s}}{9.143s^2+2.270s+1}$	0.0201
On-line	$\frac{e^{-0.99s}}{9.152s^2+2.271s+1}$	0.0202
On-line with $L = 0.1$	$\frac{e^{-s}}{10.402s^2+2.303s+1}$	0.0673

Table. 2.12: Limit cycle measurements of the extracted signal at different SNR levels for Example 6

Method	SNR (dB)	A_p	T_p	K	a_1	a_2	θ
Off-line	10	0.5262	5.44	1	9.103	2.267	0.99
	15	0.5254	5.46	1	9.141	2.312	1.01
	20	0.5249	5.44	1	9.118	2.272	0.99
On-line	10	0.5272	5.45	1	9.130	2.292	1
	15	0.5265	5.46	1	9.178	2.295	1
	20	0.5275	5.44	1	9.111	2.270	0.99

2.4.5 Identification of DC-DC buck converter

DC-DC converters are widely used in many applications, such as battery charging, photovoltaic systems, DC motor drive systems, portable electronic devices, etc. [63–66]. The performance of these applications depends on the operation of DC-DC converters. Usually, state-space averaged model is used to study and analyze the converter's performance where the open loop transfer function obtained is for a particular operating point. This neglects some of the relatively small dynamics of the actual model [67]. So the performance of the averaged model may be inaccurate for different operating conditions. Also, the dynamics of the converter do not remain same all the times, it may change with components aging, temperature, loading effect and operating conditions. This will cause a change in the dynamic model of the converter and in turn affects the closed-loop performance. To overcome this, actual dynamics of the converter need to be obtained with less computational effort. Non-parametric identification using cross correlation method and Fourier analysis is applied to identify DC-DC converters [68, 69]. These types of methods need large data for the analysis. Therefore, half limit data obtained from relay test is used in the proposed state-space method to identify the converter model.In the mathematical formulation, specified ratings of the components are considered. The exact values of the components with tolerance are generally not considered. Also during formulation, the effect of additional circuit elements, such as driver and sensor are not considered. In the relay test, the effect of additional circuits, tolerance of components and delay involved in the data processing will be reflected in the limit cycle output. Therefore, the dynamics of the entire circuit can be obtained from limit cycle.

The proposed off-line identification using DIDF approximation is applied on DC-DC buck converter shown in Fig. 2.12. The limit cycle output of the relay feedback test is used to identify the dynamic model converter. Parameter variations may disturb the symmetric limit cycle output. Therefore, the relay approximated by DIDF can be used to identify converter model during normal conditions and during parameter perturbations as well. Hence, the converter transfer function is also identified under parameter variations. Identification is done

by simulation and on real-time experiment and the performance of the identified model is validated with the closed-loop response.

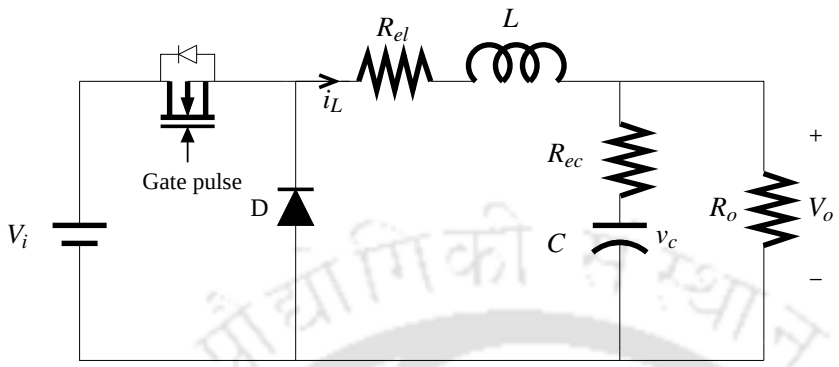

Figure 2.12: Equivalent circuit of a non-ideal buck converter.

The first step in the identification procedure using the relay is to generate sustained oscillatory output. To achieve this, the system output should be forced to intersect the negative real axis of the Nyquist curve. The system with time delay will pass through the negative real axis, as shown in Fig. 2.13. The DC-DC buck converter output is forced to oscillate by adding a delay. The delay in practical circuits is due to the circuit elements, drivers, and the data processing involved in controllers.

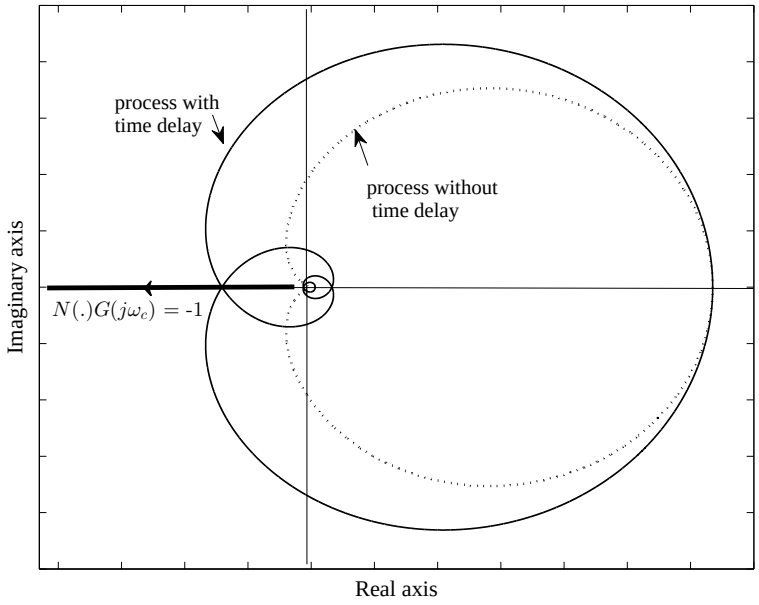

Figure 2.13: Nyquist curves

Remark: A system with time delay or a non-minimum phase system will intersect the negative real axis of a Nyquist curve. Hence, it is possible to obtain the limit cycle output from these types of systems. The DC-DC buck converter is considered to be minimum phase system i.e., there are no right half plane (RHP) zeros [25]. Therefore, a delay is added into the system. Both delay and relay heights are selected in such a way that there exists sustained limit cycle oscillations. In such case, the selection of these values are very sensitive. There is no exact method to choose the delay. However, to be realistic the delay is chosen to be 10% to 20% of the system time constant.

2.4.6 Transfer function model using the state-space average method

The buck-type DC-DC converter power stage circuit is shown in Fig. 2.12. The parasitic resistances of the capacitor and the inductor are included in the design. State-space averaging method is most commonly used for the design and analysis of converters [70, 71]. The state-space representation of the dynamic variables using the averaging method is given in the equation below:

$$\begin{bmatrix} \frac{di_L}{dt} \\ \frac{dv_c}{dt} \end{bmatrix} = \begin{bmatrix} \frac{-(R_{el}+R_{ec}R_{eq})}{L} & \frac{-R_{eq}}{L} \\ \frac{1}{C}[1-\frac{R_{ec}R_{eq}}{R_o}] & \frac{-R_{eq}}{R_oC} \end{bmatrix} \begin{bmatrix} i_L \\ v_c \end{bmatrix} \tag{2.47}$$

where $R_{eq} = \frac{R_o}{R_o+R_{ec}}$, i_L and v_c are current through inductor and voltage across the capacitor, respectively. The representation in (2.47) is utilized to find the output to control transfer function. Considering the perturbation in the duty cycle $\hat{d}(t) = d(t) - D$, the overall transfer function is given as [72, 73] (Detailed derivation is given in A.1)

$$\frac{\hat{v}_o}{\hat{d}} = \frac{R_{eq}R_o(R_{ec}Cs+1)V_{in}}{(((R_{ec}Cs+1)R_{eq}+Cs(Ls+R_{el}))R_o+R_{eq}(Ls+R_{el}))} \tag{2.48}$$

According to the design specifications (given in Appendix Table A.1), the transfer function in (2.48) will be

$$\frac{\hat{v}_o}{\hat{d}} = \frac{7.8(0.294\times10^{-5}s+1)}{5.4586\times10^{-8}s^2+0.7009\times10^{-4}s+1} \tag{2.49}$$

The above equation can be represented as

$$\frac{\hat{v}_o}{\hat{d}} = \frac{K(\theta s+1)}{a_1 s^2 + a_2 s + 1} \tag{2.50}$$

where, $K = 7.8$, $\theta = 0.294 \times 10^{-5}$, $a_1 = 5.4586 \times 10^{-8}$ and $a_2 = 0.7009 \times 10^{-4}$. The dynamics obtained with the state-space averaging method in (2.49) are compared with the relay based identification method.

2.4.7 Relay feedback test to identify DC-DC buck converter Model

The proposed relay feedback test is conducted on DC-DC buck converter and is shown in Fig. 2.14. To generate a sustained oscillatory output, a delay is added to the converter. Simulations are performed in MATLAB/Simulink and the same is verified experimentally. The design specifications of the converter are given in Appendix A.1 (Table A.1). Furthermore, the identification is carried out under parameter variations. The converter transfer func-

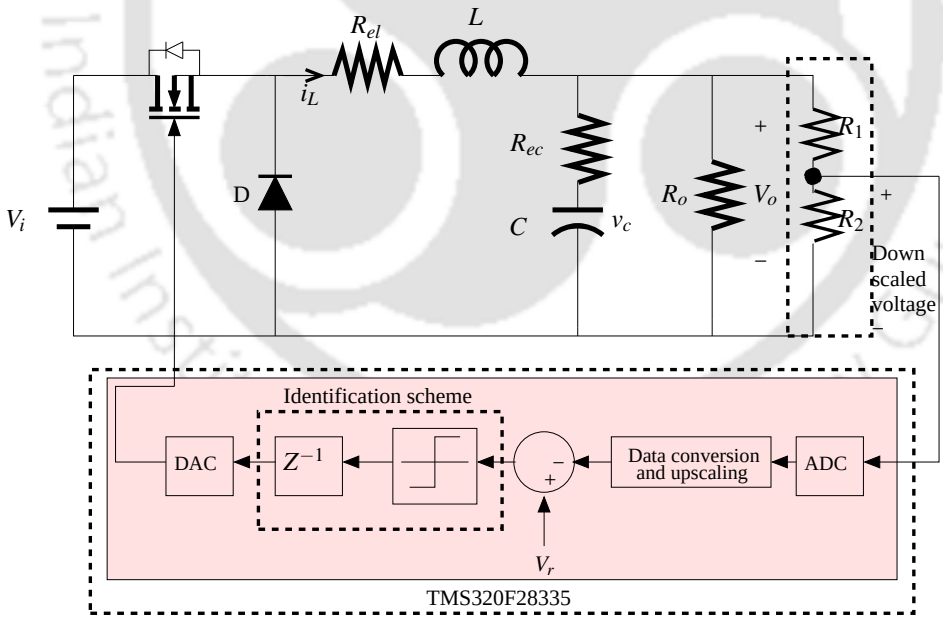

Figure 2.14: Implementation of identification test with relay.

tion obtained from averaging method (2.49) has underdamped characteristics. Therefore, the form of the converter model is considered as SOPDT underdamped model given in Eq. (2.35). As the identification is carried out in off-line, the explicit expressions for unknown process parameters a_1 and a_2 are obtained from (2.46) and (2.45), respectively. Steady state

gain K is determined from the ratio of steady state values of output and input. To get these values, a high value of $r(t)$ is set which is more than h, i.e. $(r(t) >> h)$.

During nominal conditions:

In this case, it is assumed that the converter is operating under normal conditions without any change in the design parameters.

During parameters perturbation:

Here, the parameter variations in terms of load resistance, capacitance, and input voltage are considered for the converter operating under nominal conditions.

In normal condition, the input voltage to the converter is 8 V, the load is 10 Ω, and the reference input $(r(t))$ is set to 4.5 V. The limit cycle measurements are made with respect to the reference value $(r(t))$. From both simulation and experiment, it is observed that a delay of 200 μsec and relay height of $h = 0.8$ induce limit cycle output. The required data is extracted from limit cycle output and is utilized for the identification of DC-DC buck converter.

Simulation:

The limit cycle output during nominal condition is shown in Fig. 2.15. The limit cycle oscillates with respect to the reference value. The measured values are $A_p = 1.1375$ V, $\delta_0 = 0.268$, $T_p = 0.0004$ sec, and $\theta = 200$ μsec. The system's steady state gain is 7.125 and the remaining parameters are obtained as $a_1 = 6.70718 \times 10^{-8}$ and $a_2 = 0.0009233$. The transfer function with the relay feedback method is given in the equation below:

$$G_{\hat{v}\hat{d}} = \frac{7.125e^{-2\times10^{-4}s}}{6.70718 \times 10^{-8}s^2 + 0.000923s + 1} \tag{2.51}$$

The parameters of the converter may vary depending on operating conditions. It is obvious that with the change in any of the circuit parameters, the transfer function of the system

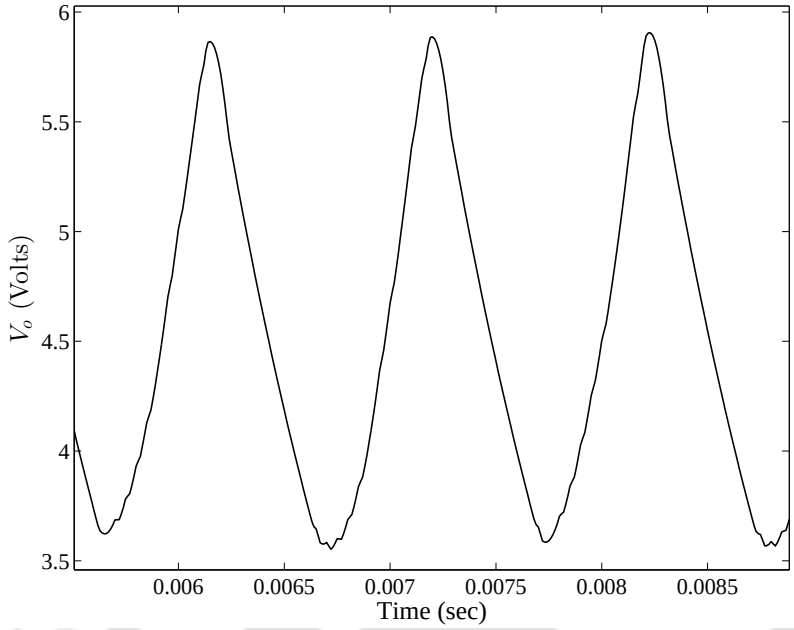

Figure 2.15: Limit cycle output from the simulation

changes. In general, the capacitance of a buck converter may decrease with time due to ageing effect. This will cause a slight change in the system transfer function. In the present work, identification is carried out with a 20% reduction in capacitance. The system parameters are obtained as $K = 7$, $\theta = 200\ \mu sec$, $a_1 = 3.4309 \times 10^{-8}$ and $a_2 = 0.0007296$. There are slight variations in the parameters K, a_1 and a_2 compared with that of nominal values.

Table. 2.13: Identified Parameters with simulation under different conditions

Cases	K	θ	a_1	a_2
Nominal	7.125	2×10^{-4}	6.7071×10^{-8}	0.000923
20% change in C 98 μF to 77 μF	7	2×10^{-4}	3.4309×10^{-8}	0.000729
change in R_L 10 Ω to 15 Ω (50%)	7.125	2×10^{-4}	1.6211×10^{-8}	0.000771
change in V_{in} 8 V to 7.5 V (6%)	6.875	2×10^{-4}	1.6211×10^{-8}	0.000885

Similarly, the parameters during the load variation from 10 Ω to 15 Ω and input voltage from 8 V to 7.5 V are tabulated in Table 2.13. According to the design specifications, it is observed that during the identification test the limit cycle exists for the variation in V_i up to 12%. Owing to this, the dynamics are shown only for 6% variation in V_i. There are differ-

ences in the dynamics during the perturbation of C, R_L and V_i. The changes are due to the variation in peak value and bias of the limit cycle. The simulation results have revealed that there is an increase in the value of a_2 compared with the state-space averaged model.

Experimental evaluation:

The obtained simulation results are verified with the experimental setup. The DC-DC buck converter is designed according to the specifications given in Table A.1. The relay is implemented on Texas Instrument DSP board TMS320F28335 [74], IRF740 MOSFET (V_{DS}=400 V and $R_{DS(on)}$=0.55 Ω) is used as a switch and IR2110 (I_O=2 A and V_{OUT}= 10-20 V) is used in the driver circuit to drive the MOSFET. The experimental setup is shown in Fig. 2.16, YOKOGAWA oscilloscope is used to monitor the output. The sensor voltage is passed through a 12-bit ADC module on the DSP board. The ePMW module generates gating signal which is fed to MOSFET through the driver circuit. The switching frequency of 20 kHz is obtained as $f_s = \dfrac{f_{p\_clk}}{2 \times TBPRD}$ by setting $TBPRD$ count as 3750 with the processor clock frequency (f_{p_clk}) 150 MHz.

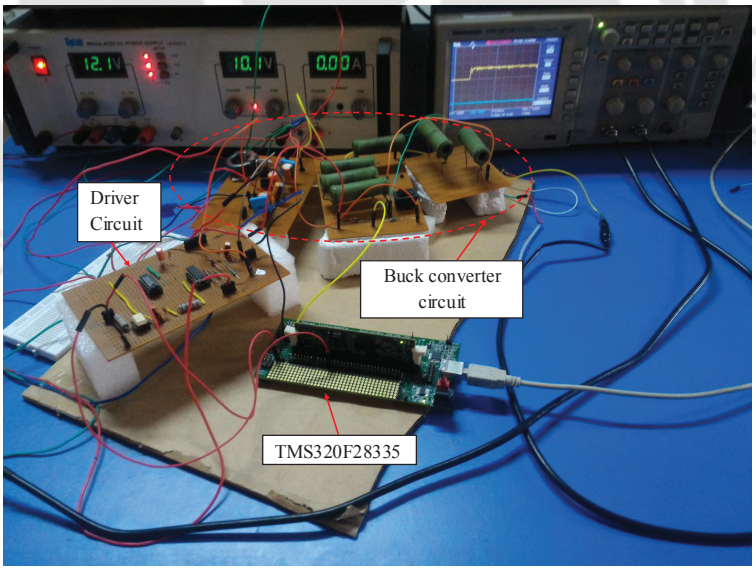

Figure 2.16: DC-DC buck converter experimental prototype

For the sake of comparison, similar settings of h and θ are chosen during simulation and experimental evaluation. When the circuit is operating under nominal conditions, symmetric limit cycle is produced and is shown in Fig. 2.17. The measurements of limit cycle are

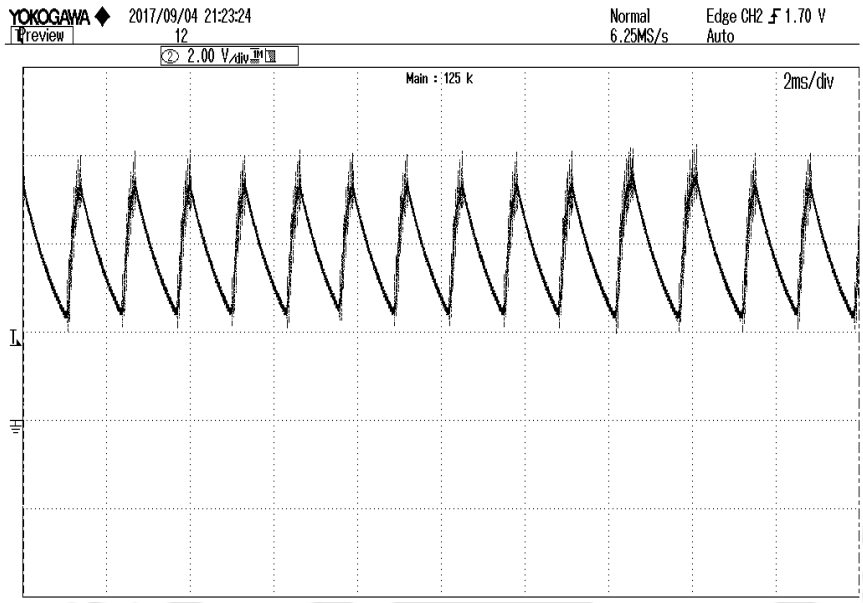

Figure 2.17: Limit cycle output Under nominal conditions

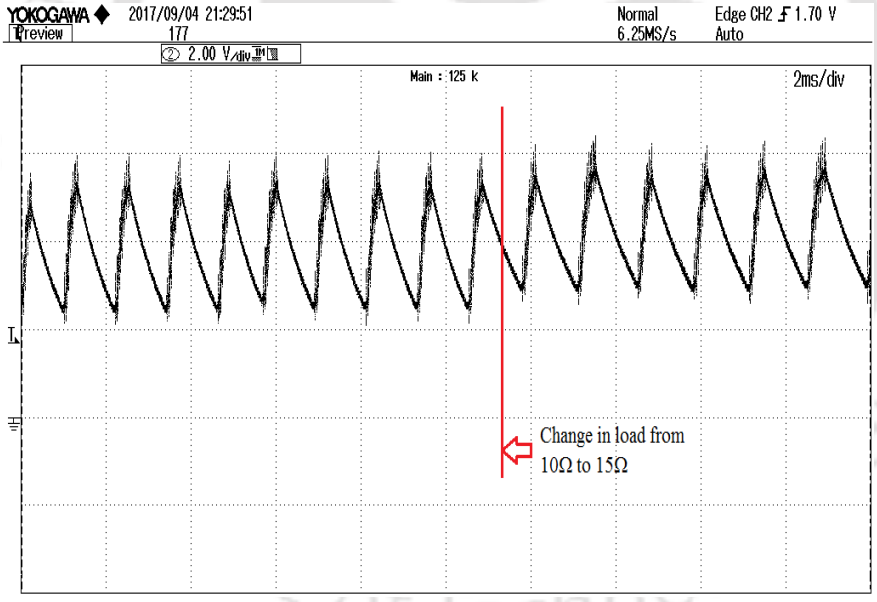

Figure 2.18: Limit cycle output during load change from 10 Ω to 15 Ω

seen to be A_p = 1.4005 V, $\delta_0 = 0.332$, T_p = 0.00059 *sec*, and θ = 223.2 μsec. The resultant parameters are a_1 = 9.4309 $\times 10^{-8}$ and a_2 = 0.000726 and the transfer function is given in (2.52).

$$G_{\hat{vd}} = \frac{6.35e^{-2.232\times10^{-4}s}}{9.4309\times10^{-8}s^2 + 0.000726s + 1} \tag{2.52}$$

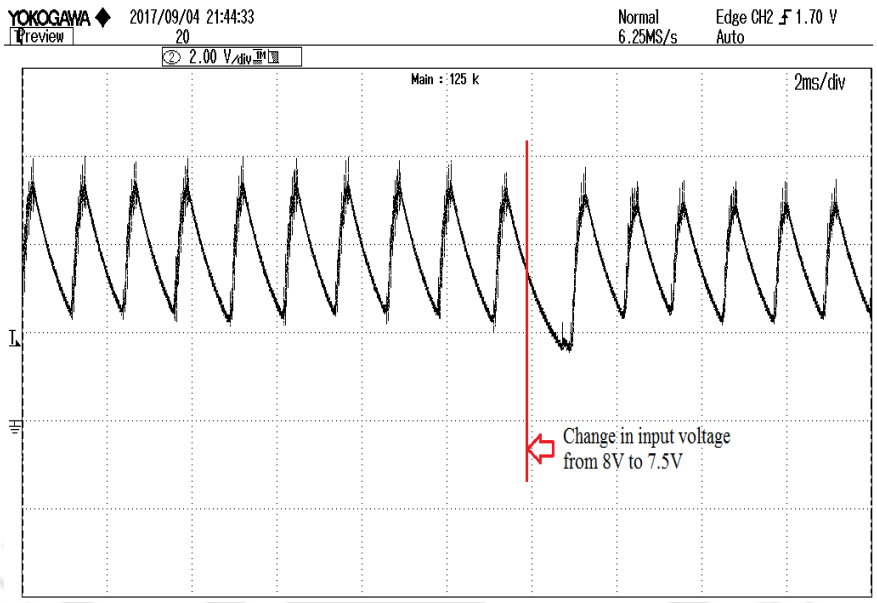

Figure 2.19: Limit cycle output during change in input voltage from 8 V to 7.5 V

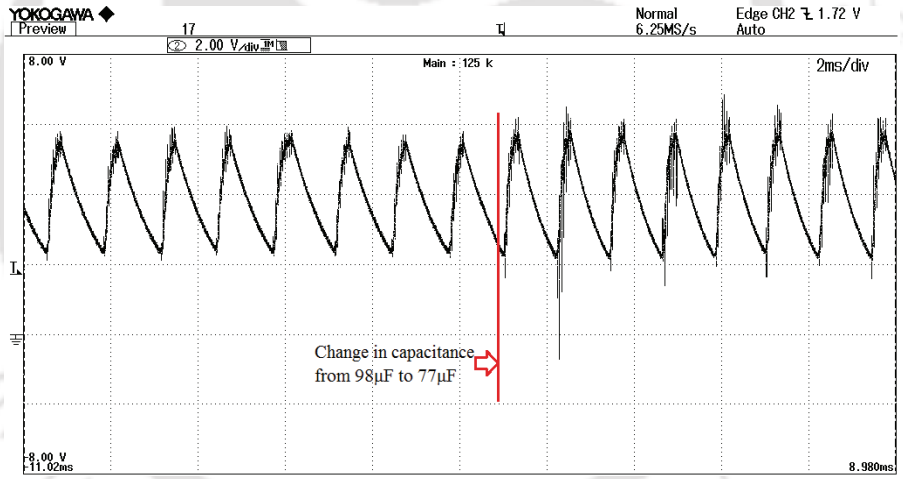

Figure 2.20: Limit cycle output during change in capacitance 98 μF to 77 μF

Experimental results during the change in load, input voltage and change in capacitance are shown in Fig. 2.18, Fig. 2.19 and Fig. 2.20, respectively. During the perturbations, limit cycle stabilizes after one or two cycles. This allows us to identify the dynamics in presence of parameter variations. System parameters during different variations are given in Table 2.14.

The results are nearly close to the simulation for all the cases. As a_2 corresponds to the coefficient of "s" this relates to the damping of the system. Any change in this value affects

Table. 2.14: Identified Parameters with experimental evaluation under different conditions

Cases	K	θ	a_1	a_2
Nominal	6.35	2.232×10^{-4}	9.4309×10^{-8}	0.000726
20% change in C 98 μF to 77 μF	6.625	2.126×10^{-4}	5.8053×10^{-8}	0.000628
change in R_L 10 Ω to 15 Ω (50%)	6.625	2.501×10^{-4}	8.4819×10^{-8}	0.000946
change in V_{in} 8 V to 7.5 V (6%)	6.075	2.789×10^{-4}	1.0325×10^{-8}	0.000513

the peak and time constant of the closed loop response. The state-space averaging method has less damping coefficient compared to that obtained from relay feedback method (both simulation and experiment). As the same dynamics are used for the controller design. There will be an effect on the closed loop response of the system with the difference in dynamics. The important data obtained from the process in the form of limit cycle output gives accurate information about the process dynamics. The accuracy of the method is seen in above examples. In the next section, the effectiveness of the identified model is validated.

Model validation test:

The identified buck converter model is verified from the closed-loop response. After performing the identification test, PID controller is connected in place of relay to validate the identified model. During the model validation test, input voltage is set to 18 V and reference voltage at 12 V. Controller parameters are tuned using the characteristic equation below:

$$1+G_p(s)G_c(s)=0 \tag{2.53}$$

where $G_p(s)$ is the identified model ($G_{\hat{v}\hat{d}}$) in simulation Eq. (2.51)/experiment Eq. (2.52)
For state-space averaging method (2.50) can be used as $G(s)$ and for the proposed SOPDT model (2.35) is used, here $e^{-\theta s}$ is represented as $(1-\theta s)$ then by substituting $G_c(s)$ the characteristic becomes

$$\frac{(a_1T_I\pm\theta T_IT_DKK_P)}{KK_P}s^3+\frac{(a_2T_I+KK_P(\pm\theta T_I+T_IT_D))}{KK_P}s^2+\frac{(T_I+KK_P(T_I\pm\theta))}{KK_P}s+1=0 \tag{2.54}$$

Here, the term with $+\theta$ corresponds to state-space averaging method and $-\theta$ to the identified SOPDT model. PID controller is designed considering that the phase margin of the system to be 50^o. According to the desired phase margin specification the equation for state-space averaging method is considered to be

$$3.250966980 \times 10^{-12}s^3 + 3.630401663 \times 10^{-8}s^2 + 0.0004485000003s + 1 = 0 \tag{2.55}$$

Substituting K, θ, a_1 and a_2 obtained from (2.49) in (2.54) and comparing it with (2.55). The controller parameters for state-space averaging method are obtained as $K_P = 0.85803$, $T_I = 0.00038$ and $T_D = 0.000080$. Similarly, for the identified SOPDT model the desired equations for simulation and experimental are given in the below expressions:

$$1.9593469 \times 10^{-11}s^3 + 2.180363 \times 10^{-7}s^2 + 0.000808s + 1 = 0 \tag{2.56}$$

$$1.4313506 \times 10^{-11}s^3 + 1.768555 \times 10^{-7}s^2 + 0.000728s + 1 = 0 \tag{2.57}$$

The controller parameters obtained for the identified simulation SOPDT model are $K_P = 0.2584$, $T_I = 0.000653$ and $T_D = 0.000032$ and for experimental model $K_P = 0.2960$, $T_I = 0.000621$ and $T_D = 0.000121$.

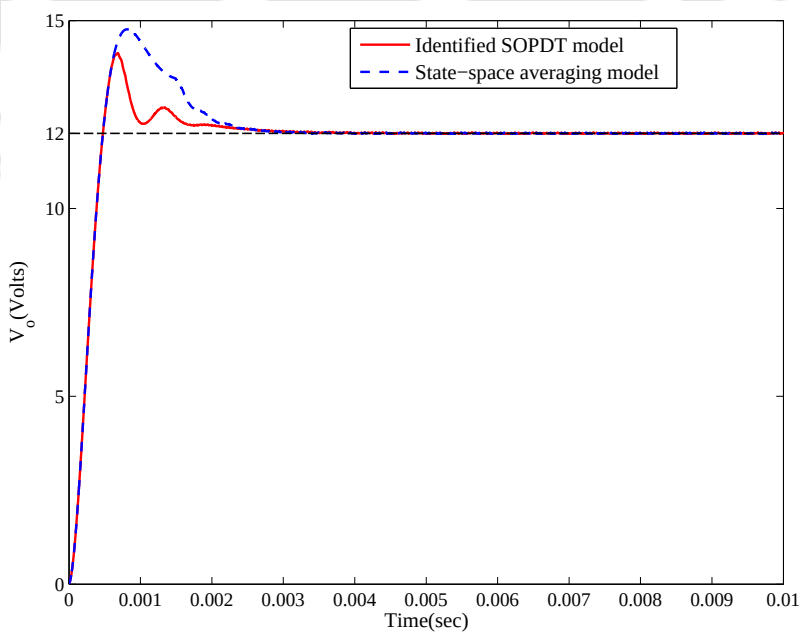

Figure 2.21: Comparison of closed-loop responses obtained from simulation

The closed-loop response obtained from simulation reveals that there is less peak overshoot in the control response during the transient condition for the identified model compared with the state-space averaging model, as shown in Fig. 2.21. The controller designed using identified model is able to track the reference value effectively.

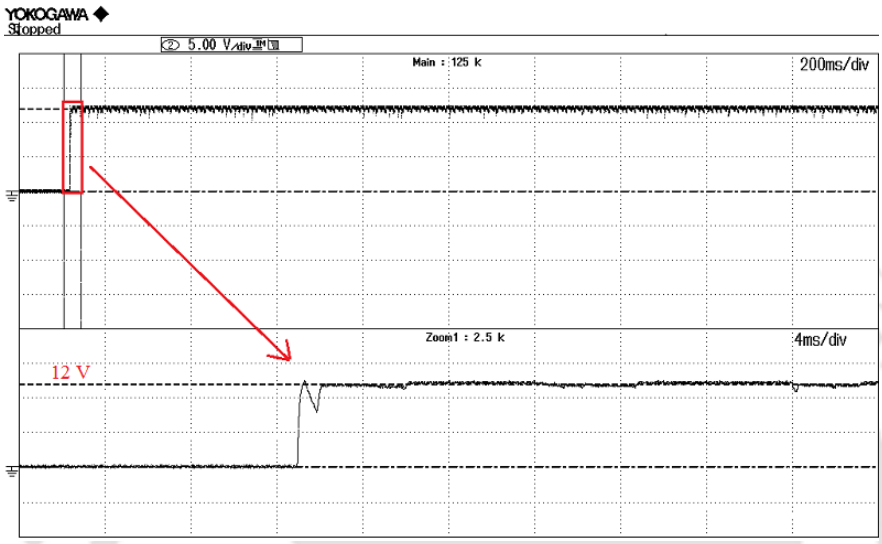

Figure 2.22: Closed-loop responses (V_o) obtained from experiment for state-space averaging model

Figure 2.23: Closed-loop responses (V_o) obtained from experiment for identified SOPDT model

The experimental results of averaging model and identified SOPDT model are given in Figs. 2.22 and 2.23, respectively. The comparison of the closed-loop responses are given in Fig.

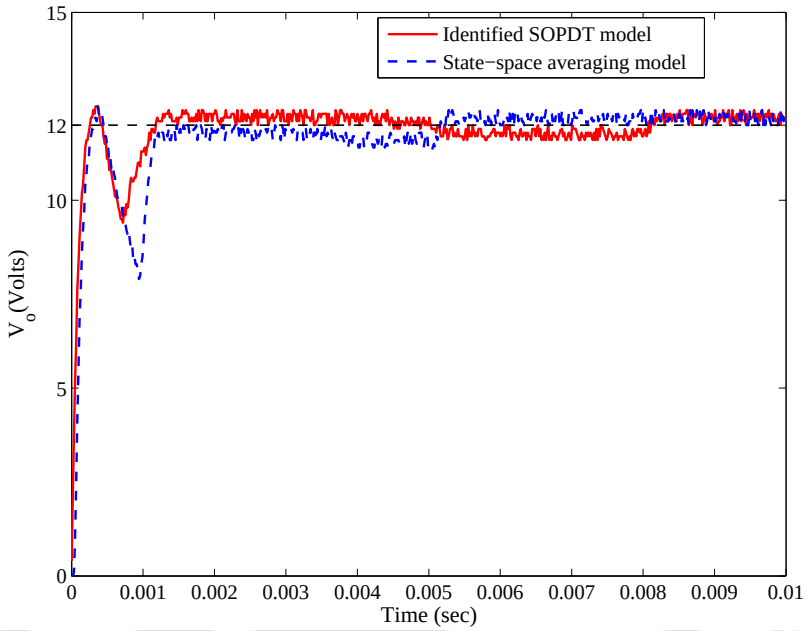

Figure 2.24: Comparison of closed-loop responses obtained from experiment

2.24. From the response, it can be observed that the identified SOPDT model suits the DC-DC buck converter. During starting both the responses have similar overshoot whereas the identified SOPDT model has less undershoot. Using relay identification, real dynamics of the converter are identified which further resulted in better response. The settling time is same for both the models which are seen in simulation as well. If there is a degradation in the performance of the converter over the time due to parametric changes, model identification using relay can be carried out to identify the converter dynamics. Using the identified model, controller can be designed. The model validation test proves that the identified model can be used for the analysis of the buck converter. The identification test gives the exact information of the converter in the from of limit cycle with which it is possible to estimate the real dynamics of the converter.

2.5 Summary

Process models are obtained from off-line and on-line relay feedback test. DIDF approximation is effectively used to estimate the process models during nominal and during load

disturbance condition. Analytical expressions for unknown process parameters of various process models are derived. These expressions require relay response information. Limit cycle output with noise is recovered using wavelet transform. Standard examples available in the literature are considered for the identification using the proposed method. The identification method is utilized to identify the DC-DC buck converter model. The performance of the identified converter model is observed from the closed-loop response. The results indicate that the obtained model works well and it can be used for the analysis of the converter.

भारतीय प्रौद्योगिकी संस्थान गुवाहाटी
Indian Institute of Technology Guwahati

भारतीय प्रौद्योगिकी संस्थान गुवाहाटी
Indian Institute of Technology Guwahati

CHAPTER 3

STATE-SPACE APPROACH FOR THE IDENTIFICATION OF FOPDT AND SOPDT PROCESSES

3.1 Introduction

Estimation of accurate process dynamics is important during control design. Irrespective of the control technique one should extract the process model which is close to the actual process. The DIDF method seen in previous Chapter 2 gives an approximate model. In the DF method the relay is approximated by a gain which is used by many authors [6–8, 15]. Many researchers have extended the relay method to get more accurate parameters. Exact expressions in the time domain are derived by Wang et al. [22] to get the process parameters for the FOPDT process. Using the information of asymmetrical limit cycles, Kaya and Atherton [27] derived expressions to identify FOPDT and SOPDT process models. Srinivasan and Chidambaram used an asymmetrical relay to estimate all the unknown parameters of SOPDT model. To obtain better parametric process models Lee and Sung [33] used integrals of the relay response to reduce the effect of higher harmonic terms. As the fundamental term becomes more dominant it will improve the accuracy of the parameter estimates. Using the relay feedback responses, Panda and Yu [30] derived time domain expressions to identify different processes. Using linear regression equations, Fedele [75] identified FOPDT pro-

cess. The area of the steady-state output is used to estimate the parameters. However, this is used for only stable lower order modeling. Panda et al. [32] developed mathematical models for integrating processes utilizing the expressions obtained from relay feedback response. Majhi and Atherton [23, 25] used the state-space approach which requires limit cycle conditions to derive the expressions for modeling FOPDT and SOPDT processes. The method can be further extended to identify process models.

In this chapter, the state-space method is used to identify the FOPDT, SOPDT and underdamped SOPDT process models. General time-domain solution is derived which can be used to identify the above mentioned processes with few modifications. The effectiveness of the method is evaluated in simulation and in real-time on the DC-DC buck converter. The noisy limit cycle is recovered using wavelet transform as given in Chapter 2. The process models are also estimated during the low-load disturbance.

3.2 Identification Structure

The off-line identification scheme shown in Fig. 2.1 is used to identify the process models. The relay feedback response is utilized to extract the parameters of the process. The necessary measurements to be made on the limit cycle are shown in Fig. 3.1.

Here, t_o and t_2 are zero crossings of the limit cycle, t_p is the time at which peak amplitude of the limit cycle occurs and t_1 is the zero crossing of the delayed relay output.

3.3 Mathematical modeling

In this section, mathematical modeling of the process models is carried out. State-space approach is used to derive the analytical expressions. The standard state-space equation is represented as

$$\dot{\mathbf{x}}(t) = \mathbf{A}\mathbf{x}(t) + \mathbf{b}u(t-\theta) \tag{3.1}$$

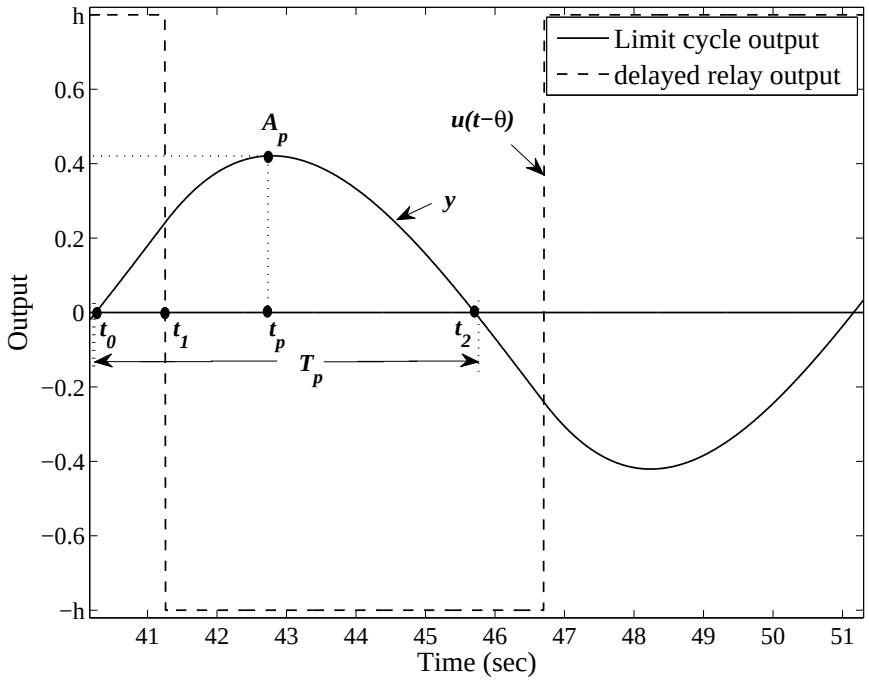

Figure 3.1: Limit cycle output and delayed input

$$y(t) = \mathbf{c}\mathbf{x}(t) \tag{3.2}$$

where $\mathbf{A}$, $\mathbf{b}$ and $\mathbf{c}$ are matrices with dimension 2×2, 2×1 and 1×2, respectively. During the relay test, it is assumed that the relay feedback response is symmetrical with half period T_p as shown in Fig. 3.1 with initial condition $\mathbf{x}(t_0)$. During the identification test the relay switches from $+h$ to $-h$ at t_0, the delayed relay output shown in Fig. 3.1 has two piecewise constant signals for positive and negative limit cycle output. Therefore, the solution for (3.1) for the time range $t_0 \le t \le t_1$ with $u(t-\theta) = h$ becomes

$$x(t) = \mathbf{e}^{\mathbf{A}(t-t_0)}\mathbf{x}(t_0) + \mathbf{A}^{-1}(\mathbf{e}^{\mathbf{A}(t-t_0)} - \mathbf{I})\mathbf{b}h \tag{3.3}$$

where $\mathbf{I}$ is the identity matrix with dimension 2×2. The solution for the time range $t_1 < t \le t_2$ is

$$x(t) = \mathbf{e}^{\mathbf{A}(t-t_1)}\mathbf{x}(t_1) - \mathbf{A}^{-1}(\mathbf{e}^{\mathbf{A}(t-t_1)} - \mathbf{I})\mathbf{b}h \tag{3.4}$$

Substituting t_2 in (3.4) gives

$$x(t_2) = \mathbf{e}^{\mathbf{A}(t_2-t_1)}\mathbf{x}(t_1) - \mathbf{A}^{-1}(\mathbf{e}^{\mathbf{A}(t_2-t_1)} - \mathbf{I})\mathbf{b}h \tag{3.5}$$

Substituting t_1 in (3.3) becomes

$$x(t_1) = \mathbf{e}^{\mathbf{A}(t_1-t_0)}\mathbf{x}(t_0) + \mathbf{A}^{-1}(\mathbf{e}^{\mathbf{A}(t_1-t_0)} - \mathbf{I})\mathbf{b}h \tag{3.6}$$

Utilizing the Eq. (3.6) in (3.5)

$$x(t_2) = \mathbf{e}^{\mathbf{A}(t_2-t_0)}\mathbf{x}(t_0) + \mathbf{A}^{-1}(\mathbf{e}^{\mathbf{A}(t_2-t_0)} - 2\mathbf{e}^{\mathbf{A}(t_2-t_1)} - \mathbf{I})\mathbf{b}h \tag{3.7}$$

The symmetric limit cycle follows $x(t_2) = -x(t_o)$. Therefore, we get

$$\mathbf{x}(t_o) = (\mathbf{I} + \mathbf{e}^{\mathbf{A}(t_2-t_0)})^{-1}\mathbf{A}^{-1}(2\mathbf{e}^{\mathbf{A}(t_2-t_1)} - \mathbf{e}^{\mathbf{A}(t_2-t_0)} - \mathbf{I})\mathbf{b}h \tag{3.8}$$

The output equation $y(t)$ for time range $t_0 \leq t \leq t_1$ is

$$y(t) = \mathbf{c}\mathbf{e}^{\mathbf{A}(t-t_0)}\mathbf{x}(t_0) + \mathbf{c}\mathbf{A}^{-1}(\mathbf{e}^{\mathbf{A}(t-t_0)} - \mathbf{I})\mathbf{b}h \tag{3.9}$$

and $y(t)$ for time range $t_1 < t \leq t_2$

$$y(t) = \mathbf{c}\mathbf{e}^{\mathbf{A}(t-t_1)}\mathbf{x}(t_1) - \mathbf{c}\mathbf{A}^{-1}(\mathbf{e}^{\mathbf{A}(t-t_1)} - \mathbf{I})\mathbf{b}h \tag{3.10}$$

Substituting (3.8) in (3.6) and utilizing the resultant equation in (3.10) will give the expression for $y(t)$. From Fig. 3.1, $t_2 - t_0 = T_p$ and $\theta = t_1 - t_0$ which reduces to

$$y(t) = \mathbf{c}\mathbf{A}^{-1}\mathbf{b}h - 2\mathbf{c}\mathbf{e}^{\mathbf{A}(t-t_1)}\mathbf{A}^{-1}(\mathbf{I} + \mathbf{e}^{\mathbf{A}T_p})^{-1}\mathbf{b}h \tag{3.11}$$

3.4 Identification of Process Models

3.4.1 SOPDT Process

The stable or unstable SOPDT process is given as

$$G_p(s) = \frac{Ke^{-\theta s}}{(\tau_1 s \pm 1)(\tau_2 s + 1)} \tag{3.12}$$

where K is steady-state gain, θ is time delay, τ_1 and τ_2 are time constants of SOPDT process. In the analysis, for unstable process it is assumed that $\tau_1 > \tau_2$. For ease in solving, Eq. (3.12)

is represented as

$$G_p(s) = \frac{K\lambda_1\lambda_2 e^{-\theta s}}{(s \mp \lambda_1)(s-\lambda_2)} \tag{3.13}$$

where $\lambda_1 = \frac{-1}{\tau_1}$ and $\lambda_2 = \frac{-1}{\tau_2}$, representing (3.13) in state-space from one obtains

$$\dot{\mathbf{x}}(t) = \begin{bmatrix} \pm\lambda_1 & 0 \\ 0 & \lambda_2 \end{bmatrix} \begin{bmatrix} x_1(t) \\ x_2(t) \end{bmatrix} + \begin{bmatrix} \pm a \\ \mp a \end{bmatrix} u(t-\theta) \tag{3.14}$$

$$y(t) = \begin{bmatrix} 1 & 1 \end{bmatrix} \mathbf{x}(t) \tag{3.15}$$

(In Appendix A.2, detailed derivation of (3.14) and (3.15) is given)

From the standard state-space representation (3.1) the matrices are given as

$$\mathbf{A} = \begin{bmatrix} \pm\lambda_1 & 0 \\ 0 & \lambda_2 \end{bmatrix}; \mathbf{b} = \begin{bmatrix} \pm a \\ \mp a \end{bmatrix}; \mathbf{c} = \begin{bmatrix} 1 & 1 \end{bmatrix} \tag{3.16}$$

where

$$a = \frac{K\lambda_1\lambda_2}{(\lambda_1 \mp \lambda_2)} \tag{3.17}$$

Stable process

To derive the expressions for the stable SOPDT process, the matrices in (3.16) are substituted in (3.11) gives the equation as

$$y(t) = \frac{Kh\lambda_1\lambda_2}{\lambda_1-\lambda_2}\left[\frac{1}{\lambda_1} - \frac{1}{\lambda_2} - \frac{2e^{\lambda_1(t-t_1)}}{\lambda_1(1+e^{\lambda_1 T_p})} + \frac{2e^{\lambda_2(t-t_1)}}{\lambda_2(1+e^{\lambda_2 T_p})}\right] \tag{3.18}$$

From the peak amplitude condition i.e., at $t = t_p$, $\dot{y}(t_p) = 0$ gives

$$e^{\lambda_2(t_p-t_1)} = \frac{(1+e^{\lambda_2 T_p})e^{\lambda_1(t_p-t_1)}}{(1+e^{\lambda_1 T_p})} \tag{3.19}$$

Substituting (3.19) in (3.18) at $t = t_p$, $y(t_p) = A_p$ which becomes

$$\chi = \frac{e^{\lambda_1(t_p-t_1)}}{1+e^{\lambda_1 T_p}} \tag{3.20}$$

where $\chi = \frac{1}{2}\left[\frac{A_p}{Kh} + 1\right]$

Using Taylor series, the exponential terms in (3.20) are approximated up to the 5^{th} order then by solving the equation, the value of λ_2 can be obtained.

The other parameter λ_1 is determined by applying second derivative to Eq. (3.18)

$$\ddot{y}(t) = \frac{Kh\lambda_1\lambda_2}{\lambda_1 - \lambda_2}\left[-\frac{2\lambda_1 e^{\lambda_1(t-t_1)}}{(1+e^{\lambda_1 T_p})} + \frac{2\lambda_2 e^{\lambda_2(t-t_1)}}{(1+e^{\lambda_2 T_p})}\right] \tag{3.21}$$

By substituting (3.19) in (3.21) at $t = t_p$ and simplifying the equation gives λ_1 as

$$\lambda_2 = \frac{-\ddot{y}(t_p)}{2\chi Kh\lambda_1} \tag{3.22}$$

The two equations (3.22) and (3.20) are used to get τ_1 and τ_2. Time delay is measured from limit cycle output as $\theta = t_1 - t_0$ and steady-state gain is assumed to be known.

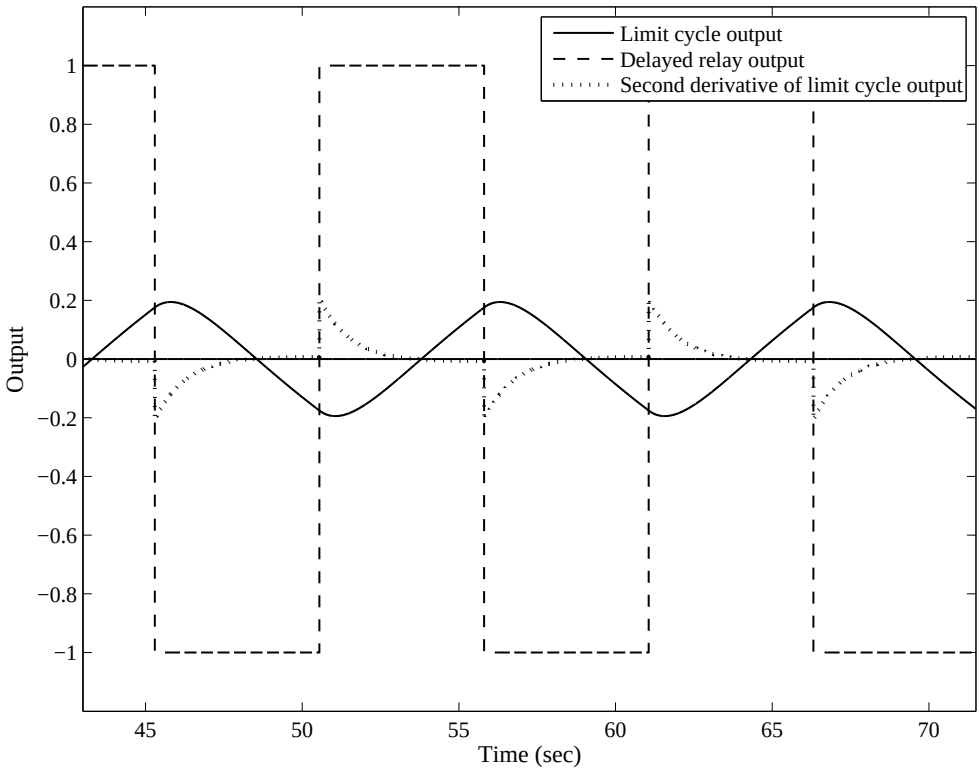

Figure 3.2: Limit cycle response and delayed relay output of Example 1

Example 1

A stable SOPDT process [11] is considered as

$$G(s) = \frac{e^{-2s}}{(10s+1)(s+1)}.$$

The relay test with setting $h = 1$ gives a limit cycle output. The measurements of the limit cycle output shown in Fig. 3.2 are $t_0 = 0$, $t_1 = 1.999$, $t_p = 2.5131$, $t_2 = 5.26$, $A_p = 0.1946$ and $\ddot{y}(t_p) = -0.12$. The value of θ is 1.999 and K is assumed to be 1. Using (3.20) and (3.22) the other two process parameters τ_1 and τ_2 are obtained as 0.9985 and 9.9700, respectively. The proposed model has an identification error (E_I) of 0.00178. Liu et al. [34] identified an SOPDT for the same process and Vivek and Chidambaram [62] identified an FOPDT model, the results are shown in Table 3.1. The identified model has better identification accuracy. Using the proposed method, process model is also obtained during small load disturbance. Nyquist plot is drawn for the identified models and is shown in Fig. 3.3. The plot shows that the identified model is close to actual process compared with the other process models. The extracted limit cycle output measurements using wavelet transform for different SNR levels are shown in Table 3.2. It is observed that the second derivative of the peak output ($\ddot{y}(t_p)$) of the recovered limit cycle has some error. This will affect the estimation of τ_2.

Table. 3.1: Identified Process models for Example 1

Method	Process model	Error (E_I)
Proposed	$\frac{e^{-1.999s}}{(9.9700s+1)(0.9985s+1)}$	0.0017
Proposed with $L = 0.1$	$\frac{e^{-2.002s}}{(9.5238s+1)(1.1355s+1)}$	0.0140
Liu et al. [34]	$\frac{1.0122e^{-2.0037s}}{(10.1178s+1)(0.992s+1)}$	0.0029
Vivek and Chidambaram [62]	$\frac{1.03e^{-2.84s}}{(11.98s+1)}$	0.0442

Table. 3.2: Limit cycle measurements of the extracted signal at different SNR levels for Example 1

SNR (dB)	A_p	$\ddot{y}(t_p)$	t_p	T_p	K	τ_1	τ_2	θ
10	0.1944	-0.145	2.49	5.25	1	10.121	0.891	2
15	0.1948	-0.155	2.49	5.26	1	10.131	0.756	2
20	0.1942	-0.150	2.48	5.25	1	10.131	0.784	1.99

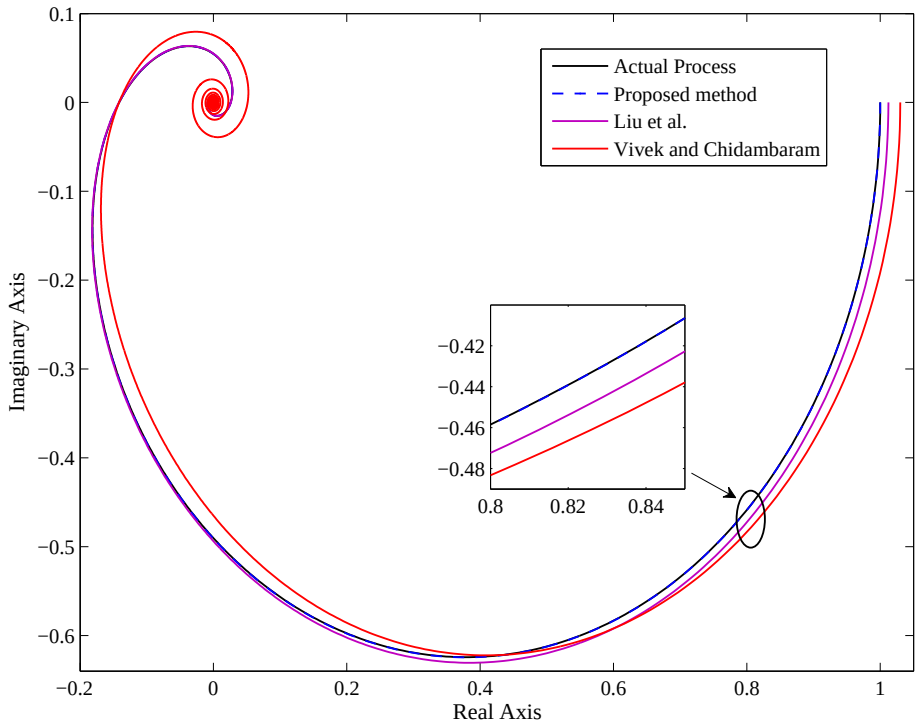

Figure 3.3: Nyquist plots for Example 1

Unstable process

For unstable SOPDT process the output equation is obtained as

$$y(t) = \frac{Kh\lambda_1\lambda_2}{\lambda_1+\lambda_2}\left[\frac{1}{\lambda_1}+\frac{1}{\lambda_2}-\frac{2e^{-\lambda_1(t-t_1)}}{\lambda_1(1+e^{-\lambda_1 T_p})}-\frac{2e^{\lambda_2(t-t_1)}}{\lambda_2(1+e^{\lambda_2 T_p})}\right] \tag{3.23}$$

The peak amplitude condition at $\dot{y}(t_p) = 0$ gives

$$e^{\lambda_2(t_p-t_1)} = \frac{(1+e^{\lambda_2 T_p})e^{-\lambda_1(t_p-t_1)}}{(1+e^{-\lambda_1 T_p})} \tag{3.24}$$

Substituting (3.24) in (3.23) at $t = t_p$ the expression becomes

$$\chi = \frac{-e^{-\lambda_1(t_p - t_1)}}{1 + e^{-\lambda_1 T_p}} \tag{3.25}$$

where $\chi = \frac{1}{2}\left[\frac{A_p}{Kh} - 1\right]$ the value of λ_2 is obtained by approximating the exponential terms up to 5^{th} order using Taylor series.

Second derivative of (3.23) is

$$\ddot{y}(t) = \frac{Kh\lambda_1\lambda_2}{\lambda_1 + \lambda_2}\left[-\frac{2\lambda_1 e^{-\lambda_1(t-t_1)}}{(1 + e^{-\lambda_1 T_p})} - \frac{2\lambda_2 e^{\lambda_2(t-t_1)}}{(1 + e^{\lambda_2 T_p})}\right] \tag{3.26}$$

At $t = t_p$ utilizing (3.25) and (3.26) in (3.27). The expression for λ_2 is obtained as

$$\lambda_2 = \frac{\ddot{y}(t_p)}{2\chi Kh\lambda_1} \tag{3.27}$$

Therefore, λ_1 and λ_2 for both stable and unstable processes are obtained from the derived equations from which the two time constants τ_1 and τ_2 can be determined. The steady-state gain is assumed to be known and the time delay θ is obtained from the Fig. 3.1 as $t_1 - t_0$.

Table. 3.3: Identified Process models for Example 2

Method	Process model	Error (E_I)
Proposed	$\frac{e^{-0.496s}}{(1.9892s-1)(0.4937s+1)}$	0.0056
Proposed with $L = 0.1$	$\frac{e^{-0.5s}}{(2.1177s-1)(0.5874s+1)}$	0.0342
Liu and Gao [35]	$\frac{1.0097e^{-1.36s}}{(2.74s-1)}$	0.2112
Vivek and Chidambaram [41]	$\frac{0.7534e^{-1.041s}}{(2.164s-1)}$	0.3595

Example 2

Let us consider an unstable SOPDT model [41] as

$$G(s) = \frac{e^{-0.5s}}{(2s-1)(0.5s+1)}.$$

The limit cycle obtained from the relay test with $h = 1$ has the following measurements $t_0 = 0$, $t_1 = 0.496$, $t_p = 1.1417$, $t_2 = 2.7703$, $A_p = 0.4482$ and $\ddot{y}(t_p) = -0.5618$. Time delay

θ is 0.496 and K is assumed to be 1. The process parameters τ_1 and τ_2 are estimated using (3.25) and (3.27) as 1.9892 and 0.4937. The identified models by Liu and Gao [35] and Vivek and Chidambaram [41] along with identification error are given in Table 3.3. The accuracy of the identification method is shown with Nyquist plot in Fig. 3.4. The identified model is more near to the actual process. The recovered signal using wavelet transform for

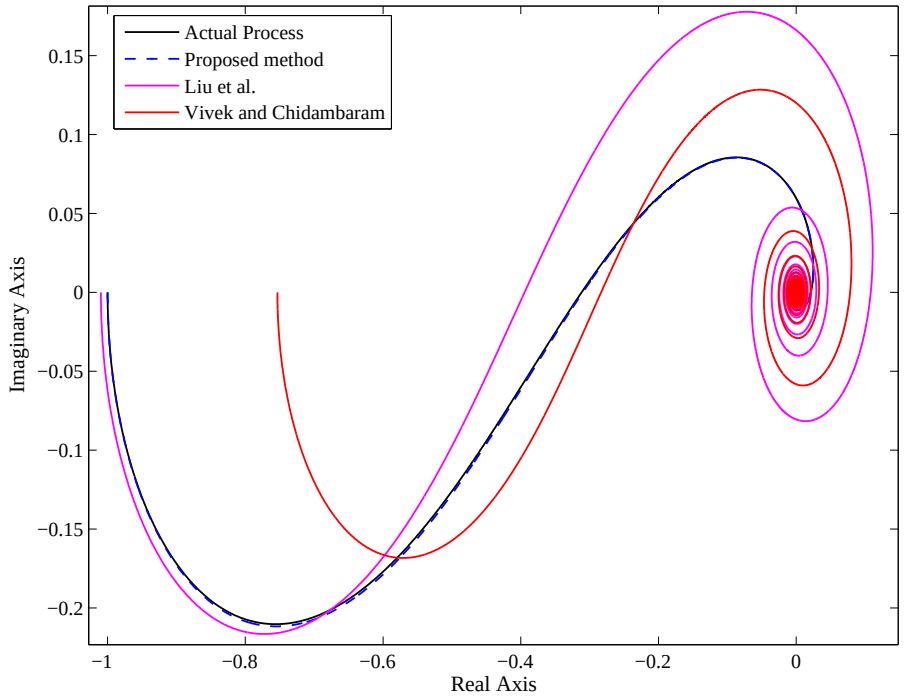

Figure 3.4: Nyquist plots for Example 2

different SNR levels are shown in Table 3.4. Compared to all the parameters there is much deviation in $\ddot{y}(t_p)$. This effects the estimation of the process parameter τ_2.

Table. 3.4: Limit cycle measurements of the extracted signal at different SNR levels for Example 2

SNR (dB)	A_p	$\ddot{y}(t_p)$	t_p	T_p	K	τ_1	τ_2	θ
10	0.4451	-0.5305	1.11	2.77	1	2.0491	0.5104	0.5
15	0.4487	-0.6435	1.18	2.76	1	1.9186	0.4464	0.49
20	0.4479	-0.8448	1.07	2.76	1	2.064	0.3165	0.49

3.4.2 FOPDT Process

The following stable or unstable FOPDT process is obtained from (3.12) by substituting $\tau_2 = 0$

$$G_p(s) = \frac{Ke^{-\theta s}}{\tau_1 s \pm 1} \tag{3.28}$$

The above equation can be represented as

$$G_p(s) = \frac{-K\lambda_1 e^{-\theta s}}{s \mp \lambda_1} \tag{3.29}$$

where $\lambda_1 = \frac{-1}{\tau_1}$, expressing FOPDT process model (3.29) in state-space from gives

$$\mathbf{A} = \pm\lambda_1 \; ; \; \mathbf{b} = -K\lambda_1 \; ; \; \mathbf{c} = 1 \tag{3.30}$$

The output equation of FOPDT process is obtained by substituting (3.30) in (3.11) as

$$y(t) = Kh\left(\mp 1 \pm \frac{2e^{\pm\lambda_1(t-t_1)}}{1+e^{\pm\lambda_1 T_p}}\right) \tag{3.31}$$

At $t = t_1$, the above equation becomes

$$y(t_1) = Kh\left(\mp 1 \pm \frac{2}{1+e^{\pm\lambda_1 T_p}}\right) \tag{3.32}$$

In FOPDT process $t_1 = t_p$ which gives $y(t_1) = y(t_p) = A_p$. Simplifying (3.32) further

$$\lambda_1 = \frac{\pm 1}{T_p} \ln\left(\frac{\pm 1}{\chi} - 1\right) \tag{3.33}$$

where $\chi = \frac{1}{2}\left[\frac{A_p}{Kh} \pm 1\right]$. Thus, from (3.33) the process parameter τ_1 can be determined and time delay θ is obtained from Fig. 3.1 and K is assumed.

Example 3

The following stable FOPDT model [31] is considered as

$$G(s) = \frac{e^{-2s}}{10s+1}.$$

The limit cycle quantities for the stable FOPDT process are $A_p = 0.182$, $T_p = 3.68$, $\theta = 2$ and K is assumed to be 1. The time constant of the process model obtained from (3.33) is $\tau_1 = 9.9972$. The identification error of the proposed model, Liu and Gao [35] and Vivek and Chidambaram [62] is given in Table 3.5. The identified model with the proposed method has

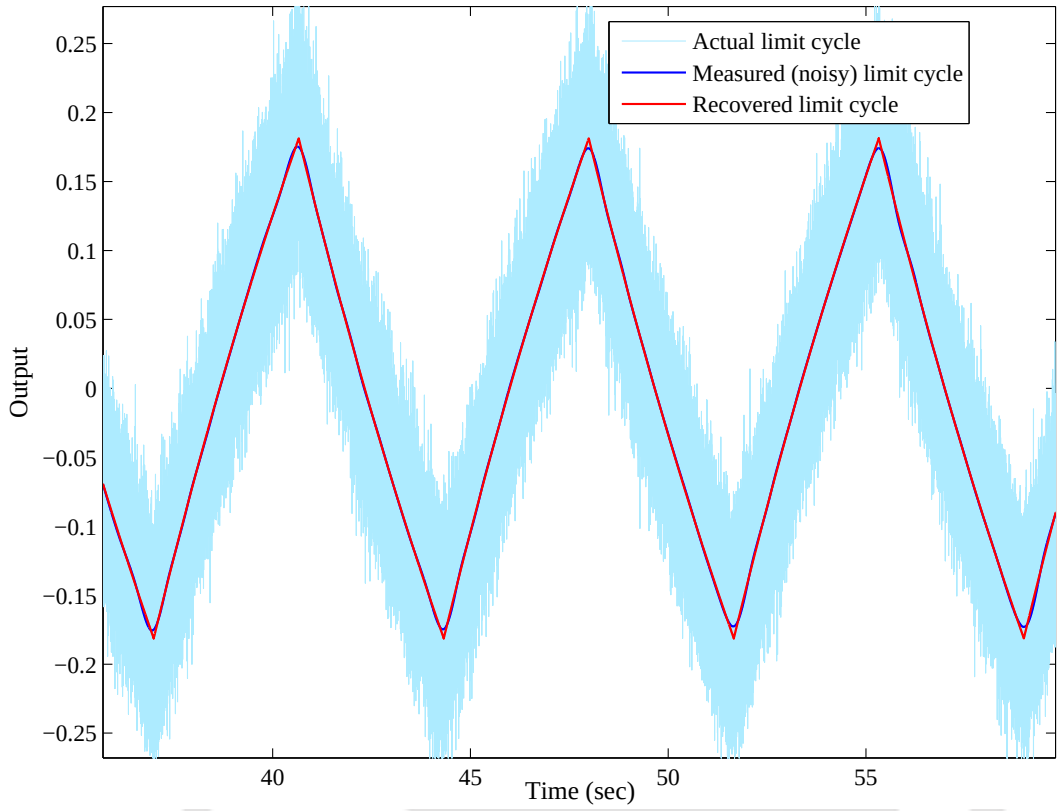

Figure 3.5: Limit cycle output of Example 3

less error. An SNR of 10dB is added at the output and is recovered using wavelet transform which is shown in Fig. 3.5. The extracted signal almost matches with the actual limit cycle output. Therefore, the process parameters are determined as $A_p = 0.1739$, $T_p = 3.66$, $\theta = 1.99$. For steady state gain $K = 1$, the time constant τ_1 is 10.416. For different SNR levels, process parameters are shown in Table 3.6.

Table. 3.5: Identified Process models for Example 3

Method	Process model	Error (E_I)
Proposed	$\frac{e^{-2s}}{9.9972s+1}$	0.0002
Proposed with $L = 0.1$	$\frac{e^{-2.003s}}{9.900s+1}$	0.0067
Liu and Gao [35]	$\frac{1.0048e^{-2.002s}}{10.049s+1}$	0.0022
Vivek and Chidambaram [62]	$\frac{0.9467e^{-2s}}{9.5028s+1}$	0.0164

Table. 3.6: Limit cycle measurements of the extracted signal at different SNR levels for Example 3

SNR (dB)	A_p	T_p	K	τ_1	θ
10	0.1739	3.66	1	10.416	1.99
15	0.1746	3.66	1	10.373	1.99
20	0.1747	3.67	1	10.395	2

Example 4

An unstable FOPDT model is considered as [62]

$$G(s) = \frac{e^{-0.5s}}{s-1}.$$

The relay test is conducted with $h = 1$, induces limit cycle output which has $A_p = 0.6597$, $T_p = 1.5681$ and $\theta = 0.5$. By assuming the steady-state gain $K = 1$, the value of τ_1 is 0.9896. The identified models are tabulated in Table 3.7. The model proposed by Vivek and Chidambaram [62] has more error compared with the identified model using the proposed method. Nyquist plot in Fig. 3.6 reveals that the identified model is near to the actual process. During a step load disturbance of magnitude $L = 0.1$, it is seen from the identified model that the identification accuracy decreases. The parameters for different SNR levels are given in Table 3.8.

Table. 3.7: Identified Process models for Example 4

Method	Process model	Error (E_I)
Proposed	$\frac{e^{-0.5s}}{0.9896s-1}$	0.0128
Proposed with $L = 0.1$	$\frac{e^{-0.5053s}}{1.1222s-1}$	0.0943
Vivek and Chidambaram [62]	$\frac{1.0638e^{-0.5127s}}{1.0832s-1}$	0.0681

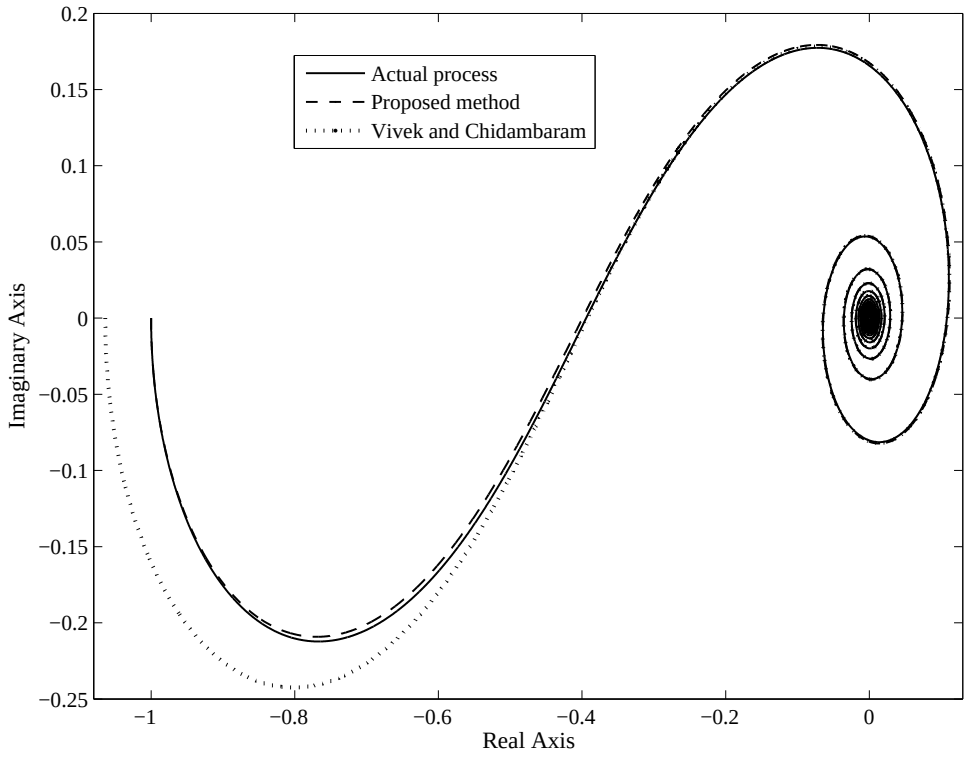

Figure 3.6: Nyquist plots for Example 4

Table. 3.8: Limit cycle measurements of the extracted signal at different SNR levels for Example 4

SNR (dB)	A_p	T_p	K	τ_1	θ
10	0.6132	1.56	1	1.092	0.5
15	0.6093	1.57	1	1.109	0.51
20	0.6093	1.57	1	1.109	0.51

3.4.3 Underdamped SOPDT Process

The general from of the underdamped model is considered as

$$G_p(s) = \frac{Ke^{-\theta s}}{a_1 s^2 + a_2 s + 1} \tag{3.34}$$

where K is steady-state gain, θ is time delay, a_1 and a_2 are the coefficients of the second order process. Eq. (3.34) is represented as

$$G_p(s) = \frac{K\lambda_1\lambda_2 e^{-\theta s}}{(s-\lambda_1)(s-\lambda_2)} \tag{3.35}$$

The eigenvalues, λ_1 and λ_2 are given as $\lambda_1 = \mu_1 - i\mu_2$ and $\lambda_2 = \mu_1 + i\mu_2$, where $\mu_1 = \frac{-a_2}{2a_1}$ and $\mu_2 = \frac{\sqrt{(4a_1 - a_2^2)}}{2a_1}$. Therefore, the coefficients of the model are given as

$$a_1 = \frac{1}{\mu_1^2 + \mu_2^2} \quad , \quad a_2 = \frac{-2\mu_1}{\mu_1^2 + \mu_2^2} \tag{3.36}$$

The state-space matrices of the underdamped SOPDT model (3.35) are

$$\mathbf{A} = \begin{bmatrix} \lambda_1 & 0 \\ 0 & \lambda_2 \end{bmatrix} ; \mathbf{b} = \begin{bmatrix} a \\ -a \end{bmatrix} ; \mathbf{c} = \begin{bmatrix} 1 & 1 \end{bmatrix} \tag{3.37}$$

where

$$a = \frac{K\lambda_1\lambda_2}{(\lambda_1 - \lambda_2)} \tag{3.38}$$

The output equation of the underdamped SOPDT model will be similar to the stable SOPDT model. Therefore, substituting the eigenvalue λ_2 of the model (3.35) in (3.20) yields

$$\chi = \frac{e^{\mu_1(t_p - t_1)} e^{i\mu_2(t_p - t_1)}}{1 + e^{\mu_1 T_p} e^{i\mu_2 T_p}} \tag{3.39}$$

where $\chi = \frac{1}{2}\left[\frac{A_p}{Kh} + 1\right]$

Upon solving the Eq. (3.39) results in the following two equations

$$\chi + \chi e^{\mu_1 T_p}\cos(\mu_2 T_p) - e^{\mu_1(t_p - t_1)}\cos(\mu_2(t_p - t_1)) \tag{3.40}$$

$$\chi e^{\mu_1 T_p}\sin(\mu_2 T_p) - e^{\mu_1(t_p - t_1)}\sin(\mu_2(t_p - t_1)) \tag{3.41}$$

By solving the two non-linear equations (3.40) and (3.41), μ_1 and μ_2 are obtained and then using (3.36) the coefficients of the underdamped SOPDT model, a_1 and a_2 are extracted. Time delay is obtained from Fig. 3.1 and the steady-state gain is assumed to be known.

Example 5

Consider the underdamped SOPDT model given in [76]

$$G(s) = \frac{e^{-s}}{9s^2 + 2.4s + 1}.$$

Relay feedback test is performed by setting $h = 1$ and a sustained limit cycle output is obtained. The measurements made on the limit cycle are $t_0 = 0$, $t_1 = 1.0001$, $t_p = 2.5287$, $T_p = 5.4488$ and $A_p = 0.5255$. Therefore, the value of θ is 1.0001 and for $K = 1$ using (3.40) and (3.41) the remaining two parameters are obtained as $a_1 = 8.9988$ and $a_2 = 2.4008$. Chen [76] approximated the underdamped SOPDT model as an FOPDT model and the identified models are given in Table 3.9. The identification error is very less for the identified model. The identified models for various SNR levels are shown in Table 3.10.

Table. 3.9: Identified Process models for Example 5

Method	Process model	Error (E_I)
Proposed	$\frac{e^{-1.0001s}}{8.9988s^2+2.4008s+1}$	0.0001
Proposed with $L = 0.1$	$\frac{e^{-s}}{9.7192s^2+2.3285s+1}$	0.0355
Chen [76]	$\frac{e^{-3.35s}}{3.96s+1}$	0.3528

Table. 3.10: Identified process models for different SNR levels for Example 5

SNR (dB)	Process model	Error (E_I)
10	$\frac{e^{-0.99s}}{9.1414s^2+2.2095s+1}$	0.0289
15	$\frac{e^{-1.01s}}{9.0547s^2+2.3901s+1}$	0.0023
20	$\frac{e^{-0.99s}}{9.0445s^2+2.3310s+1}$	0.0100

3.5 Identification of Buck converter

The relay identification method using the proposed state-space approach is verified on DC-DC buck converter. The identification procedure given in Chapter 2 (Section 2.4.5) is used to generate sustained limit cycle output. The buck converter system connected to the relay is shown in Fig. 3.7. The specifications of the converter is already presented in Appendix Table

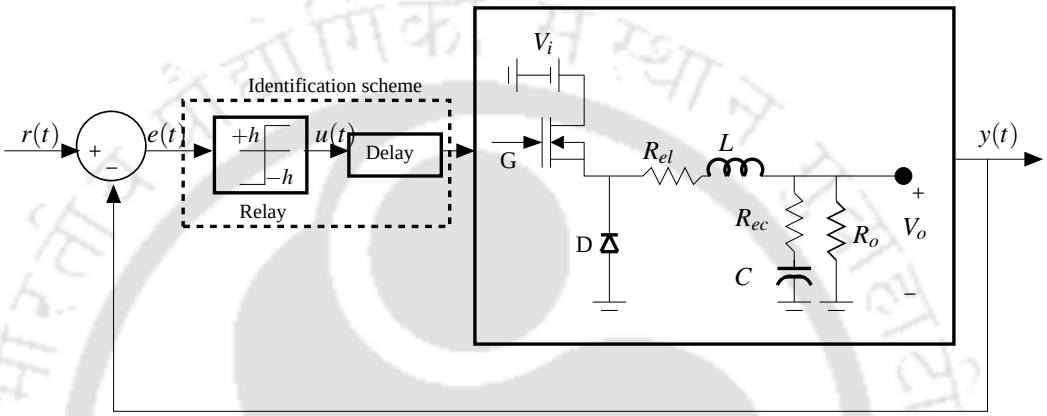

Figure 3.7: Relay identification for buck converter.

A.1 and the implementation of the identification test is shown in Fig. 2.14. Here, during the identification the input voltage (V_i) is varied from 9.5 V to 10 V. For $V_i = 9.5$ V, the averaged model is obtained from Eq. (2.48) [73] as

$$G(s) = \frac{9.38(0.291 \times 10^{-5}s + 1)}{5.402 \times 10^{-8}s^2 + 0.699 \times 10^{-4}s + 1} \tag{3.42}$$

The averaged model (3.42) has underdamped characteristics. Therefore, an underdamped model of the form (3.34) is considered for identification. The relay feedback test is performed with the following settings: $V_r = 5$ V, $h = 0.8$ and $\theta = 200$. The limit cycle response obtained from simulation has $A_p = 2.01$ V, $t_p = 2.4 \times 10^{-4}$ *sec* and T_p=5.9 $\times 10^{-4}$ *sec*. The steady state gain K is obtained from step test as $K = 8.87$. The limit cycle data is substituted in (3.40) and (3.41) and solving these equations resulted in these values, $a_1 = 7.03 \times 10^{-7}$ and $a_2 = 0.0017$. The identified SOPDT model is represented as

$$G(s) = \frac{8.87e^{-2\times10^{-4}s}}{7.0341\times10^{-7}s^2 + 0.0017s + 1} \tag{3.43}$$

There are slight variations in the dynamics between the identified and that of the averaged model. This may result in different closed-loop responses.

The effectiveness of the relay feedback test is also verified experimentally and the schematic diagram of the identification test is shown in Fig. 2.14. Identification scheme is implemented on TMS320F28335 DSP processor. Tektronix oscilloscope is used to monitor the output voltage. The experimental prototype of buck converter is shown in Fig. 2.16. Experiment is conducted with similar settings used in simulation. The limit cycle output for different conditions is shown in Fig. 3.8. The limit cycle in Fig. 3.8(a) has the measurements $\theta = 2.68 \times 10^{-4}$, t_p=2.88 $\times$ 10^{-4}, T_p = 6.08 $\times$ 10^{-4} and A_p= 1.53 V and K=6.8. The dynamic model is given by

$$G(s) = \frac{6.8e^{-2.68\times10^{-4}s}}{8.6699\times10^{-7}s^2 + 0.0019s + 1} \tag{3.44}$$

There may be frequent changes occurring in the buck converter, such as change in load and input voltage. The identification test is also performed for these changes. During the change in load resistance from 10 Ω to 15 Ω the limit cycle is shown in Fig. 3.8(b) and the model parameters are seen to be K=8.75, θ = 2.28 $\times$ 10^{-4}, a_1=7.650 $\times$ 10^{-8} and a_2=5.405 $\times$ 10^{-4}. The limit cycle for the sudden change in input voltage from 9.5 to 10 V is shown in Fig. 3.8(c) and the identified parameters are K=9.25, θ = 2.96 $\times$ 10^{-4}, a_1 = 1.186 $\times$ 10^{-8} and a_2 = 2.178 $\times$ 10^{-4}. It can be seen from the identification results that changes in the system will lead to the variations in dynamics. This model mismatch may ultimately effect the control response. Thus, if there is a degrade in the controller performance then relay can be switched on to get the actual dynamics of the system.

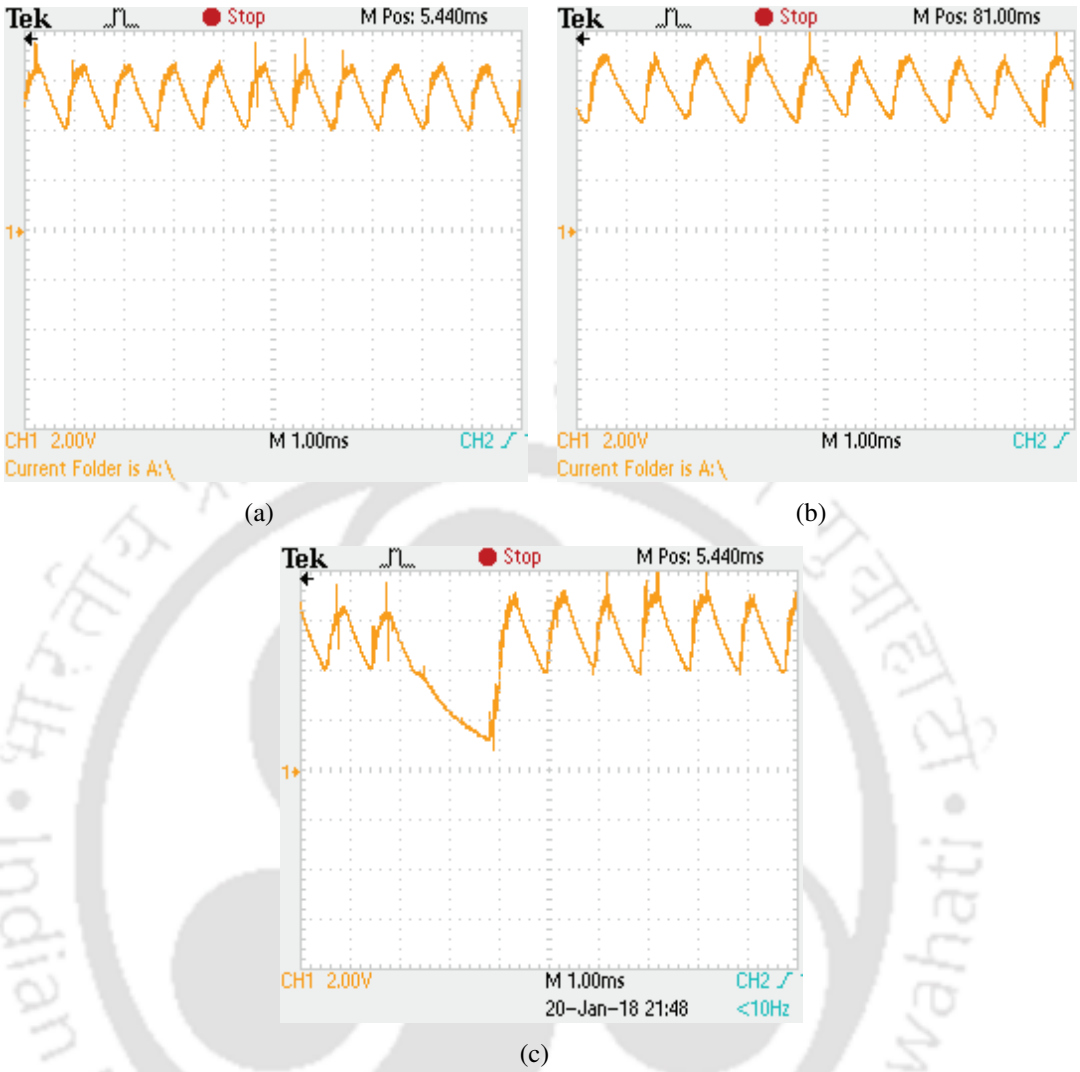

Figure 3.8: Limit cycle output (V_o) (a) under nominal condition (b) change in R_o to 15 Ω (c) change in V_i from 9.5 to 10V.

3.5.1 Validation of the identified model

The performance of the identified model from simulation (3.43) and experiment (3.45) using the relay is validated with the step response and is compared with the response obtained from the averaged model (3.42). The identification scheme shown in Fig. 2.14 is replaced with a PID controller (G_c(s)) and the tuning of the controller parameters for both the models are done for a phase margin of 50^o.

The characteristic equation for the block diagram (Fig. 3.7) with G_c(s) in the loop is written as $1 + G_c(s)G_p(s) = 0$. To bring a correlation between the chosen SOPDT model (3.34) and

that of the average model the exponential term in the numerator of the SOPDT model is approximated as $1-\theta s$. The generalized characteristic equation for the models is given in 2.54. The controller parameters are tuned using the coefficient comparison method by choosing the desired equation such that the system phase margin be 50^o. For the averaged model (3.42) the desired equation is

$$8.6712\times10^{-12}s^2+6.4165\times10^{-8}s+0.0006406s+1=0 \tag{3.45}$$

The tuning parameters for the averaged model are K_P=0.3245, T_I=0.000485 and T_D=0.0001081. Similarly, the desired equations for the identified model from simulation (3.42) and experiment (3.45) are given in (3.46) and (3.47), respectively.

$$4.4241\times10^{-13}s^2+7.6269\times10^{-7}s+0.00084s+1=0 \tag{3.46}$$

$$9.8775\times10^{-11}s^2+9.7063\times10^{-7}s+0.00063s+1=0 \tag{3.47}$$

The tuning parameters for the models are $K_P=0.545$, $T_I=0.00087$, $T_D=0.000725$ and $K_P=0.3061$, $T_I=0.000609$, $T_D=0.000949$.

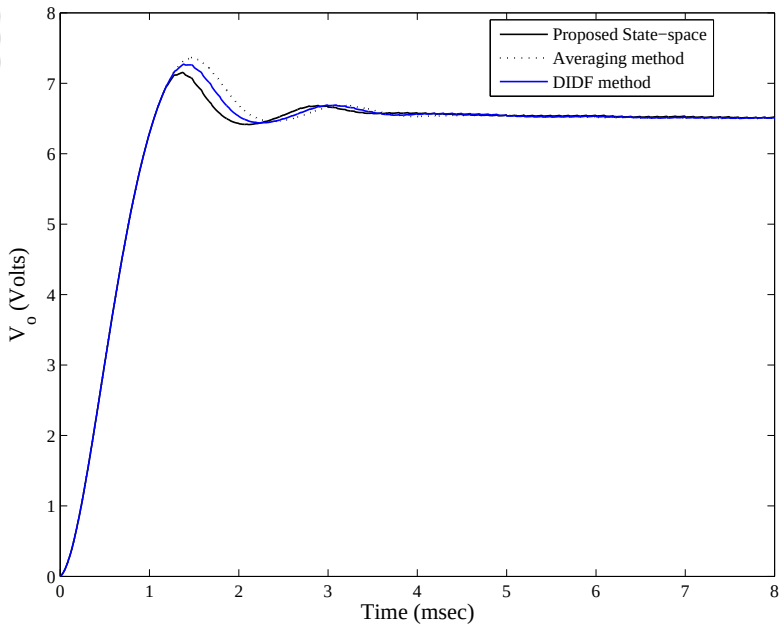

Figure 3.9: Step responses obtained from simulation

The step response is observed with the obtained controller parameters. The reference value

is set to 6.5 V and V_i to be 10 V. The simulation responses in Fig. 3.9 reveal that the identified simulation model has less peak overshoot (7.13 V) compared to the average model (7.36 V). Using the chosen design specifications DIDF model is obtained and its response is also plotted in Fig. 3.9. It has a peak overshoot of 7.26 V. The response of the identified model from experiment and averaged model are shown in Fig. 3.10 and Fig. 3.11, respectively.

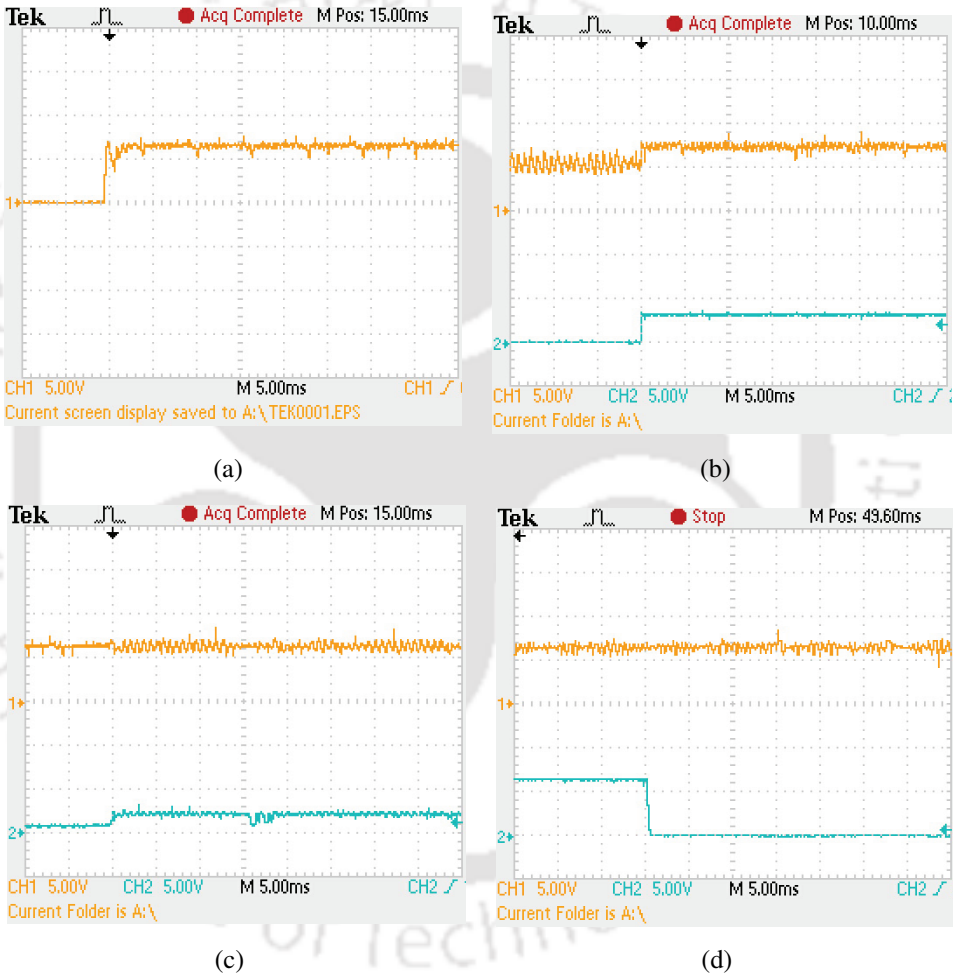

Figure 3.10: Step response (V_o) for the identified model using proposed state-space (a) For V_r=6.5V (b) change in V_r from 5 $\rightarrow$ 7 V (c) change in R_o from 10 $\rightarrow$ 15 Ω (d) change in C from 98 μF to 76 μF.

Both models track the reference value. The settling time of the identified model is 4.86 ms and for the averaged model it is 6.64 ms. The model obtained from DIDF has 5.2 ms. The response is verified for different perturbations such as change in reference value from 5 to 7 V and load resistance (R_o) from 10 Ω and 15 Ω. During the step change in reference voltage,

the output voltage of the identified model (Fig. 3.10(b)) settles at 0.48 ms and 1.08 ms for the averaged model (Fig. 3.11(b)). For the 50% change in R_o the output response of both the models is unchanged as shown in Fig. 3.10(c) and Fig. 3.11(c). During the capacitance change from 98 μF to 76 μF for $V_i = 8.5$ V and $V_r = 6$ V, the output voltage tracks the reference value. The results of DIDF method is shown in Fig. 3.12. The performance of the models is shown in Table 3.11.

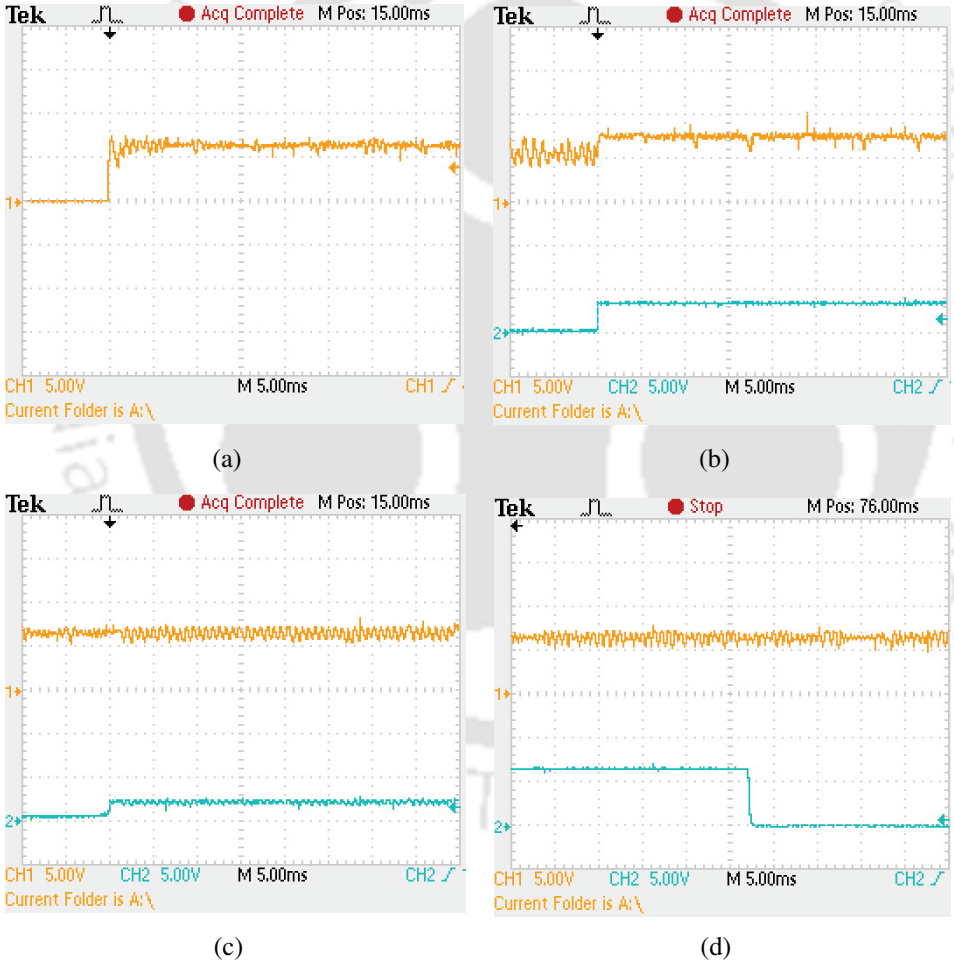

Figure 3.11: Step response (V_o) for the averaged model (a) For V_r=6.5V (b) change in V_r from 5 $\rightarrow$ 7 V (c) change in R_o from 10 $\rightarrow$ 15 Ω. (d) change in C from 98 μF to 76 μF.

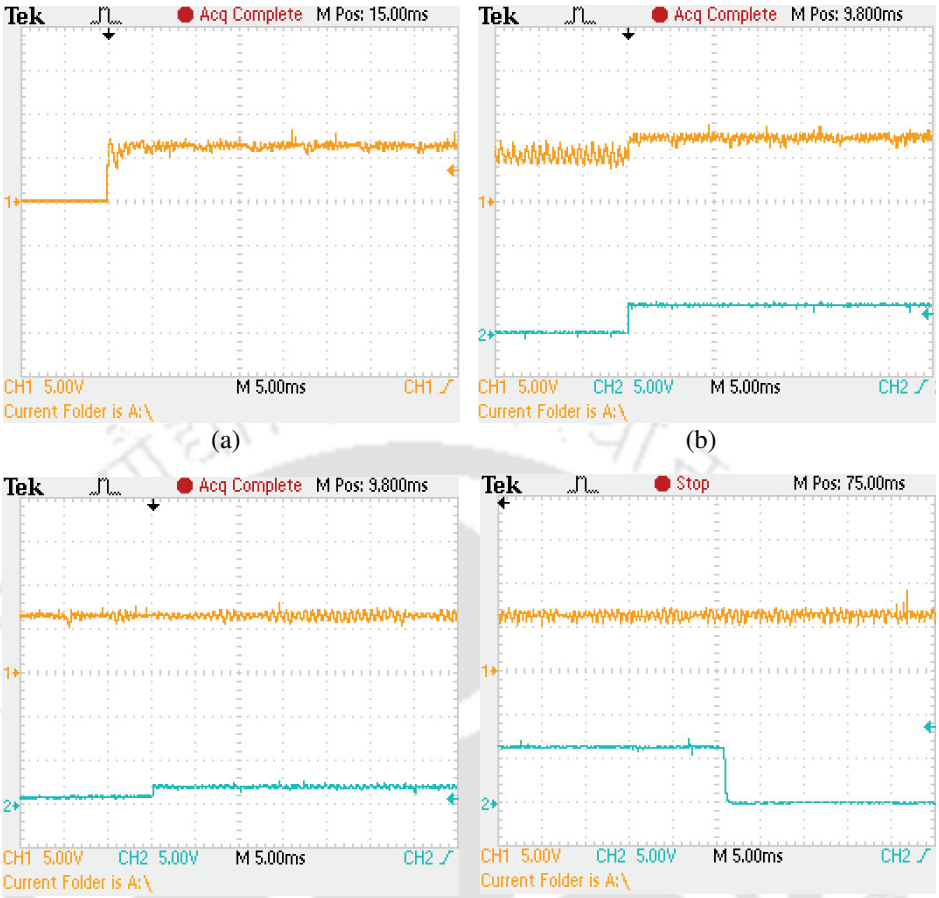

Figure 3.12: Step response (V_o) for the identified model using DIDF (a) For V_r=6.5V (b) change in V_r from 5 $\rightarrow$ 7 V (c) change in R_o from 10 $\rightarrow$ 15 Ω (d) change in C from 98 μF to 76 μF.

Table. 3.11: Performance of the models from experiment

Method	Settling Time	
	Ref 6.5V	Ref change 5V$\rightarrow$7V
Proposed state-space	4.86 ms	0.48 ms
DIDF approximation	5.2 ms	0.9 ms
Averaging method	6.64 ms	1.08 ms

3.6 Summary

Expressions to estimate FOPDT, SOPDT and underdamped process models are derived using the state-space method. Half limit cycle information obtained from relay feedback test is sufficient to determine the required parameters of the process. The estimated models with the proposed method have better identification accuracy. But during load disturbance, the identification error has increased but overall the error is not very high. The identification method is extended to identify the dynamic model of the DC-DC buck converter. The identified buck converter model has a better closed-loop response. The model performs well even during parameter perturbations.

Indian Institute of Technology Guwahati

Indian Institute of Technology Guwahati

CHAPTER 4

IDENTIFICATION AND CONTROL OF FOPDT AND SOPDT PROCESSES

4.1 Introduction

In Chapter 2 and Chapter 3, the process models were identified. In this Chapter, identification and control of FOPDT and SOPDT is performed. The proportional-integral-derivative (PID) controller is commonly used in process industries due to its ease of design. With proper tuning of the PID parameters, satisfactory performance can be obtained for different types of systems. In real-time application, a model based controller design is more effective as it includes the dynamics of the process to be controlled. Several methods have been reported in the literature for the identification of process models. Åström and Hägglund [4] conducted a relay feedback test which is known as autotune method to generate sustained oscillations. Using Åström's relay test Luyben identified the process parameters of a plant, later Shen et al., Kaya and Atherton, Atherton, Haung et al., Majhi and Atherton and Srinivasan and Chidambaram [5, 8, 15, 18, 23, 27, 31] have identified first-order-plus-dead-time (FOPDT) and second-order-plus-dead-time (SOPDT) systems from the relay feedback test. Vivek and Chidambaram [62] identified a FOPDT system using Laplace transform method by a single relay feedback test. Panda [16] estimated the parameters of a SOPDT model from the limit cycle data of the relay output. To reduce the estimation error during relay test of SOPDT critically damped system, Vivek and Chidambaram [10] considered higher order harmonics

in the relay approximation. Wang et al. used a relay (biased and unbiased) with hysteresis to estimate the unknown parameters of a FOPDT system [22]. There is a drift caused when a biased relay is used. To overcome the drift and for better estimates of the process parameters, an unbiased relay is used.

Once the process dynamics are identified, a controller can be designed depending on the obtained process dynamics. Variety of design techniques were proposed by many authors [58, 77–79] for the control of FOPDT, SOPDT and integrating systems. The tuning methods give either good set-point response or load disturbance attenuation. This depends on the objective function that is selected during the design. A tradeoff is achieved by using two controllers in the closed loop or a set-point filter along with a controller. Shamsuzzoha and Lee [48] designed a PID controller using the generalized IMC-PID method to achieve improved load disturbance rejection. The reference tracking is obtained from the set-point filter. Liu et al. [80] proposed a two-degree-of-freedom (2-DoF) control structure for the control of different unstable process models. Three controllers were present in the 2-DoF structure, one for stabilizing the process and the other two for set-point tracking and load disturbance rejection, respectively. Double feedback loops with set-point filter is proposed by Vijayan and Panda [53] to obtain better closed loop performance. Here, the inner feedback is used to stabilize the process, the outer loop for set-point tracking and the set-point filter for reducing the peak overshoot. This method has improved the performance measures. Along with the performance measure, it is very much necessary to consider the robustness during the design. The robustness is usually measured based on the maximum sensitivity (M_s) [52]. The desirable range of M_s is between 1.2 to 2.0 for stable systems. However, for unstable systems, the value is greater than 2.0. Alfaro and Vilanova [57] proposed a model reference robust tuning of 2DoF PI controllers for FOPDT and SOPDT process models. Here, the tuning equations were given for four robustness levels. The designer may select the robustness level according to the requirement. Ajmeri and Ali [54] used the direct synthesis (DS) method to control a particular class of unstable systems. In their analysis, the tuning parameter for load disturbance case with a proper value of M_s is obtained from extensive simulations. In some

of the works, the authors have presented a control strategy using the DS method. The desired tuning parameter required for the controller design is chosen depending on time delay or by curve fitting [79, 81]. In the above works, the performance evaluation for the selection of the desired tuning parameter is not directly taken into account. An attempt is made in this chapter to determine the desired tuning parameter with best performance evaluation.

In this chapter, accurate modeling of stable/unstable FOPDT and SOPDT processes is proposed using the state-space approach. Utilizing the information of limit cycle, simple explicit expressions are derived to obtain accurate dynamics of the processes. Once the process parameters are identified, then the controller (PID) is designed using the direct synthesis method. This method requires a single tuning parameter to tune the controller parameters. The main focus of the controller design (PID) is to attenuate the load disturbance. The best tuning parameter is generated from the particle swarm optimization (PSO) algorithm. Satisfactory set-point tracking is achieved using a set-point filter.

4.2 Proposed feedback structure

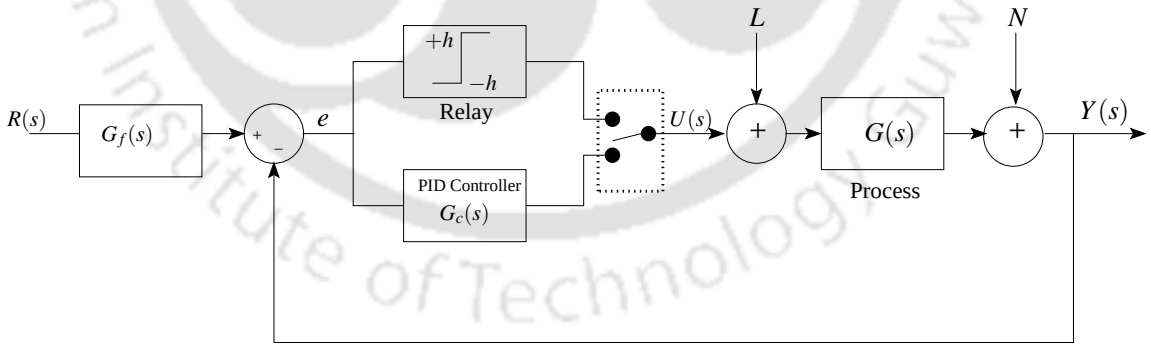

Figure 4.1: Closed loop feedback structure for identification and control

The proposed structure for identification and control is shown in Fig. 4.1 which consists of a relay, a controller and a set-point filter. Relay feedback test is performed to identify the dynamics of the unknown process. After obtaining the dynamics, the controller is designed and a closed loop response is observed. PID controller ($G_c(s)$) stabilizes the closed loop response and set-point filter ($G_f(s)$) is used to track the reference input. Several FOPDT and

SOPDT models are tested for the proposed identification and control method.

The structure of controller is chosen as

$$G_c(s) = K_P\left(1+\frac{1}{sT_I}+sT_D\right) \tag{4.1}$$

The set-point filter with set-point coefficient (β) is given by

$$G_f(s) = \frac{1}{1+s\beta T_I} \tag{4.2}$$

4.3 Identification and control of FOPDT process

Consider a stable/unstable FOPDT model of the form

$$G(s) = \frac{Ke^{-\theta s}}{s\tau_1 \pm 1} \tag{4.3}$$

Here, the parameters steady-state gain (K), time constant (τ_1) and time delay (θ) are to be estimated.

4.3.1 Expressions for process parameters

Explicit expressions are derived using the state-space method for FOPDT stable and unstable systems. Symmetrical relay with height (h) is connected with the process to be identified. Relay test results in limit cycle output shown in Fig. 4.2. The explicit expressions need the information of the limit cycle at t_0, t_1, t_2 and t_3. Here, t_0 and t_3 are zero crossings of the limit cycle, t_2 is the time at which peak of the limit cycle occurs and t_1 is the average of t_0 and t_2. Expressions are derived from t_0 to t_3 using the solution of the state equation.

The ratio of input and output of FOPDT process is written as

$$\frac{Y}{U} = \frac{Ke^{-\theta s}}{\tau_1 s \pm 1} \tag{4.4}$$

$$\dot{y} = \gamma y + \beta u(t-\theta) \tag{4.5}$$

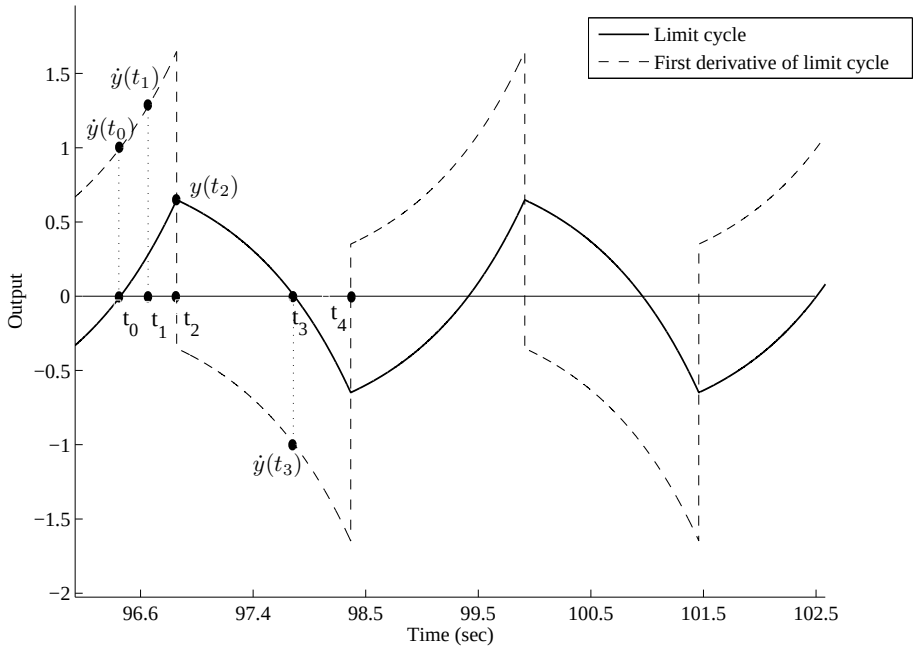

Figure 4.2: Limit cycle output and it's derivative

where $\gamma = \mp\frac{1}{\tau_1}$ and $\beta = \frac{K}{\tau_1}$

The generalized solution of FOPDT process in (4.5) is expressed as

$$y(t) = e^{\gamma(t-t_0)}y(t_0) + \int_{t_0}^{t} e^{\gamma(t-t_0)}\beta u(t-\theta)d\tau \tag{4.6}$$

The explicit expressions of process parameters are obtained using (4.6) for the time range t_0 to t_3. In this range, there are two-piecewise linear inputs $+h$ and $-h$ one from t_0 to t_2 and the other from t_2 to t_4 respectively. The solution for $t \in [t_0, t_2]$ with $y(t_0) = 0$ and $t \in (t_2, t_3]$ with $y(t_0) = y(t_2)$ is given by

$$y(t) = \gamma^{-1}(e^{\gamma t} - 1)\beta h \tag{4.7}$$

$$y(t) = e^{\gamma(t-t_2)}y(t_2) + \frac{1}{\gamma}(1 - e^{\gamma(t-t_2)})\beta h \tag{4.8}$$

The first derivative of (4.7) results in

$$\dot{y}(t) = \beta h e^{\gamma t} \tag{4.9}$$

Taking the ratio of (4.9) at time $t = t_0$ and $t = t_1$ we obtain

$$\tau_1 = \frac{\mp(t_1 - t_0)}{\ln(\frac{\dot{y}(t_1)}{\dot{y}(t_0)})} \tag{4.10}$$

Taking the first derivative of (4.8)

$$\dot{y}(t) = e^{\gamma(t-t_2)} y(t_2)\gamma - e^{\gamma(t-t_2)}\beta h \tag{4.11}$$

Arranging (4.11) at $t = t_3$ steady state gain (K) is

$$K = -\frac{1}{h}\left(\frac{\tau_1 \dot{y}(t_3)}{e^{\frac{\mp(t_3-t_2)}{\tau_1}}} \pm y(t_2)\right) \tag{4.12}$$

At $t = t_2 = \theta$ in (4.7) the time delay is expressed as

$$\theta = \mp T \ln\left(1 \mp \frac{y(t_2)}{Kh}\right) \tag{4.13}$$

Using simple expressions, the unknown process parameters are obtained for stable and unstable FOPDT process. The required limit cycle data $\dot{y}(t_0)$, $\dot{y}(t_1)$, $\dot{y}(t_3)$ and $y(t_2)$ are recorded from Fig. 4.2.

4.3.2 Controller Design

The main motive of the controller design is to obtain improved response during load disturbance. Controller parameters are tuned using Ds-d design to achieve minimum ISE. The tuning parameter 'T_c' is determined using PSO algorithm.

The desired objective function under load disturbance is given as

$$\left(\frac{Y}{L}\right)_d = \frac{\frac{T_I s}{K_P}\left(1 + \frac{\theta}{2}s\right)e^{-\theta s}}{\left(\frac{\theta}{\tau_1}T_c s + 1\right)^3} \tag{4.14}$$

The transfer function with respect to disturbance for Fig. 4.1 is written as

$$\left(\frac{Y}{L}\right) = \frac{G}{1+GG_c} \tag{4.15}$$

Substituting the process and controller transfer functions in (4.15) and comparing the denominator with (4.14) we get the expressions for controller parameters.

Controller parameters for stable and unstable processes

$$\begin{aligned} &s^3\left(\frac{\frac{\theta}{2}T_I(\tau_1 - KK_PT_D)}{KK_P}\right) + s^2\left(\frac{KK_PT_I(T_D - \frac{\theta}{2}) + T_I(\tau_1 \pm \frac{\theta}{2})}{KK_P}\right) + \\ &s\left(\frac{T_I + KK_P(\pm T_I - \frac{\theta}{2})}{KK_P}\right) + 1 = T_c^3s^3 + 3T_c^2s^2 + 3T_cs + 1 \end{aligned} \tag{4.16}$$

$$K_P = \frac{4\tau_1^4 + \tau_1^3(24T_c \pm \theta) \pm 6\tau_1^2T_c\theta \mp 12\theta T_c^2\tau_1 \mp 8\theta T_c^3}{\theta K(\tau_1 + 2T_c)^3} \tag{4.17}$$

$$T_D = \frac{\theta(\tau_1^4 + 6\tau_1^3T_c + 12\tau_1^2T_c^2 - 8\tau_1T_c^3 \mp 8\theta T_c^3)}{4\tau_1^4 + \tau_1^3(24T_c \pm \theta) \pm 6\tau_1^2T_c\theta \mp 12\theta T_c^2\tau_1 \mp 8\theta T_c^3} \tag{4.18}$$

$$T_I = \frac{1}{4}\frac{(4\tau_1^4 + \tau_1^3(24T_c \pm \theta) \pm 6\tau_1^2T_c\theta \mp 12\tau_1T_c^2\theta \mp 8T_c^3\theta)\theta}{(2\tau_1 \pm \theta)\tau_1^3} \tag{4.19}$$

The set-point coefficient β is used to track the reference its range is between 0 to 1. The desired closed loop transfer function is given as

$$\left(\frac{Y}{R}\right)_d = \frac{(1 + sT_I + s^2T_IT_D)e^{-\theta s}}{\left(\frac{\theta}{\tau_1}T_cs + 1\right)^4} \tag{4.20}$$

The transfer function for Fig. 4.1 is written as

$$\left(\frac{Y}{R}\right) = \frac{GG_cG_f}{1+GG_c} \tag{4.21}$$

The above equation is expressed as

$$\left(\frac{Y}{R}\right) = \left(\frac{Y}{L}\right) G_c G_f \tag{4.22}$$

Expressing (4.22) in terms of desired functions

$$\left(\frac{Y}{R}\right)_d = \left(\frac{Y}{L}\right)_d G_c G_f \tag{4.23}$$

Substituting the above objective functions and comparing the denominator we obtain

$$\beta = \frac{\theta T_c}{\tau_1 T_I} \tag{4.24}$$

By performing extensive simulation studies, set-point coefficient with less peak overshoot is determined as

$$\beta = 1 - \frac{\theta T_c}{\tau_1 T_I} \tag{4.25}$$

4.4 Identification and control of SOPDT process

Consider an SOPDT stable/unstable transfer function model of the form

$$G(s) = \frac{Ke^{-\theta s}}{(s\tau_1 \pm 1)(s\tau_2 + 1)} \tag{4.26}$$

where the steady state gain (K), time constants (τ_1 and τ_2 with $\tau_1 > \tau_2$) and time delay (θ) are to be estimated.

4.4.1 Expressions for process parameters

Typical process input and output waveforms during a relay feedback test are shown in Fig. 4.3. The general SOPDT model given by (4.26) is expressed as

$$\frac{Y(s)}{U(s)} = \frac{Ke^{-\theta s}}{a_1 s^2 + a_2 s \pm 1} \tag{4.27}$$

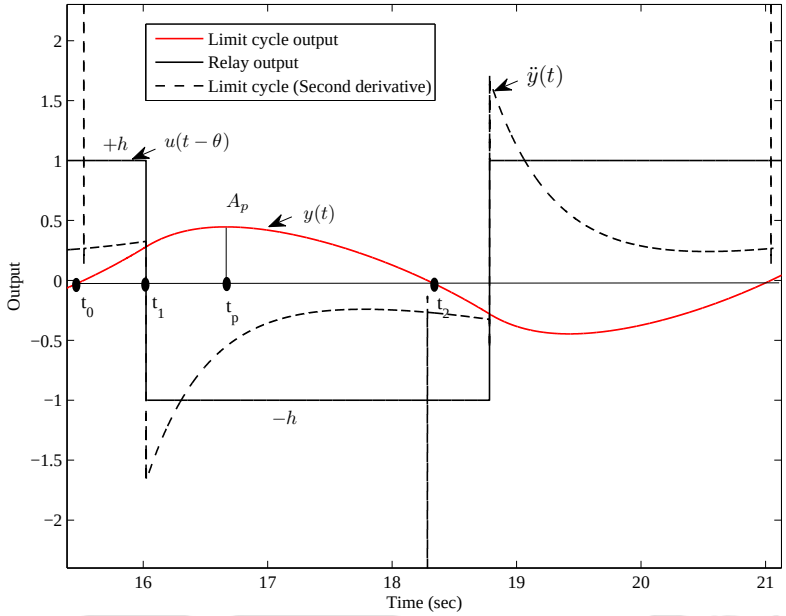

Figure 4.3: Typical relay feedback test outputs of SOPDT process

where $a_1 = \tau_1\tau_2$ and $a_2 = \tau_1 \pm \tau_2$. In state space from (4.27) can be written as

$$\begin{aligned} \dot{\mathbf{X}} &= \mathbf{A}\mathbf{X} + \mathbf{b}u(t-\theta) \\ y &= \mathbf{c}\mathbf{X} \end{aligned} \tag{4.28}$$

where

$$\mathbf{A} = \begin{bmatrix} 0 & 1 \\ -\mu_2 & -\mu_1 \end{bmatrix}; \ \mathbf{b} = \begin{bmatrix} 0 \\ \alpha \end{bmatrix}; \ \mathbf{c} = \begin{bmatrix} 1 & 0 \end{bmatrix} \tag{4.29}$$

and $\mu_1 = \frac{a_2}{a_1}$, $\mu_2 = \frac{\pm 1}{a_1}$ and $\alpha = \frac{K}{a_1}$.

The matrix $\mathbf{A}$ is expressed in terms of roots of the characteristic equation as

$$\mathbf{A} = \begin{bmatrix} 0 & 1 \\ -\lambda_1\lambda_2 & \lambda_1 + \lambda_2 \end{bmatrix} \tag{4.30}$$

where $\lambda_1 = \frac{-\mu_1}{2} - i\frac{\sqrt{4\mu_2 - \mu_1^2}}{2}$ and $\lambda_2 = \frac{-\mu_1}{2} + i\frac{\sqrt{4\mu_2 - \mu_1^2}}{2}$.

For simplicity in solving, $\mathbf{A}$ is written in diagonal form thus giving (4.28) as

$$\begin{aligned} \dot{\hat{\mathbf{X}}} &= \hat{\mathbf{A}}\hat{\mathbf{X}} + \hat{\mathbf{b}}u(t-\theta) \\ \hat{y} &= \hat{\mathbf{c}}\hat{\mathbf{X}} \end{aligned} \tag{4.31}$$

where

$$\hat{\mathbf{A}} = \begin{bmatrix} \lambda_1 & 0 \\ 0 & \lambda_2 \end{bmatrix} ; \hat{\mathbf{b}} = \begin{bmatrix} B_2 \\ -B_2 \end{bmatrix} ; \hat{\mathbf{c}} = \begin{bmatrix} 1 & 1 \end{bmatrix} \tag{4.32}$$

and $B_2 = \frac{\alpha}{\lambda_1 - \lambda_2}$. Here, $\hat{\mathbf{A}}$ is assumed to be nonsingular. (Detailed derivation is given in Appendix A.3)

The solutions of the state equations for the range $t_0 \leq t \leq t_1$ and $t_1 < t \leq t_2$ are

$$\hat{\mathbf{x}}(t) = \mathbf{e}^{\hat{\mathbf{A}}(t-t_0)}\hat{\mathbf{x}}(t_0) + \hat{\mathbf{A}}^{-1}(\mathbf{e}^{\hat{\mathbf{A}}(t-t_0)} - \mathbf{I})\hat{\mathbf{b}}h \tag{4.33}$$

and

$$\hat{\mathbf{x}}(t) = \mathbf{e}^{\hat{\mathbf{A}}(t-t_1)}\hat{\mathbf{x}}(t_1) - \hat{\mathbf{A}}^{-1}(\mathbf{e}^{\hat{\mathbf{A}}(t-t_1)} - \mathbf{I})\hat{\mathbf{b}}h \tag{4.34}$$

From the limit cycle shown in Fig. 4.3, $\theta = t_1 - t_0$ where the starting point, $t_0 = 0$ and at $t = t_1$, (4.33) becomes

$$\hat{\mathbf{x}}(t_1) = \begin{bmatrix} \hat{x}_{01}e^{\lambda_1\theta} + \frac{B_2h(e^{\lambda_1\theta}-1)}{\lambda_1} \\ \hat{x}_{02}e^{\lambda_2\theta} - \frac{B_2h(e^{\lambda_2\theta}-1)}{\lambda_2} \end{bmatrix} \tag{4.35}$$

The peak amplitude occurs at $t = t_p$ and therefore $\mathbf{x}(t)$ at t_p is

$$\hat{\mathbf{x}}(t_p) = \begin{bmatrix} \hat{x}_{\theta 1}e^{\lambda_1(t_p-\theta)} - \frac{B_2h(e^{\lambda_1(t_p-\theta)}-1)}{\lambda_1} \\ \hat{x}_{\theta 2}e^{\lambda_2(t_p-\theta)} + \frac{B_2h(e^{\lambda_2(t_p-\theta)}-1)}{\lambda_2} \end{bmatrix} \tag{4.36}$$

The expression for t_p is obtained from the condition $\hat{\mathbf{c}}\hat{\mathbf{A}}\hat{\mathbf{x}}(t_p) = 0$. After substitution and

simplification one obtains

$$\frac{e^{\lambda_1(t_p-\theta)}}{e^{\lambda_2(t_p-\theta)}} = \frac{2B_2h + e^{\lambda_2\theta}(-B_2h + \hat{x}_{02}\lambda_2)}{2B_2h + e^{\lambda_1\theta}(-B_2h - \hat{x}_{01}\lambda_1)} \tag{4.37}$$

Simplifying it further by choosing $\Gamma_1 = 2B_2h + e^{\lambda_2\theta}(-B_2h + \hat{x}_{02}\lambda_2)$ and $\Gamma_2 = 2B_2h + e^{\lambda_1\theta}(-B_2h - \hat{x}_{01}\lambda_1)$ to get the expression for t_p results in

$$t_p = \theta + \frac{ln\left(\frac{\Gamma_1}{\Gamma_2}\right)}{\lambda_1 - \lambda_2} \tag{4.38}$$

Using the output equation at $t = t_p$ from Fig. 4.3, $y(t_p) = A_p$. Therefore, the condition $\hat{\mathbf{c}}\hat{\mathbf{x}}(t_p)$=$A_p$ is used to obtain another expression.

$$\hat{x}_{\theta 1}e^{\lambda_1(t_p-\theta)} - \frac{B_2h(e^{\lambda_1(t_p-\theta)} - 1)}{\lambda_1} + \hat{x}_{\theta 2}e^{\lambda_2(t_p-\theta)} + \frac{B_2h(e^{\lambda_2(t_p-\theta)} - 1)}{\lambda_2} = A_p \tag{4.39}$$

$$\frac{\lambda_1 - \lambda_2}{\lambda_1\lambda_2}\left[\Gamma_1^{\frac{\lambda_1}{\lambda_1-\lambda_2}}\Gamma_2^{\frac{-\lambda_2}{\lambda_1-\lambda_2}} - B_2h\right] = A_p \tag{4.40}$$

From (4.33) and (4.34) using the half limit cycle condition, the initial condition is given by

$$\hat{\mathbf{x}}(t_0) = (\mathbf{I} + \mathbf{e}^{\hat{\mathbf{A}}t_2})\hat{\mathbf{A}}^{-1}(2\mathbf{e}^{\hat{\mathbf{A}}(t_2-\theta)} - \mathbf{e}^{\hat{\mathbf{A}}t_2} - \mathbf{I})\hat{\mathbf{b}}h \tag{4.41}$$

$$\hat{\mathbf{x}}(t_0) = \begin{bmatrix} B_2h\left(\frac{2e^{\lambda_1(t_2-\theta)}}{\lambda_1(1+e^{\lambda_1t_2})} - \frac{1}{\lambda_1}\right) \\ -B_2h\left(\frac{2e^{\lambda_2(t_2-\theta)}}{\lambda_2(1+e^{\lambda_2t_2})} - \frac{1}{\lambda_2}\right) \end{bmatrix} \tag{4.42}$$

For the sustained oscillations to exist, the condition is $\hat{\mathbf{c}}\hat{\mathbf{x}}(t_0) = 0$. Using this condition another non-linear equation is obtained as

$$\frac{B_2h}{\lambda_1\lambda_2}\left(\lambda_2\left(\frac{2e^{\lambda_1(t_2-\theta)}}{1+e^{\lambda_1t_2}} - 1\right) - \lambda_1\left(\frac{2e^{\lambda_2(t_2-\theta)}}{1+e^{\lambda_2t_2}} - 1\right)\right) = 0 \tag{4.43}$$

The limit cycle data such as A_p, t_1, t_p and t_2 are measured and the equations (4.38), (4.40) and (4.43) are solved simultaneously to estimate the unknown parameters τ_1, τ_2 and K.

4.4.2 Controller Design

A direct synthesis method is used to design the PID controller primarily for satisfactory load disturbance rejection. To achieve the required control objective, PID parameters are tuned from the closed loop transfer function derived with respect to load disturbance. The desired transfer function for tuning the controller parameters consists of $\frac{\theta}{\tau_s}$ ratio where, θ and τ_s are the effective time delay and time constant of the SOPDT process model, respectively.

The desired transfer function under load disturbance is chosen as

$$\left(\frac{Y}{L}\right)_d = \frac{\frac{T_I s}{K_P} e^{-\theta s}}{\left(\frac{\theta}{\tau_s} T_c s + 1\right)^3} = \frac{G}{1 + G G_c} \tag{4.44}$$

where T_c is the desired tuning parameter. Substituting the respective models of G, G_c and comparing the denominator parts we get the expression

$$\begin{aligned} s^3\left(\frac{\tau_1\tau_2 T_I}{KK_P} - T_I T_D\theta\right) + s^2\left(\frac{T_I(\tau_1 \pm \tau_2)}{KK_P} + (T_I T_D - \theta T_I)\right) + s\left(T_I - \theta \pm \frac{T_I}{KK_P}\right) + 1 \\ = T_c^3 s^3 + 3T_c^2 s^2 + 3T_c s + 1 \end{aligned} \tag{4.45}$$

Controller parameters from (4.45) for stable and unstable systems are

$$K_P = \frac{\mp T_c^3\theta^2 \mp 3T_c^2\tau_s\theta^2 + T_c(3\tau_1\tau_2\tau_s^2 + 3\tau_1\tau_s^2\theta \pm 3\tau_2\tau_s^2\theta) + \tau_1\tau_2\tau_s^3 + \tau_1\tau_s^3\theta \pm \tau_2\tau_s^3\theta}{\theta^2 K(T_c + \tau_s)^3} \tag{4.46}$$

$$T_D = \frac{\theta\left(\tau_s^3\tau_1\tau_2 + 3\tau_s^2\tau_1\tau_2 T_c + 3\tau_s\tau_1\tau_2 T_c^2 \mp T_c^3(\pm\tau_1\theta + \tau_2\theta + \theta^2)\right)}{\mp T_c^3\theta^2 \mp 3T_c^2\tau_s\theta^2 + T_c(3\tau_1\tau_2\tau_s^2 + 3\tau_1\tau_s^2\theta \pm 3\tau_2\tau_s^2\theta) + \tau_1\tau_2\tau_s^3 + \tau_1\tau_s^3\theta \pm \tau_2\tau_s^3\theta} \tag{4.47}$$

$$T_I = \frac{\theta(\mp T_c^3\theta^2 \mp 3T_c^2\tau_s\theta^2 + T_c(3\tau_1\tau_2\tau_s^2 + 3\tau_1\tau_s^2\theta \pm 3\tau_2\tau_s^2\theta) + \tau_1\tau_2\tau_s^3 + \tau_1\tau_s^3\theta \pm \tau_2\tau_s^3\theta)}{(\pm\theta^2 + \theta(\tau_1 \pm \tau_2) + \tau_1\tau_2)\tau_s^3} \tag{4.48}$$

The desired closed loop transfer function for set-point tracking is given as

$$\left(\frac{Y}{R}\right)_d = \frac{(1 + sT_I + s^2T_IT_D)e^{-\theta s}}{\left(\frac{\theta}{T}T_c s + 1\right)^4} \tag{4.49}$$

Using equations from (4.21) to (4.23) we obtain

$$\beta = \frac{\theta T_c}{\tau_s T_I} \tag{4.50}$$

As expected and verified using extensive simulation studies, β in (4.50) causes more peak overshoot in the set-point response. So the following set-point coefficient is adopted

$$\beta = 1 - \frac{\theta T_c}{\tau_s T_I} \tag{4.51}$$

4.5 Estimation of tuning parameter using PSO

The single tuning parameter required to get the tuning parameters for stable/unstable FOPDT and SOPDT processes is obtained from PSO algorithm. There are various optimization methods to maximize or minimize the objective function. The computational effort required for stochastic based methods is less compared with traditional methods. Particle swarm optimization (PSO) was developed by Eberhart and Kennedy in 1995, [82]. This is derived from a group of particles known as swarm based on the studies on bird flocking and fish schooling. These particles move in search space using the velocity vector. The velocity and best position of the particle is updated at every instant. The best value that the particle has achieved is called *pbest*. The updating process will finally guide to a global best solution (*gbest*). Let us consider a m-dimensional search space, an i^{th} particle is distributed in the space as $x_i = [x_{i1}, x_{i2}, x_{i3}\ldots\ldots, x_{im}]$ and it's velocity $v_i = [v_{i1}, v_{i2}, v_{i3}\ldots\ldots, v_{im}]$. The velocity and position are updated as

$$
\begin{aligned}
v_{im}^{t+1} &= \omega.v_{im}^{t} + C1.rand.(pbest_{im} - x_{im}^{t}) + C2.rand.(gbest - x_{im}^{t}) \\
x_{im}^{t+1} &= x_{im}^{t} + v_{im}^{t+1}
\end{aligned}
\tag{4.52}
$$

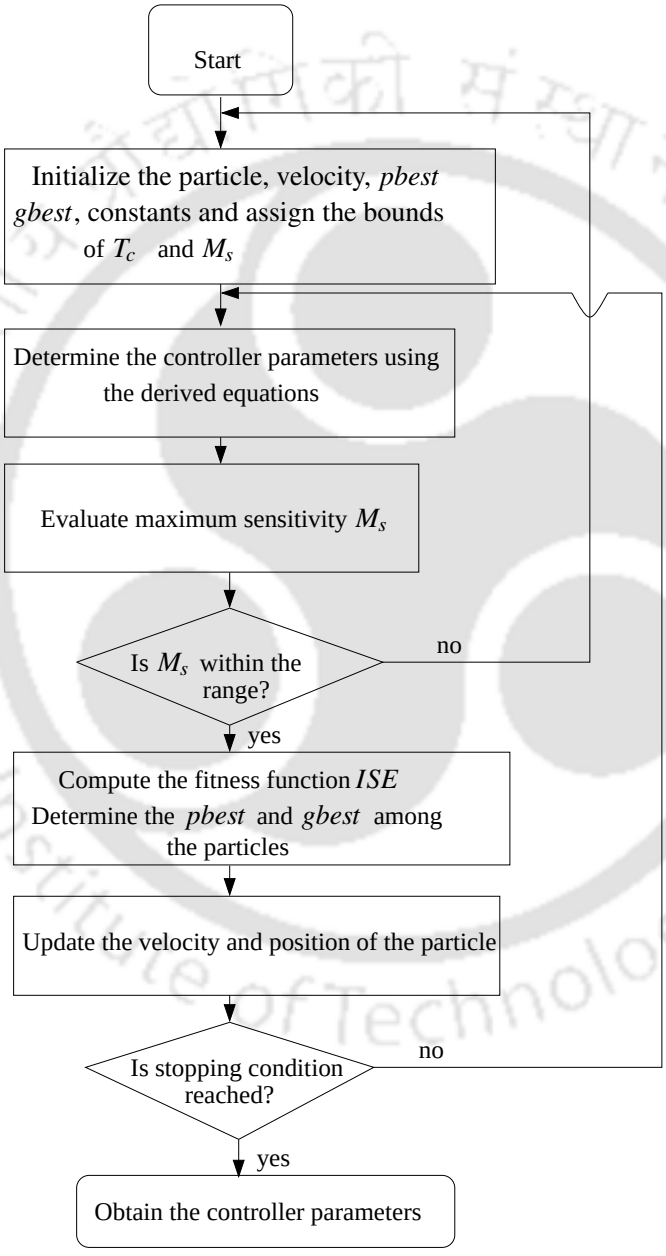

Figure 4.4: PSO algorithm flow chart

The inertia weight factor ω actually leads towards local and global search point and is given in (4.53). Here, acceleration constants $C1$, $C2$ are generally set to 2.0 and *rand* is a uniform

random number between 0 and 1.

$$\omega = \omega_{max} - \frac{\omega_{max} - \omega_{min}}{iter_{max}} iter \tag{4.53}$$

The algorithm for obtaining the best value of T_c is given in Fig. 4.4. The objective function is to minimize the integral square error (ISE) (4.54). The constraint during the search process is to maintain the value of M_s within the specified range. For stable systems, its value is maintained between $1.2 \leq M_s \leq 2.0$ and for unstable systems $1.2 \leq M_s \leq 3.0$.

The fitness function ISE is

$$ISE = \int_0^\infty e(t)^2 dt \tag{4.54}$$

where e is the error in the system. The algorithm ultimately gives us the best tuning parameters with minimum ISE.

4.6 Simulation results

The proposed identification and control method is illustrated on a few standard examples available in the literature. The process models FOPDT and SOPDT are identified initially and then the using the estimated dynamics the controller parameters and set-point coefficients are obtained. The closed-loop performances of the model (ISE (integral square error) and IAE (integral absolute error)) are evaluated.

Example 1

Consider a stable FOPDT process [31]

$$G(s) = \frac{e^{-2s}}{10s+1}$$

Limit cycle parameters for the chosen system obtained from relay test with $h = 1$ are $\dot{y}(t_0) = 0.1$, $\dot{y}(t_1) = 0.0905$, $\dot{y}(t_3) = -0.1$ and $y(t_2) = 0.1813$. The process parameters obtained from this information are $K = 1.0016$, $\tau_1 = 10.0174$ and $\theta = 2.0001$. Error for the identified process is $E_I = 0.00050$. For the same system, Liu and Gao [35] identified a FODPT stable

system which has an error of 0.00223. The model proposed by Vivek and Chidambaram [62] gives an error 0.01610. Using the relay feedback test Srinivasan and Chidambaram [31] identified FOPDT model with an error 0.1176. Therefore, the proposed model has less error compared to the earlier methods in the literature. This shows that the identified process is near to the actual process. The Nyquist plot shown in Fig. 4.5 also depicts the same i.e identified process is close to the actual process. The identified process parameters are shown in Table 4.1. To test the proposed identification method a (White Gaussian) noise with a signal to noise ratio (SNR) of 15dB is added to the system output and is recovered using wavelet transform. The extracted output results in $K = 1.3695$, $\tau_1 = 11.9862$ and $\theta = 1.6648$.

Table. 4.1: Identified process models for Example 1

Method	Process model	Error (E_I)
Proposed	$\frac{1.0016e^{-2.0001s}}{10.0174s+1}$	0.0005
Liu and Gao [35]	$\frac{1.0048e^{-2.002s}}{10.049s+1}$	0.0022
Vivek and Chidambaram [62]	$\frac{0.9467e^{-2s}}{9.5028s+1}$	0.0160
Vivek and Chidambaram [31]	$\frac{1.03e^{-2.3s}}{10.3s+1}$	0.1176

The value of 'T_c' obtained from PSO algorithm is 10.18. Using the identified process model and T_c the controller parameters are evaluated as K_P=4.6005, T_I=5.832, T_D=0.7342. According to the method proposed by Padma Sree et al. [83] the controller parameters are K_P=4.0924, T_I=5.4015, T_D=0.6323. The closed-loop response of the proposed and Padma Sree et al. method are shown is Fig. 4.6. The system is subjected to a step load disturbance of magnitude -0.5 at t=40 *sec*. Padma Sree et al. method has less set-point ISE, but there are some overshoots and undershoots. During the load disturbance, the proposed method has slightly more undershoot, but settles faster than Padma Sree et al. method. The method proposed by Vilanova et al. [52] gives an unstable response. The performance index given in Table 4.2 shows that ISE under load disturbance is less with the proposed method. The

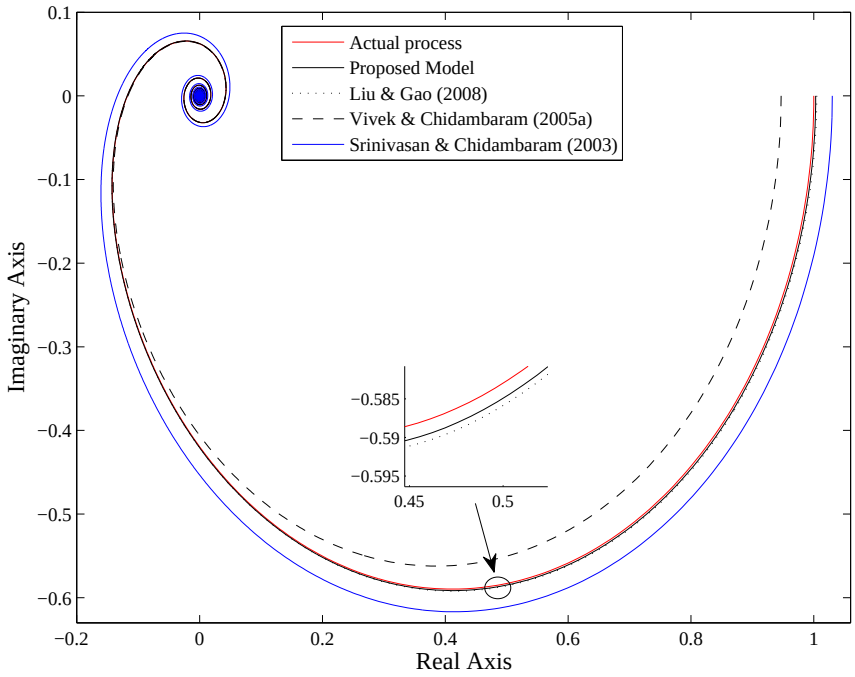

Figure 4.5: Nyquist plot for Example 1

closed-loop response during parameter perturbations (K and θ increased by 10 % and τ_1 is decreased by 5 %) is shown in Fig. 4.7. The performance indices follow the same pattern as that of the nominal case which is shown in Table 4.2. Padma Sree et al. [83] method has unstable set-point response.

Table. 4.2: ISE and IAE for Example 1

Method	Set-point		Disturbance	
	ISE	IAE	ISE	IAE
Proposed	4.040	5.379	0.042	0.633
Padma Sree et al. [83]	2.699	3.969	0.045	0.917
Perturbation	-	-	-	-
Proposed	3.900	5.051	0.049	0.633
Padma Sree et al. [83]	3.543	6.553	0.052	0.943

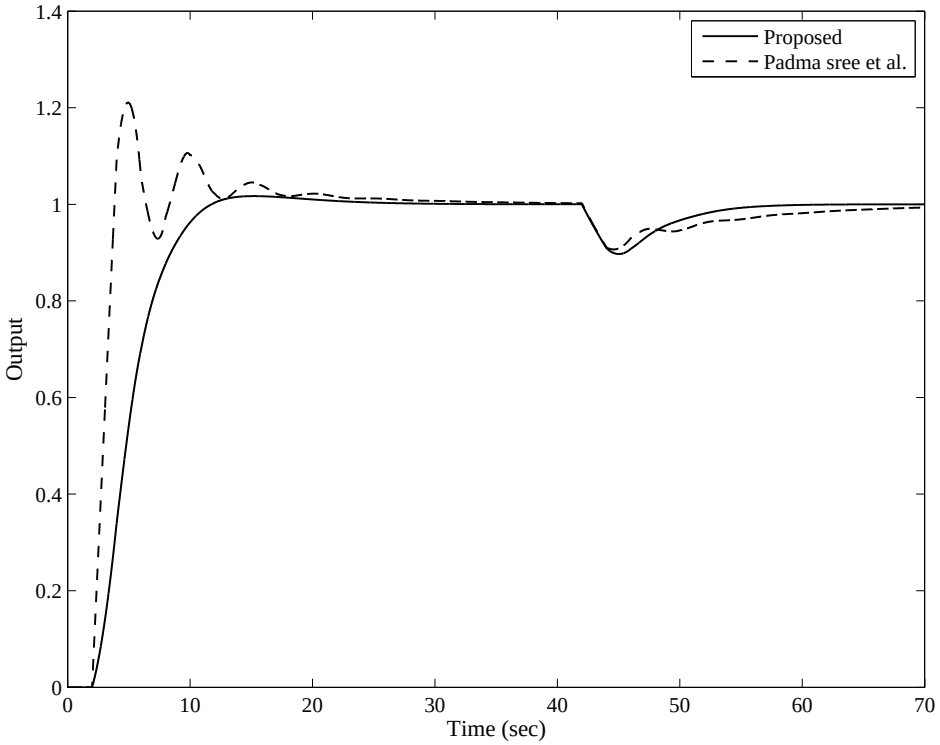

Figure 4.6: Closed loop response for Example 1

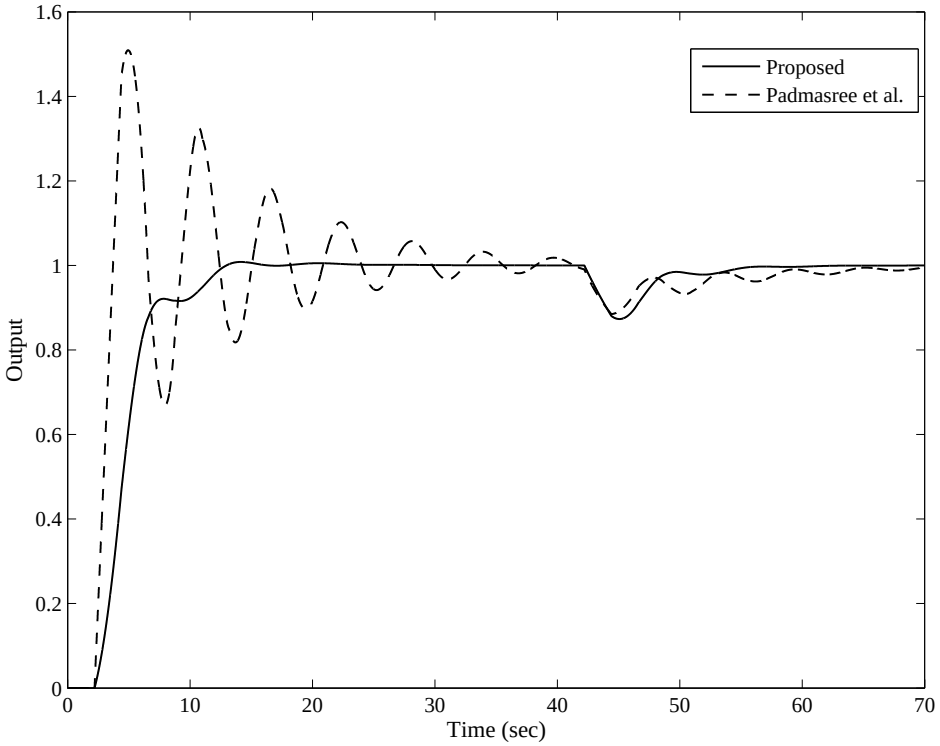

Figure 4.7: Closed-loop response with perturbations in process parameters for Example 1

Example 2

Let us consider a stable FOPDT process

$$G(s) = \frac{e^{-0.5s}}{s+1}$$

The process parameters obtained from the relay test are K=1.0015, τ_1=1.0010 and θ=0.49858. The identification error for the proposed model is 0.00957. The measurement noise with SNR of 15 dB is introduced at the system output and is denoised with the wavelet transform method. To get the required data for the identification, the derivative of the denoised signal is obtained and then the model parameters are obtained as $K = 0.7319$, $\tau_1 = 0.8635$ and $\theta = 0.5981$. The obtained process parameters are used for the controller design.

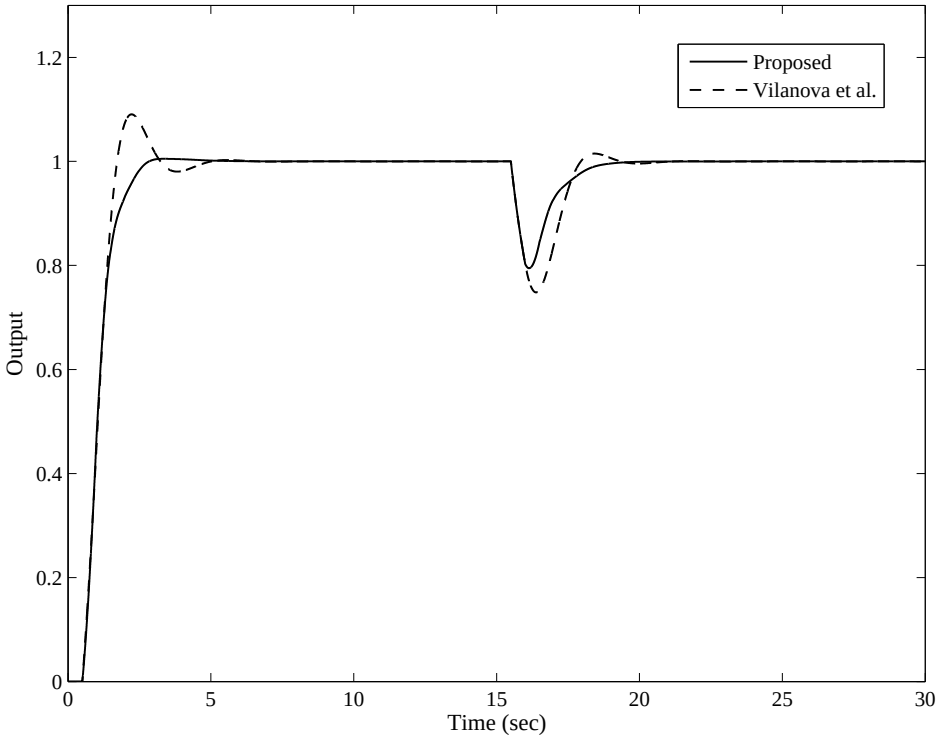

Figure 4.8: Closed loop response for Example 2

The gbest value of the tuning parameter (T_c) generated from the PSO algorithm is 0.87. Therefore, the controller parameters obtained from (4.17), (4.18) and (4.19) are $K_P = 2.033$, $T_I = 1.038$ and $T_D = 0.1774$ and M_s=1.99. The set-point coefficient β is 0.581. Vilon-

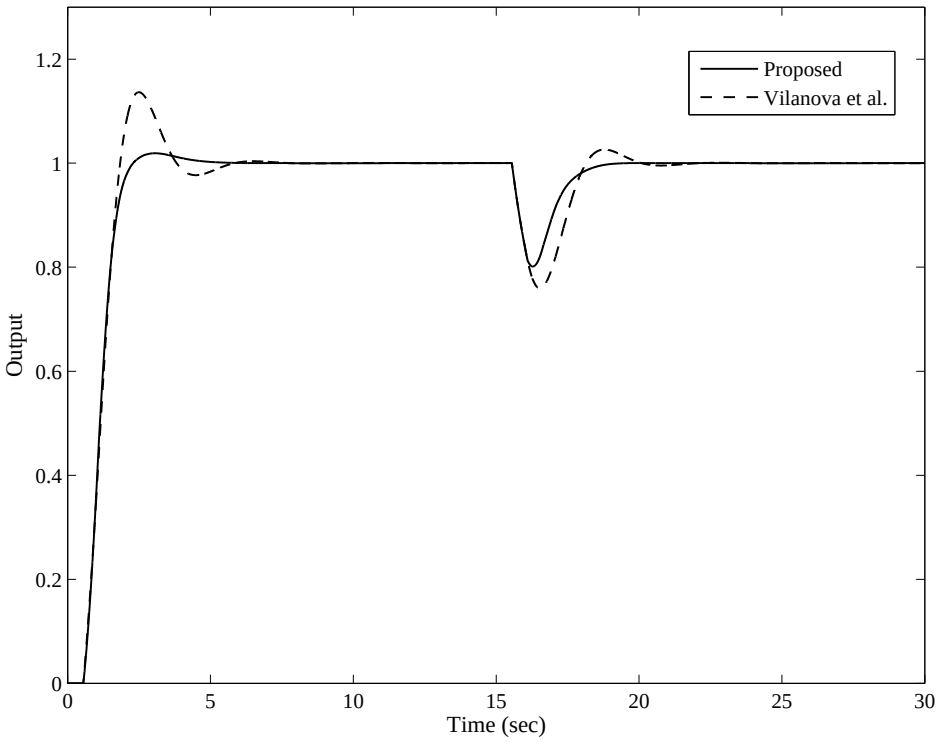

Figure 4.9: Closed-loop response with perturbations in process parameters for Example 2

Table. 4.3: ISE and IAE for Example 2

Method	Set-point		Disturbance	
	ISE	IAE	ISE	IAE
Proposed	0.884	1.139	0.034	0.258
Vilanova et al. [52]	0.879	1.164	0.064	0.358
Perturbation	-	-	-	-
Proposed	0.965	1.210	0.035	0.259
Vilanova et al. [52]	0.983	1.357	0.065	0.393

ava et al. [52] proposed the controllers $1.2462(0.5981+\frac{1}{0.8276s})$ and $1.2462(1+\frac{1}{0.8276s})$ for set-point and disturbance rejection. The closed-loop response in Fig. 4.8 shows that the proposed method has less peak overshoot in set-point response. At $t = 15sec$, the system is subjected to a unit step load disturbance of magnitude -0.5.

The magnitude of the response during load disturbance is high for Vilanova et al. method. The proposed method gives good load disturbance attenuation and the performance indices are given in Table 4.3. The proposed method is tested under parameter perturbations with K reduced by 5%, θ increased by 10% and τ_1 increased by 10%. The closed-loop response shown in Fig. 4.9 reveals that the proposed method has better performance.

Table. 4.4: Identified process models for Example 3

Method	Process model	Error (E_I)
Proposed	$\frac{1.0019e^{-0.4002s}}{1.0024s-1}$	0.0028
Liu and Gao [35]	$\frac{1.0001e^{-0.4s}}{0.9976s-1}$	0.0052
Padhy and Majhi [19]	$\frac{e^{-0.3998s}}{0.9932s-1}$	0.0137

Example 3

An unstable FOPDT process is considered as

$$G(s) = \frac{e^{-0.4s}}{s-1}$$

The recorded limit cycle parameters are $\dot{y}(t_0) = 1$, $\dot{y}(t_1) = 1.2208$, $\dot{y}(t_3) = -1$ and $y(t_2) = 0.4917$. The parameters obtained from the explicit expressions (4.10), (4.12) and (4.13) results in K=1.0019, τ_1=1.0024 and θ=0.4002. The obtained process has error $E_I = 0.00282$. The process models are tabulated in Table 4.4. The estimated FOPDT model with the proposed method has less error compared with Liu and Gao [35] and Padhy and Majhi [19], as shown in Fig. 4.10.

The tuning parameter is obtained as $T_c = 1.22$. The PID parameters obtained from (4.17), (4.18) and (4.19) are $K_P = 2.638$, $T_I = 2.671$, $T_D = 0.163$ and the value of M_s is 2.9. The closed-loop response with a unit step disturbance of magnitude -0.5 is compared with the two degree of freedom control structure proposed by Ajmeri and Ali [54] and is shown in Fig. 4.11. It is observed that there is a small peak in the set-point response with the proposed method compared with Ajmeri and Ali method. During the load disturbance, the proposed

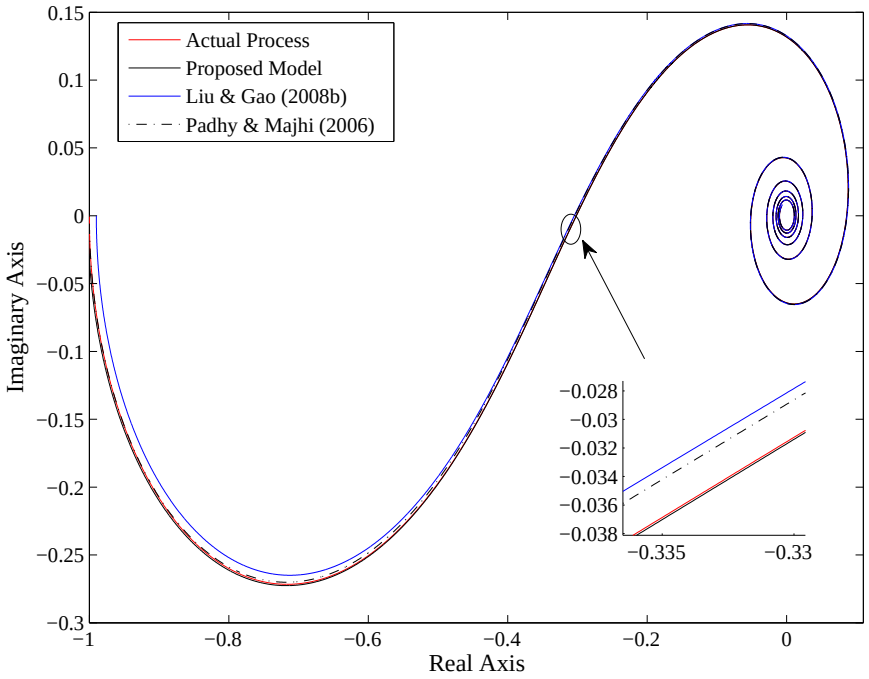

Figure 4.10: Nyquist plot for Example 3

method has less ISE. The performance parameters are shown in Table 4.5. The effectiveness of the proposed method is observed by introducing a perturbation in τ_1 by 10% $\left(\frac{e^{-0.4s}}{1.1s-1}\right)$ and the closed-loop response is shown in Fig. 4.12.

Table. 4.5: ISE and IAE for Example 3

Method	Set-point		Disturbance	
	ISE	IAE	ISE	IAE
Proposed	0.987	1.428	0.110	0.506
Ajmeri and Ali [54]	0.881	1.204	0.250	0.815
Perturbation	-	-	-	-
Proposed	1.031	1.503	0.108	0.511
Ajmeri and Ali [54]	0.936	1.319	0.244	0.831

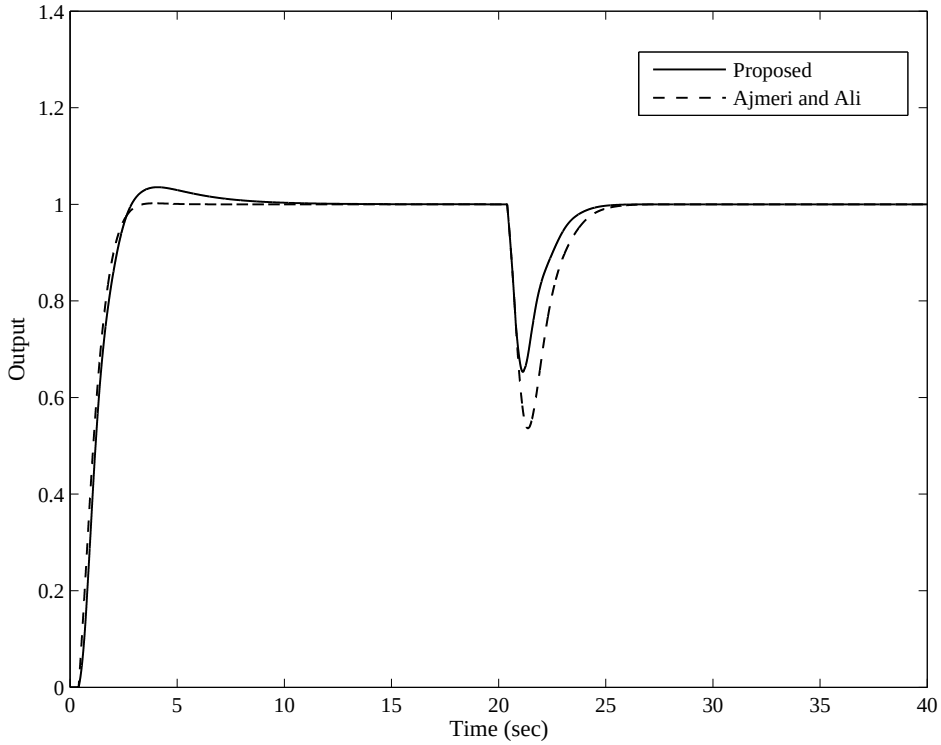

Figure 4.11: Closed loop response for Example 3

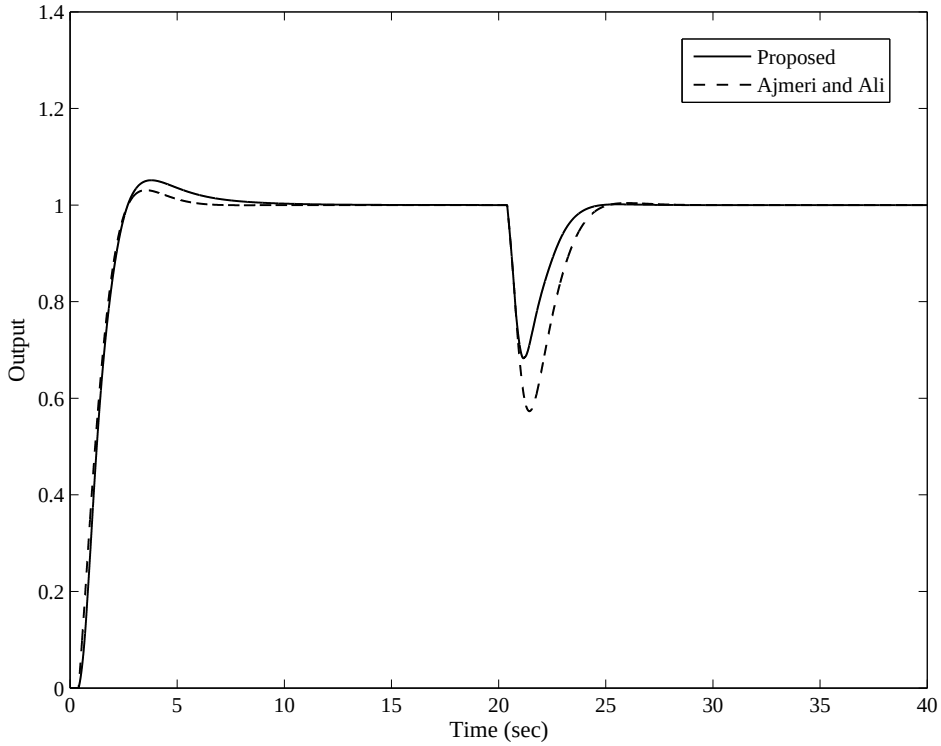

Figure 4.12: Closed loop response during parameter perturbations for Example 3

4.6.1 Example 4

Consider a stable SOPDT process

$$G(s) = \frac{2e^{-s}}{(10s+1)(5s+1)}$$

The proposed relay feedback test to the stable SOPDT process gives limit cycle output with the measured values as $t_1 = 1$, $t_p = 2.749$, $A_p = 0.1734$ and $t_2 = 6.0688$. Substituting the measurements in (4.38), (4.40) and (4.43) and solving these equations, process parameters are estimated as $K = 1.976$, $\theta = 0.999$, $\tau_1 = 9.7453$ and $\tau_2 = 5.0748$. The identified model has an error of 0.001.

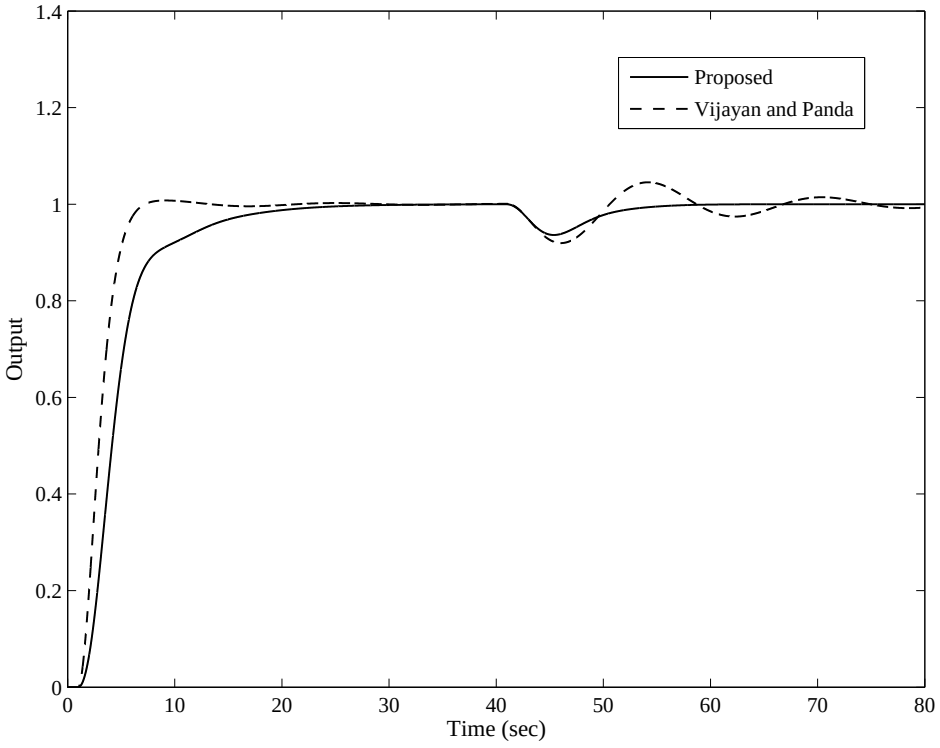

Figure 4.13: Comparison of set-point and load disturbance responses for Example 4

The tuning parameter is obtained as $T_c = 13.5$. The controller parameters for the stable SOPDT process are obtained from (4.46), (4.47) and (4.48) as $K_P = 7.870$, $T_I = 6.688$ and $T_D = 1.911$. and $M_s = 2.0$. The controller responses for the proposed method and Vijayan and Panda method [53] with a unit step load disturbance of magnitude -0.5 at time $t = 40sec$

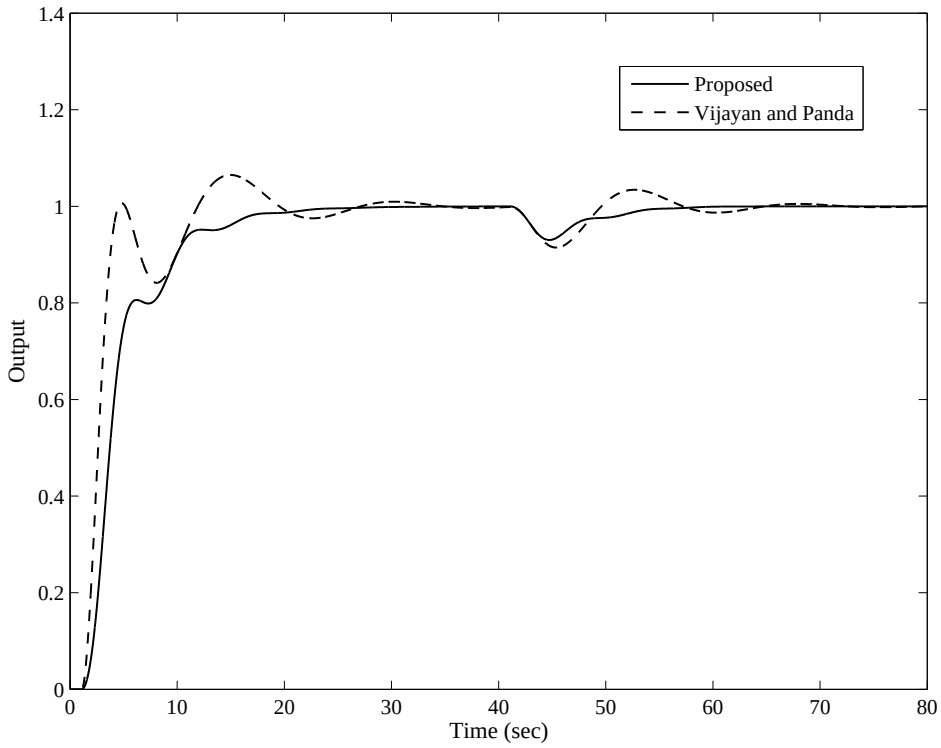

Figure 4.14: Closed loop response with perturbation of process parameters for Example 4

Table. 4.6: ISE and IAE for Example 4

Method	Set-point		Disturbance	
	ISE	IAE	ISE	IAE
Proposed	3.441	5.070	0.018	0.425
Vijayan and Panda [53]	2.419	3.186	0.039	0.905
Perturbation	-	-	-	-
Proposed	3.264	5.031	0.017	0.425
Vijayan and Panda [53]	2.318	3.786	0.031	0.662

are plotted in Fig. 4.13. A satisfactory set-point response is observed with the proposed method. The method proposed by Vijayan and Panda gives a good set-point response but during disturbance, it takes longer time to settle. The proposed method has good load disturbance rejection and the performance measures are given in Table 4.6. An *ISE* of 0.0181 is

obtained during disturbance condition which is less compared to that of Vijayan and Panda method. The method is tested under parameter variations with K and θ as $+10\%$ and time constants (τ_1 and τ_2) as -10% which is shown in Fig. 4.14. Vijayan and Panda method has more peak during load disturbance.

4.6.2 Example 5

An unstable process is considered as

$$G(s) = \frac{e^{-0.5s}}{(2s-1)(0.5s+1)}$$

The limit cycle measurements generated from relay feedback test are $t_1 = 0.5$, $t_p = 1.1407$, $A_p = 0.4464$ and $t_2 = 2.7607$. The process parameters obtained with the proposed identification method are $K = 1.0023$, $\theta = 0.5$, $\tau_1 = 2.044$ and $\tau_2 = 0.5011$. The error of the identified model is 0.00125. Using few approximations, Nema and Padhy identified the process model with an error of 0.017. Hence, the identified model is close to the actual process. The identified process is used in the PID and set-point filter design.

The controller parameters for the proposed method with $T_c = 18.4$ are $K_P = 3.170$, $T_I = 3.925$ and $T_D = 0.4341$. The proposed controller settings give the value of $M_s = 2.98$. According to the CO PI-PD scheme proposed by Nema and Padhy [58], the parameters are $K_p = 0.78$, $T_i = 1.65$, $k_f = 1.87$ and $T_d = 0.72$. The double feedback loops proposed by Vijayan and Panda [53] gives the controller parameters as $k_{c1} = 1.3977$, $k_c = 0.591$, $T_i = 2.077$, $T_d = 1.4746$ and $\lambda = 0.25$. The closed-loop responses are shown in Fig. 4.15. A step load disturbance of magnitude -0.5 is given at $t = 40sec$. The corresponding performance measures are given in Table 4.7. Vijayan and Panda [53] method has better *ISE* value during set-point tracking. But, during load disturbance, the proposed method has less *ISE* value than that proposed by Vijayan and Panda [53]. The robustness of the proposed method is tested with the plant mismatch of $\frac{1.1e^{-0.55s}}{(1.9s+1)(0.525s+1)}$. The response in Fig. 4.16 shows that the proposed method gives a satisfactory response.

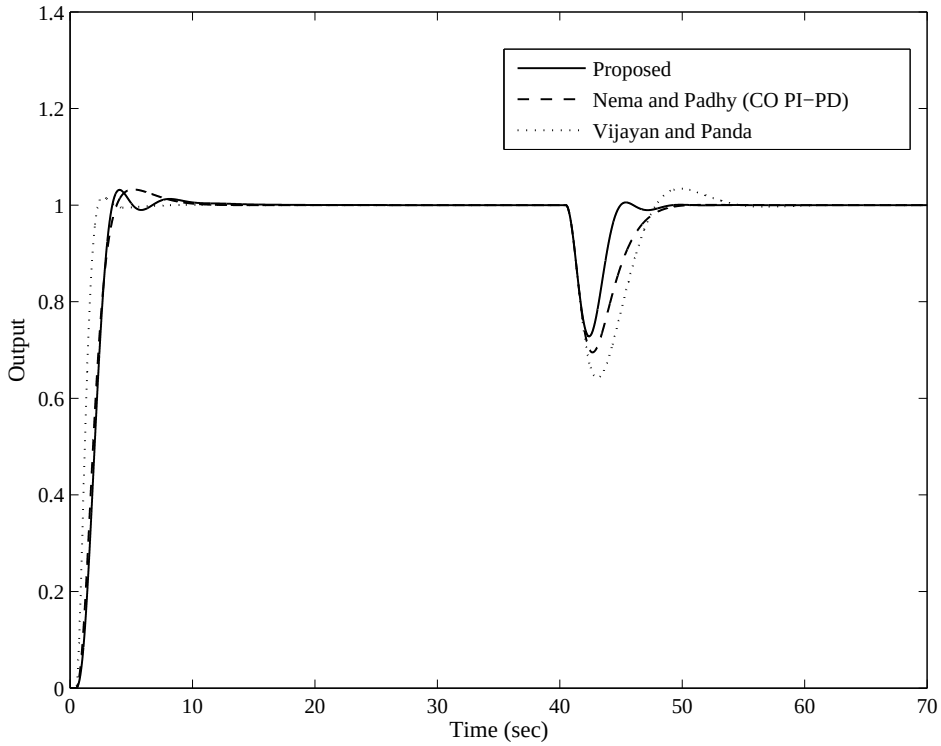

Figure 4.15: Comparison of set-point and load disturbance responses for Example 5

Table. 4.7: ISE and IAE for Example 5

Method	Set-point		Disturbance	
	ISE	IAE	ISE	IAE
Proposed	1.648	2.121	0.122	0.628
Nema and Padhy [58]	1.540	2.070	0.223	1.061
Vijayan and Panda [53]	1.022	1.281	0.238	1.523
Perturbation	-	-	-	-
Proposed	1.062	2.188	0.130	0.692
Nema and Padhy [58]	1.479	2.033	0.216	1.058
Vijayan and Panda [53]	1.043	1.668	0.346	1.308

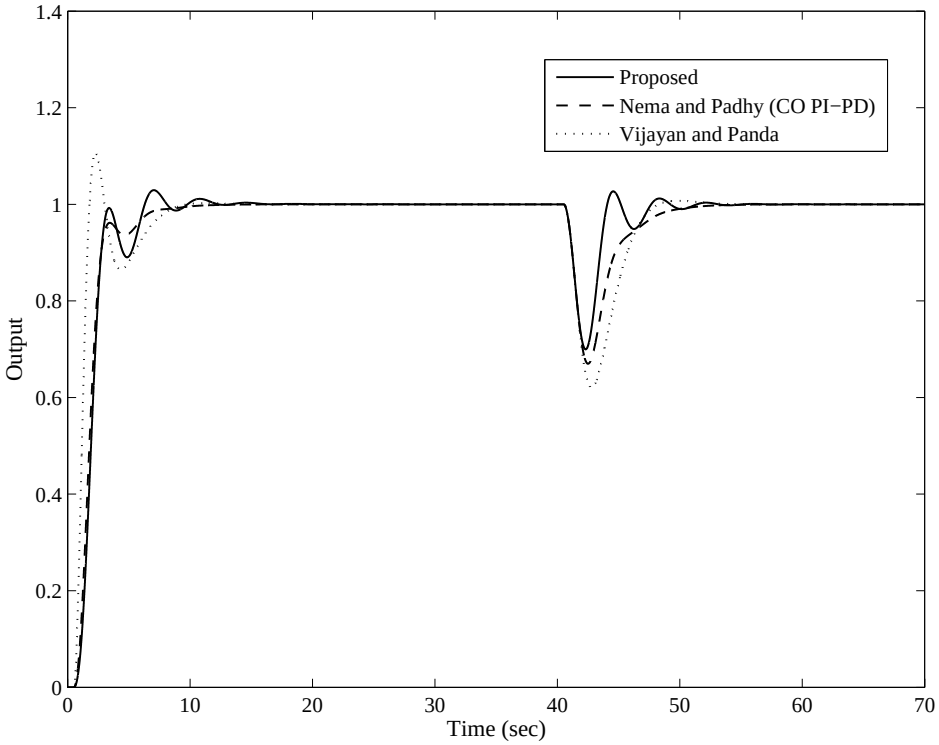

Figure 4.16: Closed loop response with perturbation of process parameters for Example 5

4.6.3 Example 6

Let us consider an unstable SOPDT process

$$G(s) = \frac{e^{-0.939s}}{(5s-1)(2.07s+1)}$$

The limit cycle information $t_1 = 0.9384$, $t_p = 3.5826$, $A_p = 0.4525$ and $t_2 = 8.241$ are used in (4.38), (4.40) and (4.43) to identify the process. The resultant process parameters are $\tau_1 = 4.9875$, $\tau_2 = 2.0666$, $K = 0.9975$ and $\theta = 0.9384$. The error of the identified model is $E_I = 0.00048$. For the same process, Nema and Padhy [58] identified the model with an error of 0.0028. However, the proposed model is very close to the real process dynamics. The best value of T_c generated from PSO algorithm is 11.64 which gives $K_P = 5.443$, $T_I = 6.836$ and $T_D = 1.4489$. The value of β and M_s are 0.77 and 2.97, respectively. Vijayan and Panda [53] controlled the same process with a double feedback loop. Nema and Padhy [78] proposed PSO PI-PD structure to control the process. The control response is shown in Fig. 4.17 with a step load disturbance of magnitude -0.5 at $t = 40sec$. It is seen that the proposed

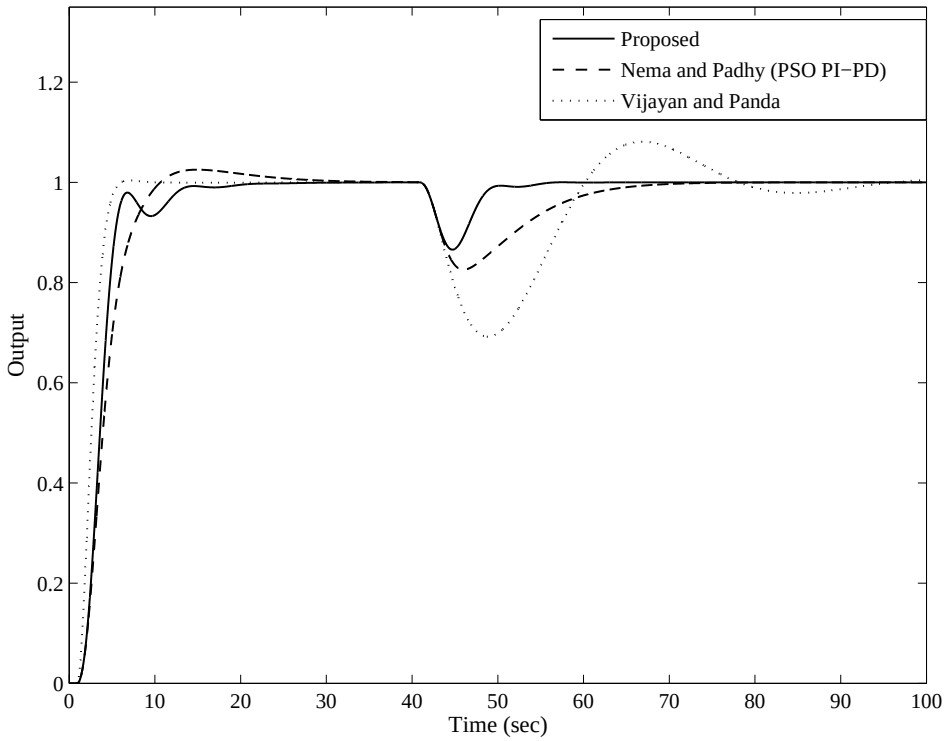

Figure 4.17: Comparison of set-point and load disturbance responses for Example 6

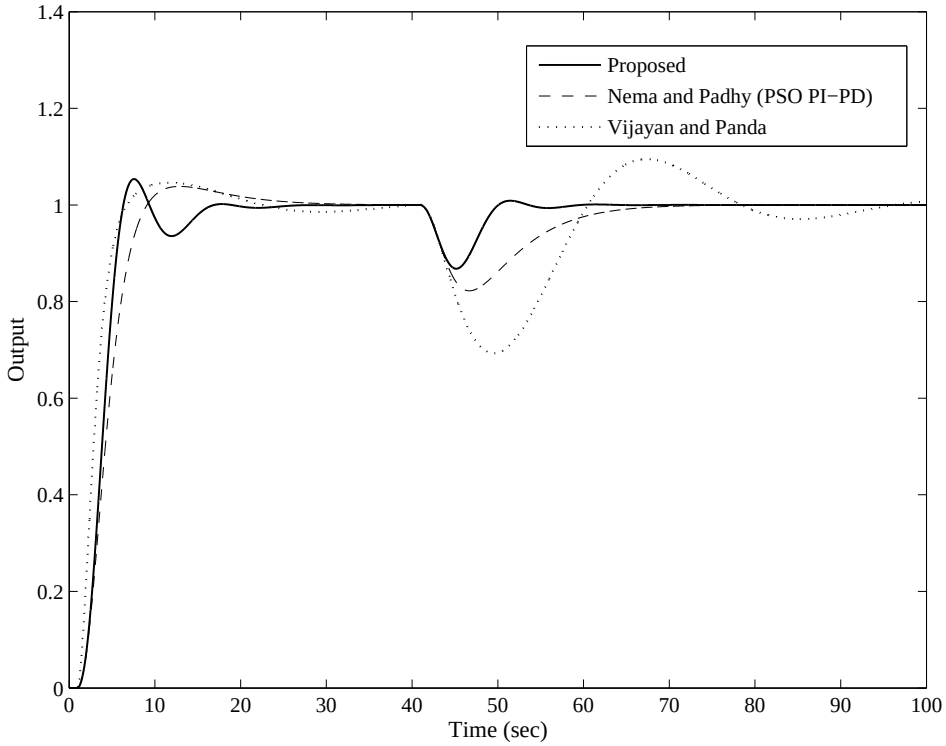

Figure 4.18: Closed loop response with +10% perturbation in time constant for Example 6

method has good load disturbance attenuation. The performance measure given in Table 4.8 shows that the value of *ISE* is very less during the load change. It is evident that the proposed method yields improved responses during load disturbances apart from the satisfactory set-point response. To check the robustness of the controller, the time constants of the process are varied to $+10\%$ and the response is shown in Fig. 4.18. The proposed method quickly tracks the reference during disturbance compared with Nema and Padhy PSO PI-PD [78] and Vijayan and Panda methods [53].

Table. 4.8: ISE and IAE for Example 6

Method	Set-point		Disturbance	
	ISE	IAE	ISE	IAE
Proposed	2.977	4.032	0.058	0.629
Nema and Padhy [78]	3.237	4.619	0.221	1.920
Vijayan and Panda [53]	2.169	2.750	0.863	4.526
Perturbation	-	-	-	-
Proposed	3.147	4.257	0.062	0.676
Nema and Padhy [78]	3.421	4.846	0.228	1.921
Vijayan and Panda [53]	2.375	3.683	0.901	4.836

4.7 Summary

The parameters of FOPDT and SOPDT stable/unstable processes are identified using state-space method. The identified models are used in the controller design. The PID controller present in the closed-loop is designed basically to reject the load disturbance. To achieve this, the required expressions are obtained using direct synthesis method. A set-point filter is used to get satisfactory set-point tracking. The required tuning parameter to find PID

parameters is determined using PSO algorithm. It gives the best tuning parameter based on error minimization. Some of the examples in literature are considered to show the efficacy of the proposed identification and control method. The simulation results have shown that the proposed method performs well during the disturbance. However, there is a slight degrade in the set-point response because the objective of the controller design is to attenuate the load disturbance.

Indian Institute of Technology Guwahati

CHAPTER 5

CONCLUSIONS AND FUTURE WORK

5.1 Conclusions

Identification of process models is essential for the analysis and controller design purpose. There are several works reported in the literature on relay based identification. To improve the identification accuracy, some modifications to the relay method are done. There is still some scope to extend this method. The key findings of the study are discussed in this section

A. Identification of FOPDT and SOPDT processes using dual-input describing function (DIDF)

The relay feedback response is utilized to identify different process models. The process parameters are estimated using the DIDF approximation. Expressions for the parameters of the process models are derived for both on-line and off-line methods. Identification is performed for nominal and during low load disturbance condition. The issue of measurement noise is a problem in process industries. Here, the identification is also done during noisy conditions. Wavelet transform is used to recover a noise-free output. The results of the identified models and Nyquist plots depicts that there is some improvement in the identification accuracy. However, during the load disturbance, the error has increased as compared with the nominal case. The proposed DIDF approximation is implemented on the DC-DC buck converter. The results indicate that the identified model has better performance. With simple analytical expressions and using important limit cycle measurements, the converter model is

extracted. Therefore, the method is proven to have less complexity.

B. State-Space approach for the Identification of FOPDT and SOPDT Processes

The estimated models using DIDF method gives approximated results. To improve the identification accuracy, the state-space method is used. Mathematical expressions to determine process parameters of FOPDT and SOPDT stable/unstable processes are derived for the off-line method. These expressions utilize half limit cycle information. The results of the identified models show that the proposed method has better accuracy. Also, the estimated parametric model of DC-DC buck converter has better closed-loop performance. The model verification test shows that the identified model can perform well during parameter perturbations as well.

C. Identification and Control of FOPDT and SOPDT Processes

The process models are identified using the state-space method and using the identified process parameters a model-based controller is designed. The identification results show that the models are near to actual process. PID controller is designed using the direct synthesis method primarily to reject the load disturbance. The required tuning parameter to obtain the controller parameters is obtained optimally from the PSO algorithm. The set-point filter tracks the reference value. Some standard well-known examples are considered to show the efficacy of the proposed method. It is evident from the closed-loop performance that there is good load disturbance attenuation. Even during parameter variations, the method is able to give a satisfactory response. The set-point point response is seen to be slightly sluggish. To achieve better set-point tracking, the design of set-point coefficient can be modified.

5.2 Scope for further work

In this thesis, some design methods are given, these can be extended further

- The DIDF method can be extended to identify the process models in presence of disturbance/offset with better accuracy.
- It is worth to do on-line identification using state-space approach. This will further enhance the identification accuracy.
- The identification methods can be applied to non-minimum phase systems. It can be implemented practically on the existing non-minimum phase converter topologies.
- In this thesis, the identification methods are used to determine a linear model. These methods can be extended to identify nonlinear processes as well.

भारतीय प्रौद्योगिकी संस्थान गुवाहाटी
Indian Institute of Technology Guwahati

LIST OF PUBLICATIONS

Journal Publications

1. Kasi V. R, Majhi S. and Gogoi, A. K., "Modeling and Estimation of DC-DC Buck Converter Dynamics using Relay Feedback Output with Performance Evaluation", *IEEE Transactions on Circuits and Systems II: Express Briefs*, (DOI: 10.1109/TCSII.2018.2843526).

2. Kasi V. R, Majhi S. and Gogoi, A. K., "Identification of DC-DC Buck Converter Dynamics using Relay Feedback Method with Experimental Validation", *IET Circuits, Devices & Systems (IET)* (DOI: 10.1049/iet-cds.2017.0542).

3. Kasi V. R, Majhi S. and Gogoi, A. K., "Identification and PID tuning techniques for stable and unstable SOPDT processes", *International Journal of Dynamics and Control (Springer)* (DOI: 10.1007/s40435-017-0362-2).

4. Kasi V. R, Majhi S. and Gogoi, A. K., "System Identification and Control of Underdamped System Using Dual Input Describing Function", *Journal of control and system Engg (Bowen Publishing)*, vol. 4(1), 51-61, 2016.

Conference Publications

1. Kasi V. R, Majhi S. and Gogoi, A. K., "Identification of higher order critically damped systems using relay feedback test", *ICPEICES 2016*, Delhi Technical University, India 2016.

2. Kasi V. R, Majhi S. and Gogoi, A. K., "Estimation of Stable FOPDT and SOPDT Process Using Dual Input Describing Function", *11^{th} Int. Conf. on Industrial and Information Systems (ICIIS 2016)*, IIT Roorkee, India 2016.

3. Kasi V. R, Majhi S. and Gogoi, A. K., "State Space Modelling of stable and unstable FOPDT processes", *11th Int. Conference on Control, Automation, Robotics and Vision (ICARV 2018)*, Singapore 2018 (submitted).

APPENDIX A

SUPPLEMENTARY MATERIALS

A.1 State-space average Modelling

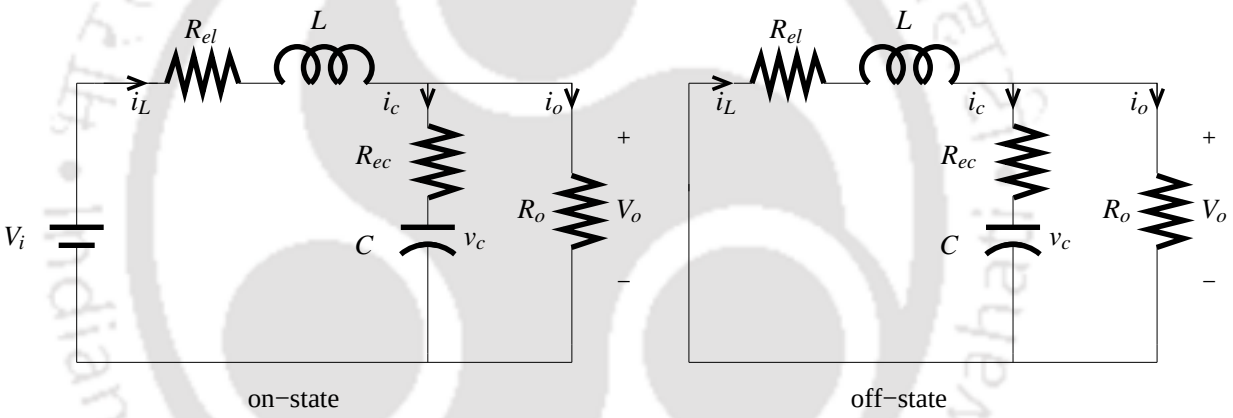

Figure A.1: Buck converter circuit during on and off states.

The buck converter shown in Fig. 2.12 has two states (on and off states). To derive the converter transfer function, the dynamic equations obtained from both the states with dynamic variables i_L and v_c are utilized.

During on-state, the switch is connected to the source as shown in Fig. A.1 and by applying Kirchoff's voltage and current (KVL and KCL), the equations are obtained as

$$V_i = L\frac{di_L}{dt} + i_L R_{eL} + V_o \tag{A.1}$$

Where V_o can be written as

$$V_o = i_c R_{ec} + v_c \tag{A.2}$$

From the circuit, $i_c = i_L - i_o$ and $i_o = \frac{V_o}{R_o}$ gives

$$V_o = i_L R_{ec} - \frac{V_o}{R_o} R_{ec} + v_c \tag{A.3}$$

$$V_i = L\frac{di_L}{dt} + i_L(R_{eL} + R_{ec}R_{eq}) + v_c R_{eq} \tag{A.4}$$

Expressing in terms of the state variable i_L gives

$$\frac{di_L}{dt} = -i_L\left(\frac{R_L + R_c R_{eq}}{L}\right) - v_c\frac{R_{eq}}{L} + \frac{V_i}{L} \tag{A.5}$$

The output equation (A.3) can be simplified as

$$V_o = i_L R_{ec} R_{eq} + v_c R_{eq} \tag{A.6}$$

The other equation is obtained from KCL as

$$i_L = i_c + i_o \tag{A.7}$$

$$C\frac{dv_c}{dt} = i_L - \frac{V_o}{R_o} \tag{A.8}$$

Substituting V_o in (A.8) gives

$$\frac{dv_c}{dt} = i_L\frac{1}{C}\left[1 - \frac{R_{ec}R_{eq}}{R_o}\right] - v_c\frac{R_{eq}}{CR_o} \tag{A.9}$$

During off-state, applying KVL to the circuit shown in Fig. A.1 gives the following equation

$$v_L = -i_L R_{el} - V_o \tag{A.10}$$

Where the output voltage V_o can be obtained as $V_o = i_L R_{ec} R_{eq} + v_c R_{eq}$. Therefore, Eq. (A.10) becomes

$$\frac{di_L}{dt} = -i_L\frac{1}{L}(R_{el} + R_{ec}R_{eq}) - v_c\frac{R_{eq}}{L} \tag{A.11}$$

From the KCL the equation is obtained as

$$\frac{dv_c}{dt} = i_L\frac{1}{C}\left[1 - \frac{R_{ec}R_{eq}}{R_o}\right] - v_c\frac{R_{eq}}{R_o C} \tag{A.12}$$

Representing the equations (A.5), (A.9) and (A.11), (A.12) in state-space form as:

During on-state,

$$\dot{\mathbf{x}} = \mathbf{A}_1\mathbf{x} + \mathbf{b}_1 V_i \tag{A.13}$$

$$V_o = \mathbf{c}_1\mathbf{x} \tag{A.14}$$

During off-state,

$$\dot{\mathbf{x}} = \mathbf{A}_2\mathbf{x} + \mathbf{b}_2 V_i \tag{A.15}$$

$$V_o = \mathbf{c}_2\mathbf{x} \tag{A.16}$$

The matrices are given as

$$\mathbf{A}_1 = \begin{bmatrix} -\left(\frac{R_L + R_c R_{eq}}{L}\right) & -\frac{R_{eq}}{L} \\ \frac{1}{C}\left[1 - \frac{R_{ec}R_{eq}}{R_o}\right] & -\frac{R_{eq}}{CR_o} \end{bmatrix} ; \mathbf{b}_1 = \begin{bmatrix} \frac{1}{L} \\ 0 \end{bmatrix} ; \mathbf{c}_1 = \begin{bmatrix} R_{ec}R_{eq} & R_{eq} \end{bmatrix} \tag{A.17}$$

$$\mathbf{A}_2 = \begin{bmatrix} -\frac{1}{L}(R_{el} + R_{ec}R_{eq}) & -\frac{R_{eq}}{L} \\ \frac{1}{C}\left[1 - \frac{R_{ec}R_{eq}}{R_o}\right] & -\frac{R_{eq}}{R_o C} \end{bmatrix} ; \mathbf{b}_2 = \begin{bmatrix} 0 \\ 0 \end{bmatrix} ; \mathbf{c}_2 = \begin{bmatrix} R_{ec}R_{eq} & R_{eq} \end{bmatrix} \tag{A.18}$$

Where $\mathbf{x} = \begin{bmatrix} i_L \\ v_c \end{bmatrix}$

The small signal model is obtained as [72]

$$\dot{\hat{\mathbf{x}}} = \mathbf{A}\hat{\mathbf{x}} + \mathbf{b}\hat{V}_i + [(\mathbf{A}_1 - \mathbf{A}_2)\mathbf{X} + (\mathbf{b}_1 - \mathbf{b}_2)V_i]\hat{d} \tag{A.19}$$

$$\hat{\mathbf{y}} = \mathbf{c}\mathbf{x} + (\mathbf{c}_1 - \mathbf{c}_2)\mathbf{X}\hat{d} \tag{A.20}$$

Where $\mathbf{A} = \mathbf{A}_1 D + \mathbf{A}_2(1-D)$, $\mathbf{b} = \mathbf{b}_1 D + \mathbf{b}_2(1-D)$ and $\mathbf{c} = \mathbf{c}_1 D + \mathbf{c}_2(1-D)$.

Therefore, the transfer function $\frac{\hat{v}_o}{\hat{d}}$ is obtained as

$$\frac{\hat{v}_o}{\hat{d}} = \frac{R_{eq}R_o(R_{ec}Cs+1)V_{in}}{(((R_{ec}Cs+1)R_{eq}+Cs(Ls+R_{el}))R_o+R_{eq}(Ls+R_{el}))} \tag{A.21}$$

Table. A.1: Buck converter specifications

Design parameters	Value
Input voltage (V_i)	18 V
Inductance (L)	0.560 mH
Inductor ESR (R_l)	0.12 Ω
Capacitance (C)	98 μF
Capacitor ESR (R_c)	0.365 Ω
Converter output voltage (V_o)	6 V
Load resistance (R_L)	10 Ω
Duty cycle (D)	0.3
Switching frequency (f_s)	20 kHz

A.2 Detailed derivation of the expressions (3.14) and (3.15)

The transfer function given in (3.13) can be represented as

$$\frac{Y(s)}{U(s)e^{-\theta s}} = \frac{K\lambda_1\lambda_2}{(s\mp\lambda_1)(s-\lambda_2)} \tag{A.22}$$

Taking partial fractions of (A.22) and rearranging gives

$$\frac{Y(s)}{U(s)e^{-\theta s}} = a\left[\pm\frac{1}{(s\mp\lambda_1)}\mp\frac{1}{(s-\lambda_2)}\right] \tag{A.23}$$

where

$$a = \frac{\pm\lambda_1\lambda_2}{\lambda_1\mp\lambda_2} \tag{A.24}$$

Let us represent

$$Y(s) = Y_1(s)+Y_2(s) \tag{A.25}$$

Therefore, Eq. (A.24) is written as

$$\frac{Y_1(s)}{U(s)e^{-\theta s}} + \frac{Y_2(s)}{U(s)e^{-\theta s}} = \pm\frac{a}{(s-\lambda_1)} \mp \frac{a}{(s-\lambda_2)} \tag{A.26}$$

The above equation is separated into two equations as

$$Y_1(s)\,(s-\lambda_1) = \pm aU(s)e^{-\theta s} \tag{A.27}$$

$$Y_2(s)\,(s-\lambda_2) = \mp aU(s)e^{-\theta s} \tag{A.28}$$

Applying inverse Laplace transform to (A.27), (A.28) and (A.25) gives

$$\dot{y}_1(t) \mp \lambda_1 y_1(t) = au(t-\theta) \tag{A.29}$$

$$\dot{y}_2(t) - \lambda_2 y_2(t) = -au(t-\theta) \tag{A.30}$$

$$y(t) = y_1(t) + y_2(t) \tag{A.31}$$

Let

$$x_1(t) = y_1(t); \qquad x_2(t) = y_2(t) \tag{A.32}$$

Therefore, (A.29), (A.30) and (A.31) becomes

$$\dot{x}_1(t) = \pm\lambda_1 x_1(t) \pm au(t-\theta) \tag{A.33}$$

$$\dot{x}_2(t) = \lambda_2 x_2(t) \mp au(t-\theta) \tag{A.34}$$

$$y(t) = x_1(t) + x_2(t) \tag{A.35}$$

The two equations (A.33) and (A.34) can be represented in state-space from as

$$\begin{bmatrix} \dot{x}_1(t) \\ \dot{x}_2(t) \end{bmatrix} = \begin{bmatrix} \pm\lambda_1 & 0 \\ 0 & \lambda_2 \end{bmatrix} \begin{bmatrix} x_1(t) \\ x_2(t) \end{bmatrix} + \begin{bmatrix} \pm a \\ \mp a \end{bmatrix} u(t-\theta) \tag{A.36}$$

The output equation (A.35) becomes

$$y(t) = \begin{bmatrix} 1 & 1 \end{bmatrix} \mathbf{x}(t) \tag{A.37}$$

Representing (A.36) and (A.37) in the following standard state-space form

$$\dot{\mathbf{x}}(t) = \mathbf{A}\mathbf{x}(t) + \mathbf{b}u(t-\theta) \tag{A.38}$$

$$y(t) = \mathbf{c}\mathbf{x}(t) \tag{A.39}$$

Hence,

$$\mathbf{A} = \begin{bmatrix} \pm\lambda_1 & 0 \\ 0 & \lambda_2 \end{bmatrix}; \mathbf{b} = \begin{bmatrix} \pm a \\ \mp a \end{bmatrix}; \mathbf{c} = \begin{bmatrix} 1 & 1 \end{bmatrix} \tag{A.40}$$

A.3 Detailed derivation of the expressions (4.29) and (4.30)

Consider the transfer function given in (4.27) in the following form

$$\frac{Y(s)}{U(s)} = \frac{Ke^{-\theta s}}{a_1 s^2 + a_2 s \pm 1} \tag{A.41}$$

Taking the inverse Laplace transform of (A.41), we obtain

$$\ddot{y}(t) = -\frac{a_2}{a_1}\dot{y}(t) \mp \frac{1}{a_1}y(t) + \frac{K}{a_1}u(t-\theta) \tag{A.42}$$

Let

$$x_1(t) = y(t); \qquad x_2(t) = \dot{y}(t) = \dot{x}_1(t) \tag{A.43}$$

Therefore, (A.42) is becomes

$$\dot{x}_2(t) = -\frac{a_2}{a_1}x_2(t) \mp \frac{1}{a_1}x_1(t) + \frac{K}{a_1}u(t-\theta) \tag{A.44}$$

Representing (A.44) in controllable canonical form as

$$\begin{bmatrix} \dot{x}_1(t) \\ \dot{x}_2(t) \end{bmatrix} = \begin{bmatrix} 0 & 1 \\ -\left(\pm\frac{1}{a_1}\right) & -\left(\frac{a_2}{a_1}\right) \end{bmatrix} \begin{bmatrix} x_1(t) \\ x_2(t) \end{bmatrix} + \begin{bmatrix} 0 \\ \frac{K}{a_1} \end{bmatrix} u(t-\theta) \tag{A.45}$$

$$y(t) = \begin{bmatrix} 1 & 0 \end{bmatrix} \mathbf{x}(t) \tag{A.46}$$

Let

$$\mu_1 = \frac{a_2}{a_1}; \quad \mu_2 = \frac{\pm 1}{a_1} \quad and \quad \alpha = \frac{K}{a_1} \tag{A.47}$$

Therefore, according to standard state-space form the matrices of (A.45) are represented as

$$\mathbf{A} = \begin{bmatrix} 0 & 1 \\ -\mu_2 & -\mu_1 \end{bmatrix}; \ \mathbf{b} = \begin{bmatrix} 0 \\ \alpha \end{bmatrix}; \ \mathbf{c} = \begin{bmatrix} 1 & 0 \end{bmatrix} \tag{A.48}$$

Expressing matrix **A** in terms of roots of characteristic equation as

$$\mathbf{A} = \begin{bmatrix} 0 & 1 \\ -\lambda_1\lambda_2 & \lambda_1 + \lambda_2 \end{bmatrix} \tag{A.49}$$

where $\lambda_1 = \frac{-\mu_1}{2} - i\frac{\sqrt{4\mu_2 - \mu_1^2}}{2}$ and $\lambda_2 = \frac{-\mu_1}{2} + i\frac{\sqrt{4\mu_2 - \mu_1^2}}{2}$. For the analysis purpose the matrix **A** need to be transformed into diagonal form. The transformation matrix **M** (eigenvectors of **A**) is

$$\mathbf{M} = \begin{bmatrix} 1 & 1 \\ \lambda_1 & \lambda_2 \end{bmatrix} \tag{A.50}$$

and the matrices are given as

$$\hat{\mathbf{A}} = \mathbf{M}^{-1}\mathbf{A}\mathbf{M}; \quad \hat{\mathbf{b}} = \mathbf{M}^{-1}\mathbf{b}; \quad \hat{\mathbf{c}} = \mathbf{c}\mathbf{M} \tag{A.51}$$

Hence, the transformed matrices are obtained as

$$\hat{\mathbf{A}} = \begin{bmatrix} \lambda_1 & 0 \\ 0 & \lambda_2 \end{bmatrix}; \ \hat{\mathbf{b}} = \begin{bmatrix} \frac{\alpha}{(\lambda_1 - \lambda_2)} \\ \frac{-\alpha}{(\lambda_1 - \lambda_2)} \end{bmatrix}; \ \hat{\mathbf{c}} = \begin{bmatrix} 1 & 1 \end{bmatrix} \tag{A.52}$$

भारतीय प्रौद्योगिकी संस्थान गुवाहाटी
Indian Institute of Technology Guwahati

REFERENCES

[1] C.-C. Yu, *Autotuning of PID controllers: a relay feedback approach*. Springer Science & Business Media, 2006.

[2] S. Majhi, *Advanced control theory: a relay feedback approach*. Cengage Learning Asia, 2009.

[3] Q.-G. Wang, T. H. Lee, and L. Chong, *Relay feedback: analysis, identification and control*. Springer Science & Business Media, 2012.

[4] K. J. Åström and T. Hägglund, "Automatic tuning of simple regulators with specifications on phase and amplitude margins," *Automatica*, vol. 20 (5), pp. 645–651, 1984.

[5] W. L. Luyben, "Derivations of transfer functions for highly non-linear distillationcolumns," *Ind. Eng. Chem. Res.*, vol. 26, pp. 2490–2495, 1987.

[6] R. C. Chang, S. H. Shen, and C. C. Yu, "Derivation of transfer function from relay feedback systems," *Ind. Eng. Chem. Res.*, vol. 31, no. 3, pp. 855–860, 1992.

[7] G. Marchetti, C. Scali, and D. Lewin, "Identification and control of open-loop unstable processes by relay methods," *Automatica*, vol. 37, no. 12, pp. 2049–2055, 2001.

[8] H.-P. Huang, J.-C. Jeng, and K.-Y. Luo, "Auto-tune system using single-run relay feedback test and model-based controller design," *J. Process Control*, vol. 15, no. 6, pp. 713–727, 2005.

[9] K. Lavanya, B. Umamaheswari, and R. C. Panda, "Identification of second order plus dead time systems using relay feedback test," *Indian Chemical Engineer*, vol. 48(2), pp. 94–102, 2006.

[10] S. Vivek and M. Chidambaram, "An improved relay auto tuning of PID controllers for critically damped SOPTD systems," *Chem. Eng. Commun.*, vol. 199, no. 11, pp. 1437–1462, 2012.

[11] W. Li, E. Eskinat, and W. L. Luyben, "An improved autotune identification method," *Ind. Eng. Chem. Res.*, vol. 30, no. 7, pp. 1530–1541, 1991.

[12] A. Leva, "PID autotuning algorithm based on relay feedback," *IEE Proceedings D-Control Theory and Applications*, vol. 140, no. 5, pp. 328–338, 1993.

[13] C. Scali, G. Marchetti, and D. Semino, "Relay with additional delay for identification and autotuning of completely unknown processes," *Industrial & engineering chemistry research*, vol. 38, no. 5, pp. 1987–1997, 1999.

[14] S. H. Shen, J. S. Wu, and C. C. Yu, "Use of biased-relay feedback for system identification," *AIChE Journal*, vol. 42, no. 4, pp. 1174–1180, 1996.

[15] ——, "Autotune identification under load disturbance," *Ind. Eng. Chem. Res.*, vol. 35, no. 5, pp. 1642–1651, 1996.

[16] R. C. Panda, "Estimation of parameters of under-damped second order plus dead time processes using relay feedback," *Comp. Chem. Eng.*, vol. 30, no. 5, pp. 832–837, 2006.

[17] S. W. Sung and J. Lee, "Relay feedback method under large static disturbances," *Automatica*, vol. 42, no. 2, pp. 353–356, 2006.

[18] D. P. Atherton, "Relay autotuning: an overview and alternative approach," *Ind. Eng. Chem. Res.*, vol. 45, no. 12, pp. 4075–4080, 2006.

[19] P. K. Padhy and S. Majhi, "Relay based PI-PD design for stable and unstable FOPDT processes," *Comp. Chem. Eng.*, vol. 30, no. 5, pp. 790–796, 2006.

[20] Bajarangbali and S. Majhi, "Identification of underdamped process dynamics," *Systems Science & Control Engineering*, vol. 2, no. 1, pp. 541–548, 2014.

[21] J. Berner, T. Hägglund, and K. J. Åström, "Asymmetric relay autotuning–practical features for industrial use," *Control Engineering Practice*, vol. 54, pp. 231–245, 2016.

[22] Q. G. Wang, C. C. Hang, and B. Zou, "Low-order modeling from relay feedback," *Ind. Eng. Chem. Res.*, vol. 36, no. 2, pp. 375–381, 1997.

[23] S. Majhi and D. Atherton, "Autotuning and controller design for processes with small time delays," *IEE Proceedings-Control Theory and Applications*, vol. 146, no. 5, pp. 415–425, 1999.

[24] ——, "Online tuning of controllers for an unstable FOPDT process," *IEE Proceedings-Control Theory and Applications*, vol. 147, no. 4, pp. 421–427, 2000.

[25] S. Majhi, "Relay based identification of processes with time delay," *J. Process Control*, vol. 17, pp. 93–101, 2007.

[26] I. Kaya and D. Atherton, "An improved parameter estimation method using limit cycle data," in *Int. Conf. Control*, 1998, pp. 682–687.

[27] I. Kaya and D. P. Atherton, "Parameter estimation from relay autotuning with asymmetric limit cycle data," *J. Process Control*, vol. 11, no. 4, pp. 429 – 439, 2001.

[28] T. Thyagarajan and C.-C. Yu, "Improved autotuning using shape factor from relay feedback," *IFAC Proceedings Volumes*, vol. 35, no. 1, pp. 443–448, 2002.

[29] R. C. Panda and C. C. Yu, "Analytical expressions for relay feedback responses," *J. Process Control*, vol. 13, no. 6, pp. 489–501, 2003.

[30] R. Panda and C.-C. Yu, "Shape factor of relay response curves and its use in autotuning," *J. Process Control*, vol. 15, no. 8, pp. 893–906, 2005.

[31] K. Srinivasan and M. Chidambaram, "Modified relay feedback method for improved system identification," *Comp. Chem. Eng.*, vol. 27, pp. 727–732, 2003.

[32] R.C.Panda, V. Vijayan, V. Sujatha, P. Deepa, D. Manamali, and A. B. Mandal, "Parameter estimation of integrating and time delay processes using single relay feedback test," *ISA Transactions*, vol. 50, no. 4, pp. 529 – 537, 2011.

[33] J. Lee, S. W. Sung, and T. F. Edgar, "Integrals of relay feedback responses for extracting process information," *AIChE Journal*, vol. 53, no. 9, 2007.

[34] T. Liu, F. Gao, and Y. Wang, "A systematic approach for on-line identification of second order process model from relay feedback test," *AIChE Journal*, vol. 54, no. 6, pp. 1560–1578, 2008.

[35] T. Liu and F. Gao, "Alternative identification algorithms for obtaining a first-order stable/unstable process model from a single relay feedback test," *Ind. Eng. Chem. Res.*, vol. 47, no. 4, pp. 1140–1149, 2008.

[36] Bajarangbali and S. Majhi, "Identification of FOPDT and SOPDT process dynamics using closed loop test," *ISA Transactions*, vol. 53, no. 4, pp. 1223 – 1231, 2014.

[37] J. H. Park, H. I. Park, and I.-B. Lee, "Closed-loop on-line process identification using a proportional controller," *Chemical engineering science*, vol. 53, no. 9, pp. 1713–1724, 1998.

[38] I. Ananth and M. Chidambaram, "Closed-loop identification of transfer function model for unstable systems," *J. Franklin Inst*, vol. 336, no. 7, pp. 1055–1061, 1999.

[39] R. P. Sree and M. Chidambaram, "Improved closed loop identification of transfer function model for unstable systems," *J. Franklin Inst*, vol. 343, no. 2, pp. 152–160, 2006.

[40] T. Liu, Q. G. Wang, and H. P. Huang, "A tutorial review on process identification from step or relay feedback test," *J. Process Control*, vol. 23, pp. 1597–1623, 2013.

[41] S. Vivek and M. Chidambaram, "An improved relay auto tuning of PID controllers for unstable FOPDT systems," *Comp. Chem. Eng.*, vol. 29, pp. 2060–2068, 2005.

[42] K. J. Åström and P. Eykhoff, "System identificationa survey," *Automatica*, vol. 7, no. 2, pp. 123–162, 1971.

[43] J. G. Ziegler and N. B. Nichols, "Optimum settings for automatic controllers," *trans. ASME*, vol. 64, no. 11, 1942.

[44] C. C. Hang, K. J. Åström, and W. K. Ho, "Refinements of the Ziegler–Nichols tuning formula," in *IEE Proceedings D (Control Theory and Applications)*, vol. 138, no. 2, 1991, pp. 111–118.

[45] M. Morari and E. Zafiriou, *Robust process control*. Englewood Cliffs, NJ: Prentice-Hall, 1989.

[46] W. K. Ho, C. C. Hang, and L. S. Cao, "Tuning of PID controllers based on gain and phase margin specifications," *Automatica*, vol. 31, no. 3, pp. 497–502, 1995.

[47] S. Skogestad, "Simple analytic rules for model reduction and PID controller tuning," *J. process control*, vol. 13, no. 4, pp. 291–309, 2003.

[48] M. Shamsuzzoha and M. Lee, "IMC- PID controller design for improved disturbance rejection of time-delayed processes," *Ind. Eng. Chem. Res.*, vol. 46, no. 7, pp. 2077–2091, 2007.

[49] G. Prashanti and M. Chidambaram, "Set-point weighted PID controllers for unstable systems," *J. Franklin Inst*, vol. 337, pp. 201–215, 2000.

[50] T. Sugie and T. Yoshikawa, "General solution of robust tracking problem in two-degree-of-freedom control systems," *IEEE Trans. Autom. Control*, vol. 31, no. 6, pp. 552–554, 1986.

[51] Y. Lee, S. Park, M. Lee, and C. Brosilow, "PID controller tuning for desired closed-loop responses for si/so systems," *AIChE journal*, vol. 44, no. 1, pp. 106–115, 1998.

[52] R. Vilanova, V. M. Alfaro, and O. Arrietia, "Simple robust autotuning rules for 2-DoF PI controllers," *ISA Transactions*, vol. 51, no. 2, pp. 30 – 41, 2012.

[53] V. Vijayan and R. C. Panda, "Design of PID controllers in double feedback loops for SISO systems with set-point filters," *ISA Transactions*, vol. 51, pp. 514 – 521, 2012.

[54] M. Ajmeri and A. Ali, "Two degree freedom control scheme for unstable processes with small time delay," *ISA Transactions*, vol. 56, pp. 308 – 326, 2015.

[55] W. K. Ho, C. C. Hang, and J. Zhou, "Self-tuning PID control of a plant with under-damped response with specifications on gain and phase margins," *IEEE Trans. Control Syst. Technol.*, vol. 5, no. 4, pp. 446–452, 1997.

[56] I. Kaya, "Tuning PI controllers for stable processes with specifications on gain and phase margins," *ISA Transactions*, vol. 43, pp. 297 – 304, 2004.

[57] V. M. Alfaro and R. Vilanova, "Model-reference robust tuning of 2-DoF PI controllers for first- and second-order plus dead-time controlled processes," *J. Process Control*, vol. 22, pp. 359 – 374, 2012.

[58] S. Nema and P. K. Padhy, "Identification and cuckoo PI-PD controller design for stable and unstable processes," *Trans. Inst. Meas. Control*, vol. 37, no. 6, pp. 708–720, 2015.

[59] R. Toscano, "A simple robust PI/PID controller design via numerical optimization approach," *J. process control*, vol. 15, no. 1, pp. 81–88, 2005.

[60] W. E. Vander Velde, *Multiple-input describing functions and nonlinear system design*. McGraw-Hill, New York, 1968.

[61] S. Mallat, "A theory for multiresolution signal decomposition: The wavelet representation," *IEEE Trans. Pattern Anal. Mach. Intell.*, vol. 11, no. 7, pp. 674–693, April 1989.

[62] S. Vivek and M. Chidambaram, "Identification using single symmetrical relay feedback test," *Comp. Chem. Eng.*, vol. 29, pp. 1625–1630, 2005.

[63] H. Renaudineau, J.-P. Martin, B. Nahid-Mobarakeh, and S. Pierfederici, "DC-DC converters dynamic modeling with state observer-based parameter estimation," *IEEE Trans. Power Electron.*, vol. 30, no. 6, pp. 3356–3363, 2015.

[64] J.-M. Wang and S.-T. Wu, "Sensorless control scheme for synchronous buck converter," *IET Circuits, Devices & Systems*, vol. 10, no. 3, pp. 181–191, 2016.

[65] E. Babaei, K. Varesi, and N. Vosoughi, "Calculation of critical inductance in n-input buck dc–dc converter," *IET Power Electronics*, vol. 9, no. 12, pp. 2434–2444, 2016.

[66] J. Wang, S. Li, B. W. Jun Yang, and Q. Li, "Finite-time disturbance observer based non-singular terminal sliding-mode control for pulse width modulation based DC-DC buck converters with mismatched load disturbances," *IET Power Electronics*, vol. 9, no. 9, pp. 1995–2002, 2016.

[67] J. G. Kassakian, M. F. Schlecht, and G. C. Verghese, *Principles of power electronics*. Addison-Wesley, USA, 1991.

[68] B. Miao, R. Zane, and D. Maksimovic, "System identification of power converters with digital control through cross-correlation methods," *IEEE Trans. Power Electron.*, vol. 20, no. 5, pp. 1093–1099, 2005.

[69] B. Johansson and M. Lenells, "Possibilities of obtaining small-signal models of DC-to-DC power converters by means of system identification," in *Telecomm. Energy Conf.* IEEE, 2000, pp. 65–75.

[70] A. N. Vargas, L. P. Sampaio, L. Acho, L. Zhang, and J. B. do Val, "Optimal control of DC-DC buck converter via linear systems with inaccessible markovian jumping modes," *IEEE Trans. Control Syst. Technol.*, vol. 24, no. 5, pp. 1820–1827, 2016.

[71] W. Xiao, W. G. Dunford, P. R. Palmer, and A. Capel, "Regulation of photovoltaic voltage," *IEEE Trans. Ind. Electron.*, vol. 54, no. 3, pp. 1365–1374, 2007.

[72] R. Middlebrook and S. Cuk, "A general unified approach to modelling switching-converter power stages," in *Proc. IEEE Power Electron. Specialist Conf.* IEEE, 1976, pp. 18–34.

[73] R. W. Erickson and D. Maksimovic, *Fundamentals of power electronics*. Springer Science & Business Media, 2007.

[74] http://www.ti.com/lit/ds/symlink/tms320f28232.pdf.

[75] G. Fedele, "A new method to estimate a first-order plus time delay model from step response," *Journal of the Franklin Institute*, vol. 346, no. 1, pp. 1–9, 2009.

[76] C. L. Chen, "A simple method for on-line identification and controller tuning," *AIChE journal*, vol. 35, no. 12, pp. 2037–2039, 1989.

[77] D. Chen and D. E. Seborg, "PI/PID controller design based on direct synthesis and disturbance rejection," *Ind. Eng. Chem. Res.*, vol. 41, pp. 4807–4822, 2002.

[78] S. Nema and P. K. Padhy, "PI-PD controller for stable and unstable processes," *International Journal of Systems, Control and Communications*, vol. 5, no. 2, pp. 156–165, 2013.

[79] M. Ajmeri and A. Ali, "Direct synthesis based tuning of the parallel control structure for integrating processes," *Int J Syst Sci*, vol. 46, no. 13, pp. 2461–2473, 2015.

[80] T. Liu, W. Zhang, and D. Gu, "Analytical design of two-degree-of-freedom control scheme for open-loop unstable processes with time delay," *J. Process Control*, vol. 15, no. 5, pp. 559–572, 2005.

[81] A. S. Rao, V. Rao, and M. Chidambaram, "Direct synthesis-based controller design for integrating processes with time delay," *J. Franklin Inst*, vol. 346, no. 1, pp. 38 – 56, 2009.

[82] Z. Gaing, "A particle swarm optimization approach for optimum design of PID controller in AVR system," *IEEE Transactions on Energy Conversion*, vol. 19, no. 12, pp. 384 – 391, 2004.

[83] R. P. Sree, M. Srinivas, and M. Chidambaram, "A simple method of tuning PID controllers for stable and unstable foptd systems," *Computers & chemical engineering*, vol. 28, no. 11, pp. 2201–2218, 2004.